STRUCTURES AND THERMAL DECOMPOSITIONS

OF

PSEUDOPOLYMORPHS OF SULFONAMIDE DRUGS

A thesis submitted to the

UNIVERSITY OF CAPE TOWN

in fulfilment of the requirements for the degree of

MASTER OF SCIENCE

BY

INNOCENT PHILANI SHABALALA *B.Sc(Hons), Cape Town*

Department of Chemistry
University of Cape Town
Rondebosch
7700
Republic of South Africa

September 1994

ACKNOWLEDGEMENTS

I wish to extend sincere thanks to

Professor M R Caira, for his patient and enthusiastic supervision,

Professor L R Nassimbeni for his support of this work and good humour,

AECI (Limited) for a Postgraduate fellowship and for sending me Happy Birthday cards, and lastly,

the moral and spiritual support of my family.

PUBLICATIONS AND CONFERENCE PROCEEDINGS

Parts of this thesis have been published:

1. "X-ray Structural Studies and Physicochemical Characterization of the 1-Butanol, 1-Pentanol and 1,4-Dioxane Solvates of Succinylsulfathiazole".
   Susan A. Bourne, Mino R. Caira, Luigi R. Nassimbeni and Innocent Shabalala: *J.Pharm.Sci.* **83**, 887, (1994).

2. "Pseudopolymorphism of Sulfathiazole:Characterization of Solvates of Sulfathiazole with Substituted Pyridines".
   Mino R. Caira, Luigi R. Nassimbeni and Innocent Shabalala: *in preparation.*

Parts of this thesis have been presented at the following:

South African Chemical Institute Young Chemist's Meeting, Eikendal Vineyards, **Stellenbosch,** 23 November 1992.

The Fourteenth Annual Congress of the Academy of Pharmaceutical Sciences, **Durban,** 21-23 June 1993.

AECI Limited Postgraduate Research Fellowship Seminar, **Modderfontein,** 7-8 October 1993.

UCT Chemistry Research Conference, **Cape Town,** 9-11 February 1994.

The Fifteenth Annual Congress of the Academy of Pharmaceutical Sciences, **Grahamstown,** 26-29 June 1994.

ABSTRACT

Pseudopolymorphs of two sulfonamide drugs, namely sulfathiazole and succinylsulfathiazole, have been prepared by recrystallization of the drugs from various organic solvents and their properties have been studied by several physicochemical methods.

Thermal Analysis involving Thermal Gravimetry (TG) and Differential Scanning Calorimetry (DSC) were used to investigate such thermal properties of the crystals as stabilities, desolvation processes and their kinetics as well as the melting of pure polymorphic forms of the drugs resulting from desolvation.

Complementary studies of the compounds using X-ray powder diffraction (XRD) and DSC allowed identification and assignment of the products of desolvation i.e. polymorphs.

Single crystal studies were carried out by X-ray diffraction methods. Interesting structural features such as crystal packing modes, hydrogen bonding schemes, cavity versus channel occupation by guest molecules and host conformations were investigated.

From a high level of agreement of results obtained using these methods, the pseudopolymorphs and polymorphs studied were characterized unambiguously.

GLOSSARY OF ABBREVIATIONS USED

Fig.	Figure
H	host
G	guest
e.s.d	estimated standard deviation
s.o.f.	site occupancy factor
CFOM	combined figure of merit
D_m	measured density
D_C	calculated density
X_b	mole fraction of 1-butanol
X_p	mole fraction of 1-pentanol
GLC	Gas Liquid Chromatography
DSC	Differential Scanning Calorimetry
TGA	Thermogravimetric Analysis
ΔH	enthalpy change
m.p.	melting point
b.p.	boiling point
T	temperature
E	normalized structure factor
Ea	activation energy
R	gas constant (8.31441 $JK^{-1}mol^{-1}$)
V	unit cell volume
XRD	X-ray diffraction
Z	number of asymmetric units per unit cell
ST	sulfathiazole
SST	succinylsulfathiazole
SSTHYD	hydrate of SST
SSTANHYD	anhydrous form of SST
SSTDI	1,4-dioxane solvate of SST
SSTBU	1-butanol solvate of SST
SSTPE	1-pentanol solvate of SST
STPY	pyridine solvate of ST
STPY1	2-methylpyridine solvate of ST
STPY2	3-methylpyridine solvate of ST
STPY26	2,6-dimethylpyridine solvate of ST
MOD	modification
HI-HIII	hydrates of SST
T_{ons}	onset temperature

TABLE OF CONTENTS

CHAPTER 11: THERMAL ANALYSIS AND THE KINETICS OF DESOLVATION

CHAPTER 1

SUBCONTENTS

INTRODUCTION

1.1 A GENERAL OVERVIEW OF INCLUSION COMPOUNDS

Although the chemistry of inclusion compounds has had a long history[1], it is only in recent years that significant advances were made in this field of research. The discovery of new clathrates and hosts, includes graphite intercalates[2], ß-quinol H_2S clathrate[3], cyclodextrin inclusion compounds[4], the Hofmann's inclusion compound of nickel cyanide ammonia with benzene[5], inclusion compounds of triphenylmethane[6], compounds of tri-o-thymotide[7], Dianin's compound[8], the choleic acids[9], urea[10] and phenol[11] inclusion compounds.

While the principal focus of this study is the inclusion compounds of drug substances, a brief overview of the classification and nomenclature of inclusion compounds warrants attention in order to understand how and why drugs form clathrates.

1.2 DEFINITIONS AND CLASSIFICATION

Molecular compounds in which one component, specifically the *host,* forms a cage structure encapsulating the other, termed *guest,* are known as *clathrates*[12]. One of the most up-to-date classification systems, that of Weber and Josel[13] takes into account the two main criteria, namely:-

- the type of host-guest interactions, and

- the topology of the host-guest aggregate.

In the former criterion a distinction is made between **complexes** and **clathrates.** Those aggregates in which coordination exists between host and guest components are defined as complexes. A typical example of a complex is the one between 18-crown-6 and ammonium bromide[14] **(Fig.1.1 (a))**. On the other hand, a true clathrate is a host-guest aggregate in which the guest is retained by steric barriers formed by the host structure. The compound, 4-p-hydroxyphenyl-2,2,4-trimethylchroman[15] shown in **Fig.1.1.(b))** is one such example.

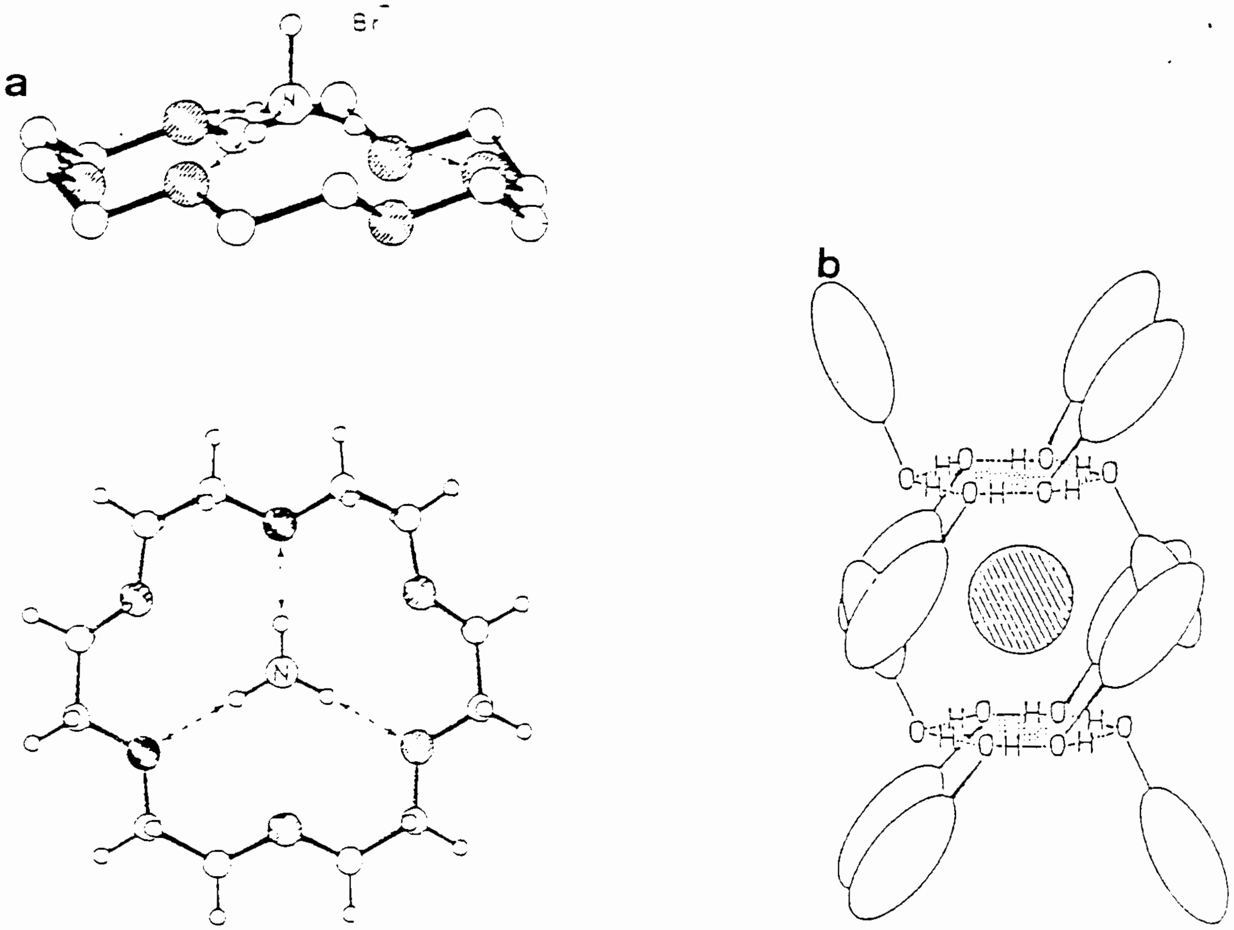

Figure 1.1 Examples of (a) 18-crown-6 ammonium bromide complex in two perspectives[14], and (b) host guest matrix of the compound, 4-*p*-hydroxyphenyl-2,2,4- trimethylchroman[15].

With respect to topological considerations a distinction is made between intramolecular host-guest aggregates which form host cavities and are thus referred to as cavitates, and extramolecular aggregates in which lattice voids are filled by guest molecules.

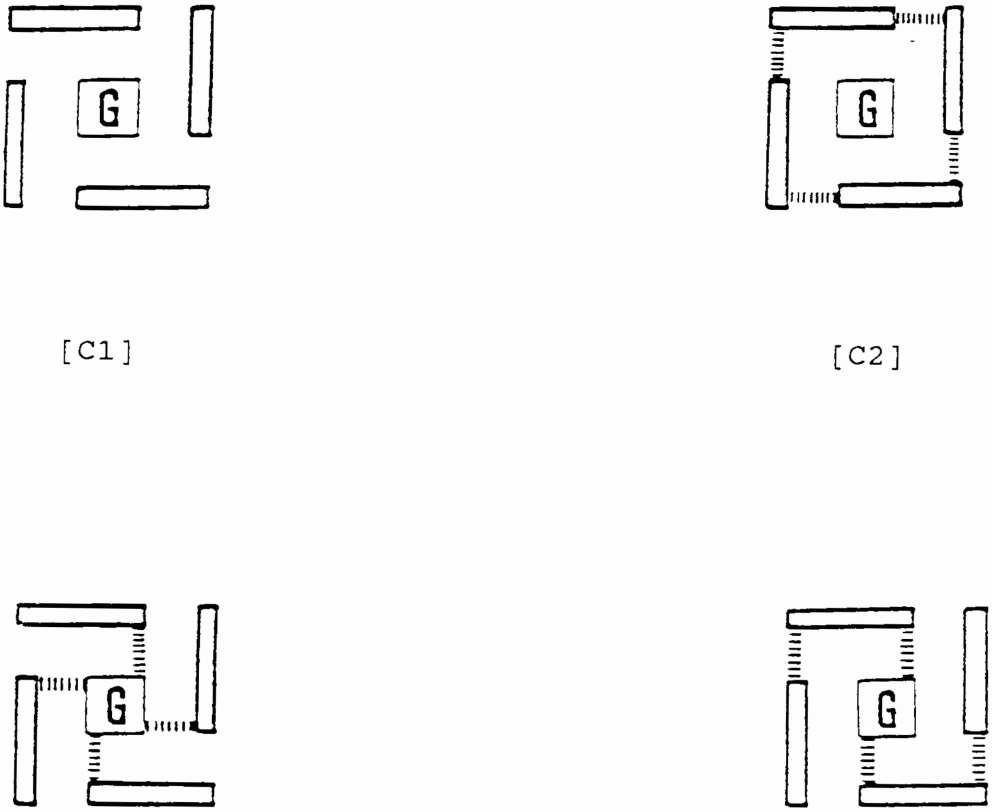

[C1]

[C2]

[C3]

[C4]

Figure 1.2 Schematic Representation of Host-Guest Types[13].

[C1] - there are no coordinative interactions; guest is held by purely steric barriers of the host lattice. This is a *true clathrate.*

[C2] - there are interactions between the host components only resulting in a *coordination-assisted clathrate host lattice.*

[C3] - this is a *coordinato clathrate* with coordinative host-guest interactions only.

[C4] - here a combination of both host-host and host-guest interactions is taking place. The aggregate is referred to as *coordinato clathrate in a coordination-assisted host lattice.*

1.3 INCLUSION COMPOUNDS OF DRUG SUBSTANCES

In a plethora of well-documented examples of clathrates lies yet another large pool of clathrate compounds; those host-guest aggregates in which at least one component is a therapeutically-active molecule, i.e. a drug.
Inclusion compounds of drug substances are of great utility in the pharmaceutical industry, having many practical and research applications.
Examples of these compounds include the solvates of cephaloglycin (**Figure** 1.3) and cephalexin [16-17] (**Figure 1.4**). These antibiotics occur in a wide variety of solvated crystal forms.

Haleblian and McCrone[18] have adequately documented the argument that the pharmaceutical chemists should become familiar with the crystallizing properties of drugs in order to control the crystal form, habit, size, size distribution, degree of crystallinity, and state of aggregation of the drug particles. These parameters, according to the argument, often determine the acceptability of bulk properties such as mixing, tabletting, filling, dusting, *etc.* and pharmaceutical performance such as dissolution, bioavailability, chemical and physical stability, suspendibility and rheology.

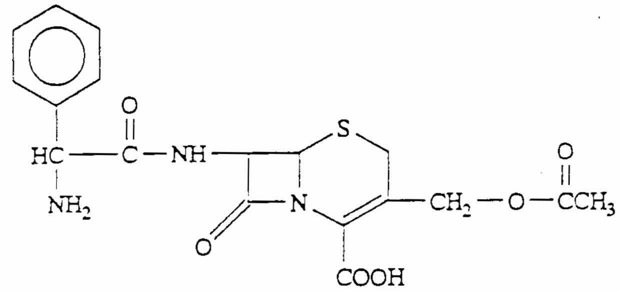

1.3 Cephaloglycin

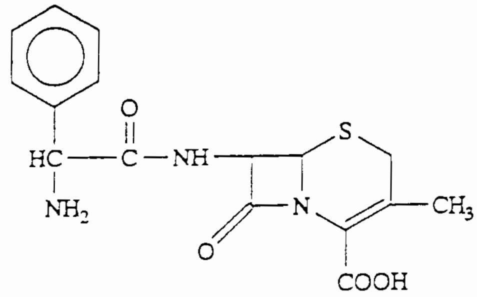

1.4 Cephalexin

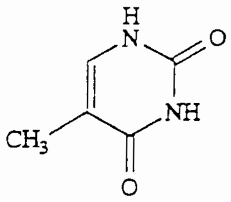

1.5 Thymine

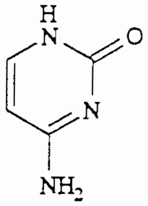

1.6 Cytosine

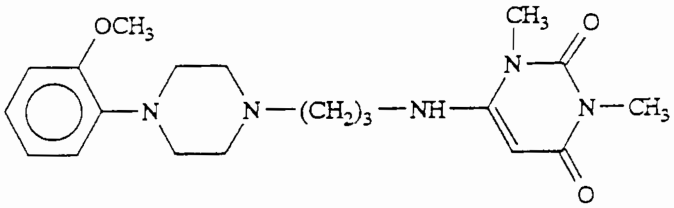

1.7 Urapidil

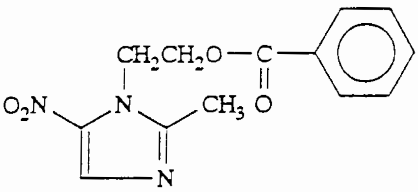

1.8 Metronidazole benzoate

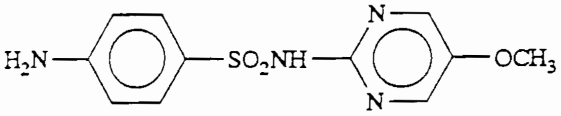

1.9 5-Methoxysulfadiazine

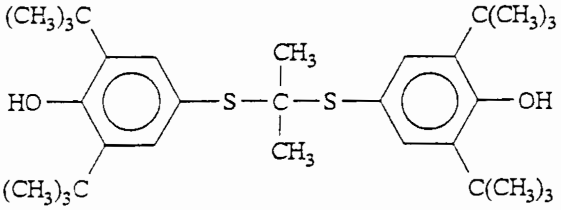

1.10 Probucol

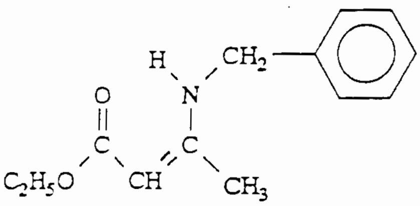

1.11 Ethyl-β-benzylaminocrotonate
(Z-structure)

Figure 1.3-1.11 Examples of drug compounds whose polymorphic and inclusion properties have been characterized.

Between 1962 and 1978 alone it was confirmed that more than 1000 crystal structures of solvates had been determined already[19]. Subsequent to that, Clark reviewed crystallographic studies of hydrates[20]. In general, quite a large number of drugs and other biologically-active compounds retain the solvent of crystallization, i.e. they form solvates.

A LIST OF SEVERAL SOLVATE-FORMING DRUGS

	DRUG	REFERENCE	YEAR
i.	Hydrocortisone acetate	21	1955
ii.	Erythromycin	22	1953
iii.	Cholesterol	23	1963
iv.	Ampicillin	24	1965
v.	Cephaloridine	25	1968
vi.	Chloramphenicol	26	1971
vii.	Sulfanilamide	27	1972
viii.	Nitrofurmethone	28	1972

Of interest as well, is the inclusion of water of crystallization to form hydrates, for example, thymine hydrate[29] **(Figure 1.5)** and cytosine hydrate[29] **(Figure 1.6)**. **Figure 1.12** is the stereoscopic view of the crystal packing of thymine hydrate showing tunnels of water molecules running parallel to the c axis[29]. The water molecules exit preferentially along these channels upon dehydration.

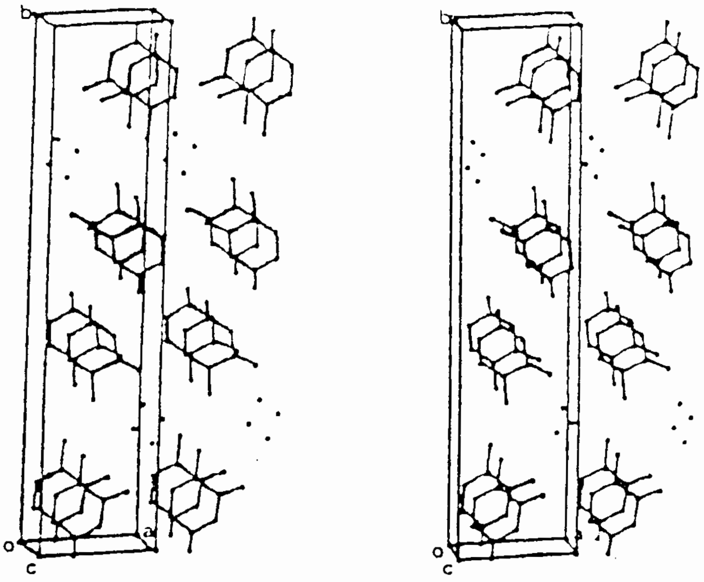

Figure 1.12 Stereoscopic view of the crystal packing of thymine hydrate[29].

1.3.1 RECENT STUDIES OF DRUG INCLUSION COMPOUNDS

The molecular features which provoke the curiosity of the solid-state chemist include the conformations of drug molecules in the host-guest aggregates, the drug:solvent stoichiometries and the type and strength of host-guest binding. It is a stimulating exercise to compare and contrast these features in a series of structurally-related crystalline solvates.

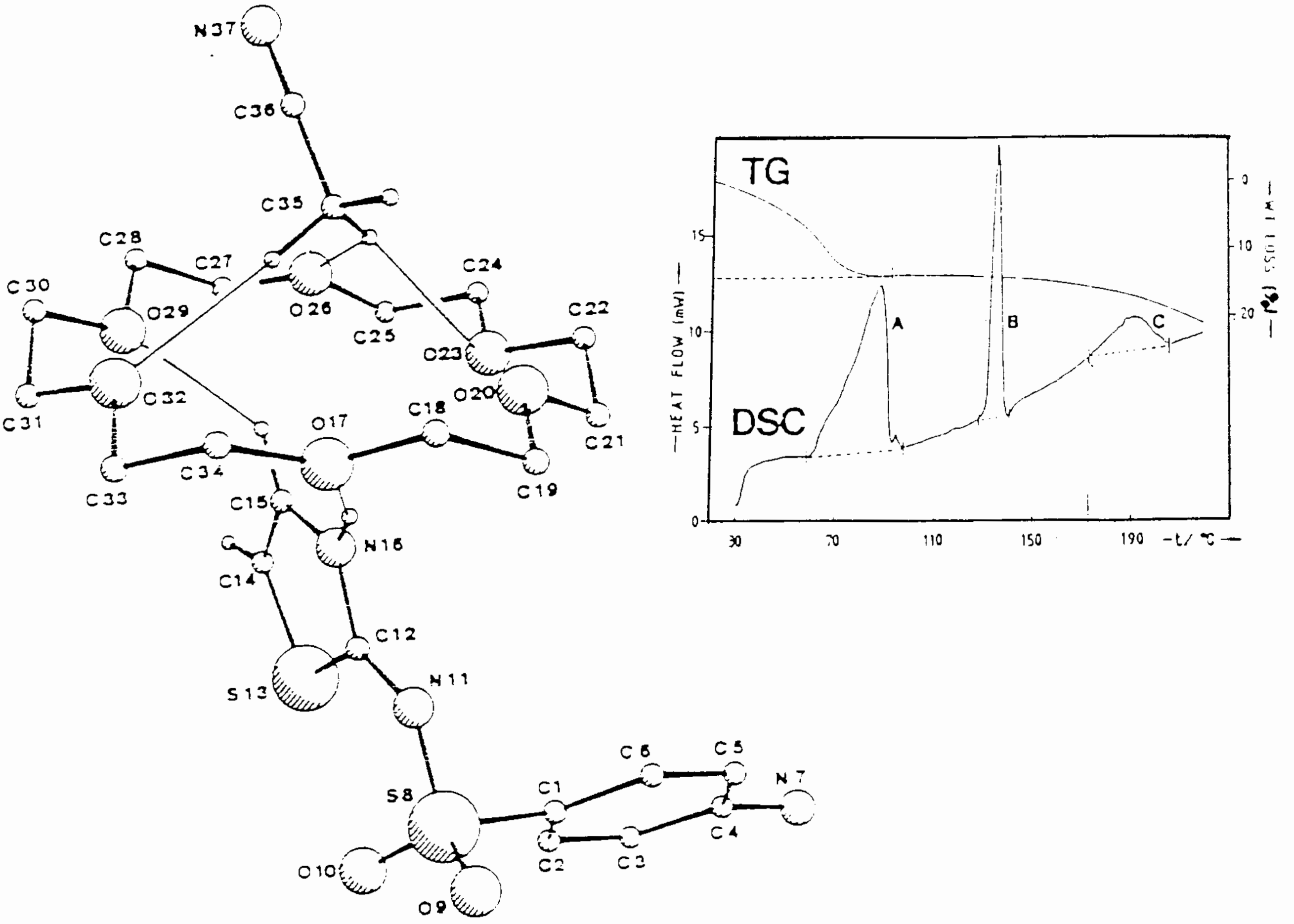

Figure 1.13 1,4,7,10,13,16-hexaoxacyclooctadecane-4-amino-*N*-2-thiazolylbenzenesulfonamide-ethanenitrile (1:1:1) complex[30], and its TG-DSC thermograms.

Most recently[30], a rare case of face differentiation in the 1:1:1 ternary inclusion complex of 18-crown-6 ligated by acetonitrile and sulfathiazole was investigated.

Figure 1.13 shows the structure of this compound. The authors have advanced a precise description of cavitate binding. Acetonitrile (**CH_3CN**) and sulfathiazole (**$C_9H_9N_3O_2S_2$**) molecules are ligated to the opposite faces of the macrocycle 18-crown-6 to form a 1:1:1 ternary inclusion compound. The dominant intermolecular associations are **C–H···O** and **N–H···O** hydrogen bonds.

Furthermore, the TGA-DSC thermal degradation profiles, **Figure 1.13**, indicate that CH_3CN is rapidly lost leaving the sulfathiazole:18-crown-6 species which undergoes a phase change before collapsing at approximately 448K. Similar studies have been conducted on a methanol solvate and hydrates of the antihypertensive drug, urapidil[31-32] (**Figure 1.7**), the monohydrate of metronidazole benzoate[33] (**Figure 1.8**), and inclusion compounds with 5-methoxysulfadiazine[34] (**Figure 1.9**).

Cyclodextrins (shown in **Figure 1.14**), the basket-shaped macrocyclic oligosaccharides consisting of six or more α-1,4-linked D-glucose units have also found place in the lofty themes of enclathration and molecular recognition.

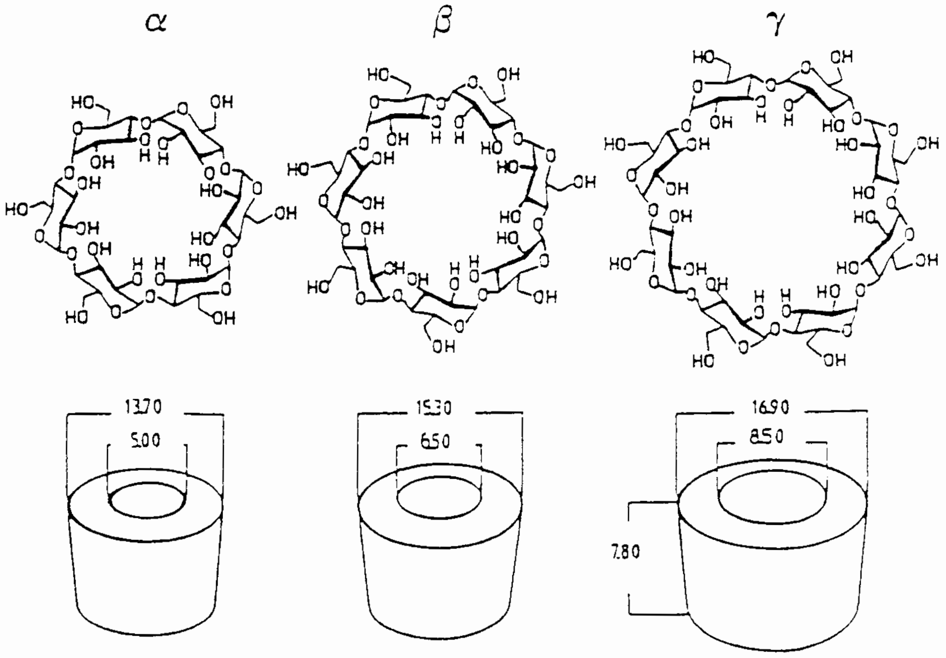

Figure 1.14 α-,β- and γ- cyclodextrins with lengths (Å) and ring sizes indicated[35].

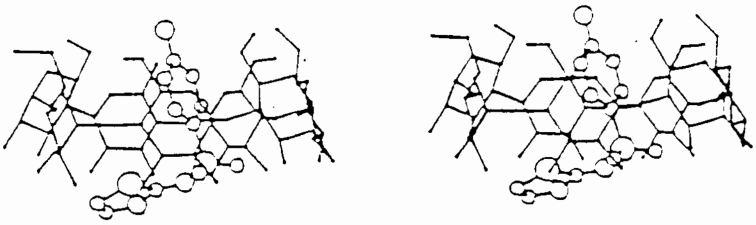

Figure 1.15 Stereo diagram of Sulfathiazole complexed with ß-cyclodextrin[36].

Caira *et al* have crystallized and fully characterized the inclusion complex of ß-cyclodextrin with sulfathiazole[36] (see **Figure 1.15**). The study formed part of the well-known approach to achieve stable drug preparation by encapsulating the drug molecules in cyclodextrins. Such modification generally results in improved drug bioavailability[37]. It is a rather important modification especially with drugs of low aqueous solubilities like sulfathiazole.

The authors[35] have exploited the potential pharmaceutical application together with the purely academic exercise of appreciating the topology, molecular conformation and the intricate host-guest binding within the complex.

Besides these recent developments, other systematic studies of many drug solvates involving distinct drug classes like barbiturates and steroids[38], sulfonamides[39] and antibiotics[40] have accumulated in the pharmaceutical literature.

1.3.2 POLYMORPHISM AND PSEUDOPOLYMORPHISM OF DRUGS

It has long been established that a given drug substance, when studied more closely, may exist in more than one crystal form. These may be solvated forms, i.e. ***pseudopolymorphs*** possessing the properties of inclusion compounds, or the different pure, non-solvated forms i.e. ***polymorphs*** of the drug which result from temperature-mediated processes like enthalpic desolvation. The foregoing terminology is rather loose but it is frequently used in the literature[41-43]. In Byrn's "Solid State Chemistry of Drugs"[29], these terms are defined and used cautiously in order to avoid confusion.

Polymorph is a broad term reserved for the different solvates and/or anhydrates of a given compound having different crystal structures resulting in different crystal habits and X-ray diffraction patterns. However, the term 'polymorph' is used exclusively to refer to the unsolvated, pure forms of the same drug in this text. As mentioned earlier, steroids, barbiturates and sulfonamides have been reported to exhibit concrete evidence of polymorphism. Phase transformations can be induced by heat or mechanical stresses and other solvent-mediated processes, such as recrystallization from mixtures instead of pure solvents. As yet, it is not possible to predict whether or not a given compound will exhibit polymorphism[44].

Further distinction is made between ***conformational*** and ***configurational*** polymorphism.

A polymorph is said to be conformational if a molecule adopts significantly different conformations in its crystal forms. Probucol **(Figure 1.10)**, a cholesterol-lowering agent used in the treatment of atherosclerotic lesions and diabetes mellitus exists in at least two conformers in the solid state[45]. One conformer is highly symmetrical whereas the other one is clearly not **(Figure 1.16)**. In the symmetrical conformer the C-S-C-S-C chain is extended with the molecular symmetry approximating to C_{2v}, while the two torsion angles, S-C-S-C approximate to 80° and 165° in the less symmetrical conformer.

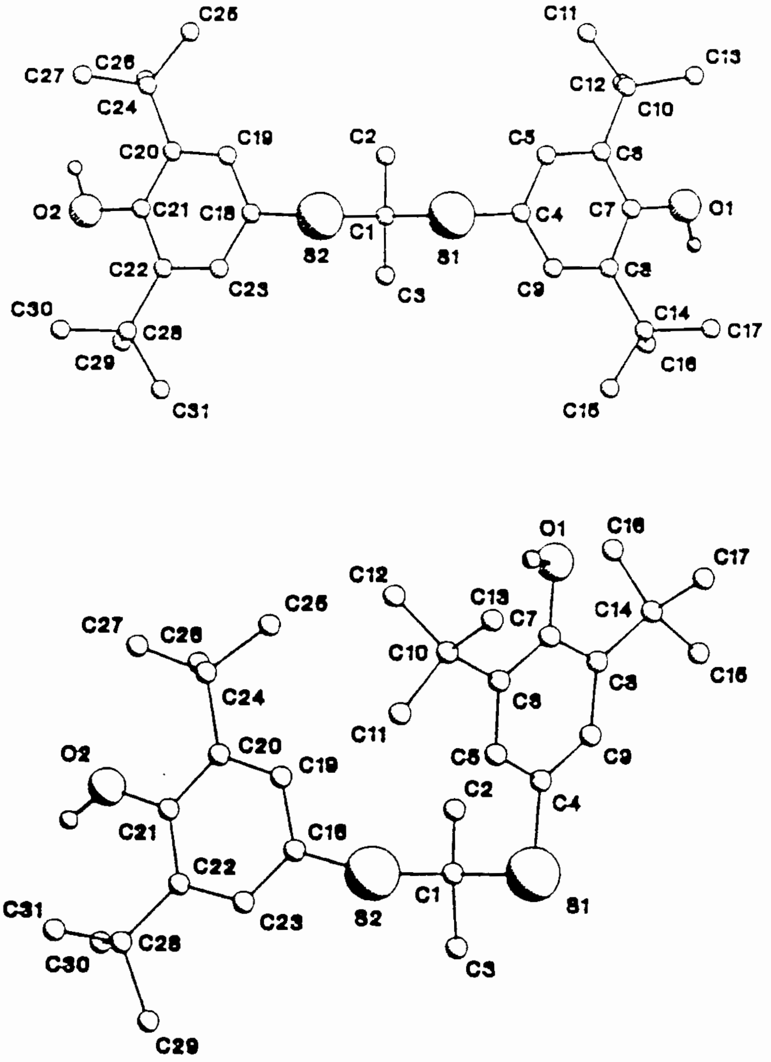

Figure 1.16 An illustration of conformational polymorphism of probucol[45].

Some drug molecules exist in different configurations in the solid state. These may be cis-trans- isomers or tautomers, crystallizing in separate forms. The consequence of this phenomenon is the ability to isolate and study the configurational polymorphs independently. A number of researchers conducted studies on the Schiff's base, ethyl ß-benzylaminocrotonate (**Figures 1.11** and

1.17) and found that the lower-melting configurational polymorph (m.p. 23°C) has the cis-structure, whereas the higher-melting one (m.p. 75-80°C) has the trans-structure[46-49]. On the other hand, if the crystallization of the drug results in the solvent of crystallization being entrapped, whether in stoichiometric or non-stoichiometric amounts, these compounds are referred to as ***solvates***. The term '***hydrates***' is used if the solvent of crystallization is water. Codeine hydrochloride[50], mercaptopurine[51], piroxicam[52], spironolactone[53] and many others have been investigated for solvate/hydrate formation.

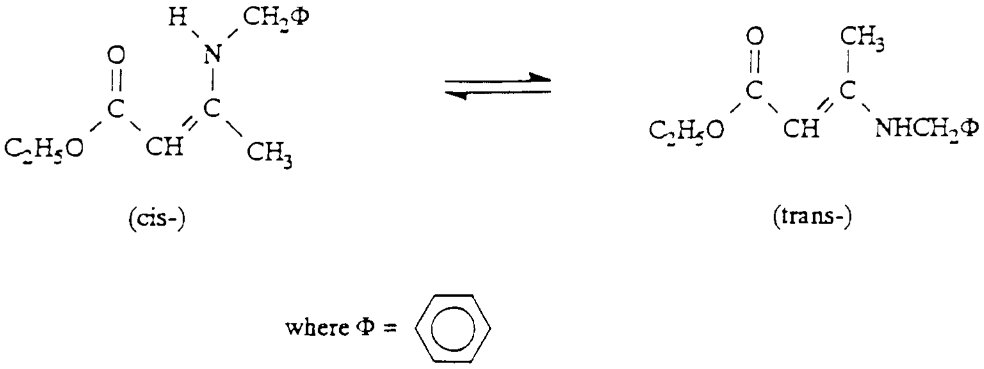

Figure 1.17 The cis- and trans- configurational polymorphs of ethyl ß-benzylaminocrotonate[49].

The central focus of this work is on the behaviour of pseudopolymorphic solvates. Hence a more detailed account is warranted. In most compounds of this type, solvent of crystallization plays an important role in holding the crystal together. Hydrogen bonding is the most common mode of association between the drug and the solvent molecules. Some solvates collapse and recrystallize in a new crystal form upon heating. Enclathration (dealt with in 1.2), is common in solvates with the solvent molecules acting as fillers that occupy voids or channels in the crystal. Sometimes, the desolvation process does not destroy the original crystal structure. Pfeiffer *et al* reported the behaviour of cephalosporin solvates that can be desolvated and resolvated at will without greatly affecting the powder diffraction pattern of the original species[54]. Byrn[29] refers to this phenomenon as ***crystal pseudopolymorphism.***

1.4 PHYSICOCHEMICAL TECHNIQUES USED TO INVESTIGATE THE DESOLVATION PROCESSES

This discussion of physicochemical techniques is not intended to develop rigorous theoretical explanations of how these techniques work since there exists an abundance of literature on this subject. The intention here is to focus on those specific techniques which were used especially in this work to assist the full and unambiguous characterization of the solvates obtained.

1.4.1 THERMAL DECOMPOSITION OF DRUG SOLVATES (TGA-DSC)

Byrn[29] cites four main steps involved in the desolvation of polymorphic and pseudopolymorphic solvates.
These are:-

1. **Molecular loosening** in which the nucleation and loosening of the crystal packing take place so that the solvent can escape.
2. **Breaking of the host-solvent** hydrogen bonds or other associations, happens after step one before the solvent can exit the crystal.
3. **Solid-solution formation** which happens at the early stages of the product formation.
4. **Separation of product** (sometimes referred to as 'topotactic' reaction), giving randomly oriented crystals whose orientation is often determined by the starting material.

Thermogravimetric Analysis (TGA) and Differential Scanning Calorimetry (DSC) are often used complementarily to investigate these enthalpic processes. Perrier and Byrn performed TGA studies at the heating rate of 6°Cmin^{-1} with the hydrates of caffeine, theophylline, cytosine and deoxyadenosine to analyse both the crystal packing and hydrogen bondings[55]. The temperature at which 2% of the water had been lost was taken to be the threshold temperature of desolvation. Due to the evolution of quantitative DSC it has become possible to evaluate important thermodynamic parameters such as enthalpies ΔH

of guest release and host fusion together with the highly reproducible onset temperatures accompanying these processes[56]. In addition to this, any intermediate phase changes and even impurities may be detectable.

The schematic TGA and DSC traces shown in **Figure 1.18** illustrate weight loss associated with desolvation (TGA) and endothermic peaks A and B (DSC) accompanying the desolvation step and melting of the host respectively. In the diagram, symbol ß represents the inclusion compound and *α* represents its unsolvated form (detailed explanations of these phases are given later in **Chapter 6**).

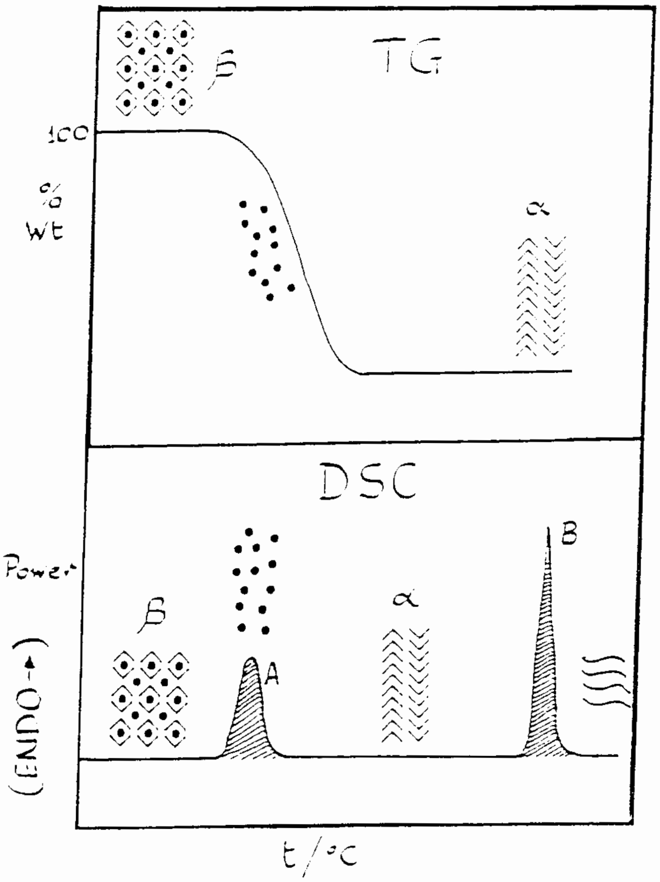

Figure 1.18 Schematic representation of chemical events as evidenced by TG-DSC techniques[57].

1.4.2 ALLIED TECHNIQUES

In order to achieve complete physical characterization of the compounds obtained, other techniques such as X-ray diffraction (XRD), microanalysis and density measurements had to be invoked. XRD is particularly indispensable in discriminating between polymorphs of the same drug since it acts as a 'fingerprinting' tool. If careful attention is paid to effects such as impurities, preferred crystal orientation and particle size during an XRD experiment the resulting diffractograms can be indicative of the polymorphic and psuedopolymorphic behaviour.

1.4.3 PRACTICAL SIGNIFICANCE OF POLYMORPHISM

The importance of polymorphism is evident in the statement that one crystalline modification of the drug may show ten times the solubility of another form of the same drug with a resulting change in bioavailability[44].

The stability of polymorphs became a pertinent issue when the "Federal Register" in 1978* stipulated that all marketed drugs should bear the expiration date after which the drug may no longer be sold[29]. The Register also prescribed the storage conditions under which the expiration date applies. The ability to control the bulk properties (mixing, tabletting, filling, dusting, etc.) depends on adequate knowledge of the polymorphic types and stabilities.

* Sept 29

Failure to successfully investigate polymorphism early in the lifetime of the drug could result in toxic drug formulation. Haleblian *et al*[18] have quoted cases of suspensions, solutions and suppositories where polymorphic changes take place due to conversion from metastable to stable forms. This conversion may be accompanied by crystal growth, thus resulting in undesirable particle size distribution.

Another case of the possible consequence of choosing a wrong polymorph for administration was evident in a recent study of the drug mebendazole, in mice[58]. Of the three polymorphic forms of mebendazole designated A, B and C by the authors, polymorph A was found to be the least toxic and effective against *T.spirallis* in mice while B was found to be the most toxic after oral administration.

1.5 SULFONAMIDE DRUGS

1.5.1 HISTORICAL BACKGROUND

Sulfonamides were discovered through the studies of Ehrlich on the selective binding of dyes to microorganisms[60-62]. In 1932, Domagk demonstrated that the red dye, Prontosil rubrum (**Figure 1.20**) could be used to effectively prevent the death of mice injected with haemolytic streptococcus[62].

The name Streptozon was adopted in order to market prontosil rubrum as a chemotherapeutic agent for *in vivo* cure. A major step was taken by Bovet in 1936 who showed that sulfanilamide **(Figure 1.21)**, a reduction product of prontosil rubrum was an effective bacterial inhibitor both *in vitro* as well as *in vivo* and that the whole process occurs in the liver[63-68]. **Figure 1.19** below is a simplistic reaction scheme showing what happens in the liver.

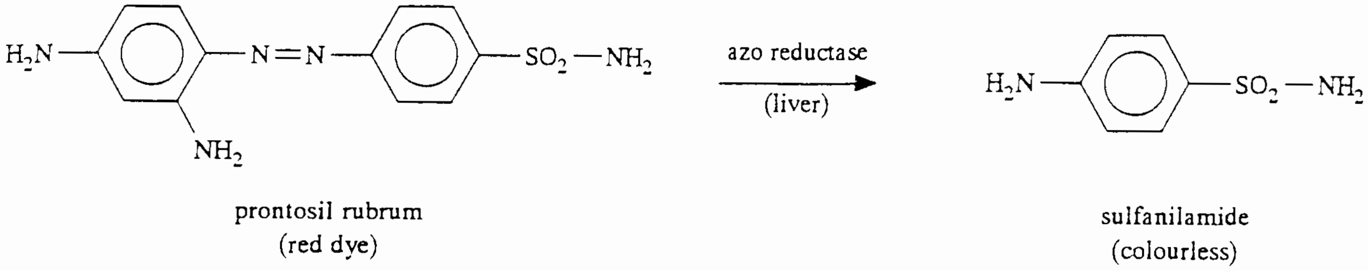

Figure 1.19 *In vivo* reduction of prontosil rubrum to sulfanilamide in the liver.

Of historical importance is the fact that prontosil rubrum and sulfanilamide effectively reduced the number of deaths due to streptococcal infections quite dramatically in England and Wales in 1935. Another sulfonamide, namely sulfapyridine **(Figure 1.22)** was prescribed to Sir Winston Churchill in 1943, during the Second World War, when he contracted pneumonia in his trip to Africa.

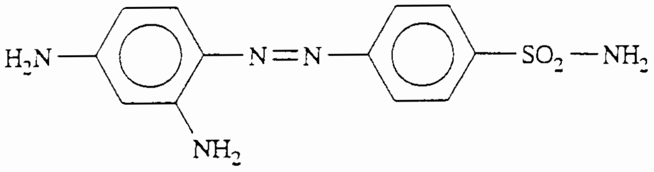

1.20 Prontosil rubrum

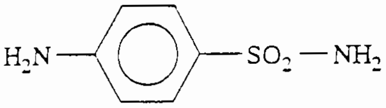

1.21 Sulfanilamide

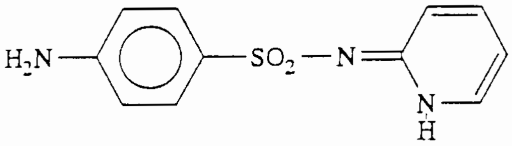

1.22 Sulfapyridine

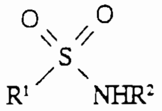

R^1 = aryl or heteroaryl group
R^2 = H, alkyl or acyl group

1.23 Sulfonamide group

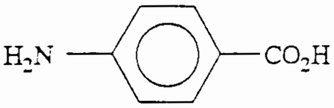

1.24 *p*-aminobenzoic acid (PABA)

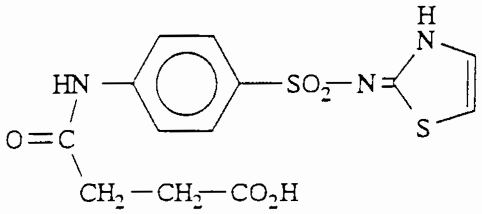

1.25 Succinylsulfathiazole

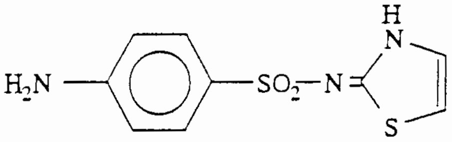

1.26 Sulfathiazole

Figure 1.20-1.26 Several Sulfonamide drugs whose pharmacological action and solid state chemistry have been investigated.

1.5.2 ANTIBACTERIAL ACTION OF SULFONAMIDES

In the research that was conducted with azo dye compounds it became popular to introduce the sulfonamide group (**Figure 1.23**) as it was believed that *in vivo/in vitro* potencies observed were due to this moiety. The fact that sulfanilamide exhibited bacteriostatic properties both *in vivo* and *in vitro* suggested that prontosil itself was not the active drug species but that it acted as a prodrug, being reduced *in vivo* to produce the active metabolite sulfanilamide[69]. It was suggested that the compound which competitively inhibited the action of sulfanilamide was *p*-aminobenzoic acid (PABA) **(Figure 1.24)**, a carboxylic acid of similar structure to sulfanilamide[70]. Hence sulfonamides are enzyme inhibitors. Their action is to inhibit the process of dihydrofolate synthesis on which bacterial growth depends. PABA, with which sulfonamides compete, is a crucial intermediate in the formation of dihydrofolate.

1.5.3 THE IMPORTANCE OF SULFONAMIDES

Sulfonamides were the first group of drug compounds to be widely used as specific antibacterial agents[71]. This discovery spurred a great many new companies willing to research into the scope and limitations of this group of compounds. The popular and authoritative opinion maintains that the entire modern pharmaceutical industry owes much to the discovery of the sulfonamides[71]. It was the development of sulfonamide chemistry that led to the design of evaluated clinical trials and hence the observations on their side effects. Sulfonamide derivatives have other important chemotherapeutic uses, for example some are used as diuretics[72-73], orally-active hypoglycaemic agents[74] and others as carbonic anhydrase inhibitors. The clinical use of sulfonamides laid the foundation for the whole of medicinal chemistry[75-76].

Typical Sulfonamides

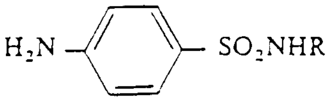

Generic name	R	pK_a	Comments
Sulfaguanidine (9)	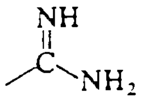	Basic	Poorly absorbed, locally acting, used in gastro-instestinal infections
Sulfathiazole (18)	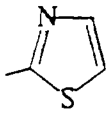	7.25	Well absorbed, rapidly excreted
Sulfacetamide	—COME	5.4	Well absorbed, used in eye infections
Sulfamethoxazole	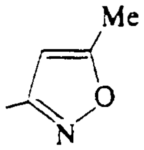	6.0	Well absorbed, moderate excretion
Sulfadiazine	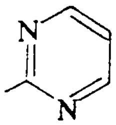	6.52	Well absorbed, moderate excretion
Sulfamethoxine	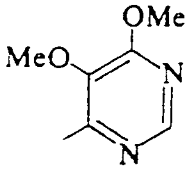	6.1	Well absorbed, slowly excreted, used in dysentery, *etc.*

Figure 1.27 Table of typical sulfonamides listing their structures and properties.

1.5.4 SULFONAMIDE INCLUSION CHEMISTRY

Literature abounds with numerous well-documented studies of polymorphs, solvates, anhydrates and complexes of sulphur-containing drugs.

Specific examples of some of these drugs are

(a) Sulfamethoxydiazine[77-78]

(b) Sulfabenzamides[79]

(c) Sulfaguanidine[79]

(d) Sulfapyridine[79]

(e) Sulfamethoxypyridazine[79]

(f) Sulfamethoxazole[79-80]

The inclusion of 1,4-dioxane, chloroform and tetrahydrofuran in 5-methoxysulfadiazine has been recently investigated[34]. In an attempt to gather more information on the crystallizing properties of the named compound, the study addressed several unresolved questions, including the exact stoichiometric compositions, reasons for the unusually stable solvates and the predominance of the common desolvation product as well as the very nature of solvent inclusion[81-84]. In the light of solvent molecules occupying cavities created by host-host interactions, the solvates were accordingly described as *coordination-assisted clathrates*, (see **Fig.1, C2**) and **Fig.1.28 (a)-(c))**. All three compounds are based on a common isostructural host framework in which the host forms centrosymmetric dimers via a pair of **N-H···N** hydrogen bonds as shown in **Figure 1.28(d)**.

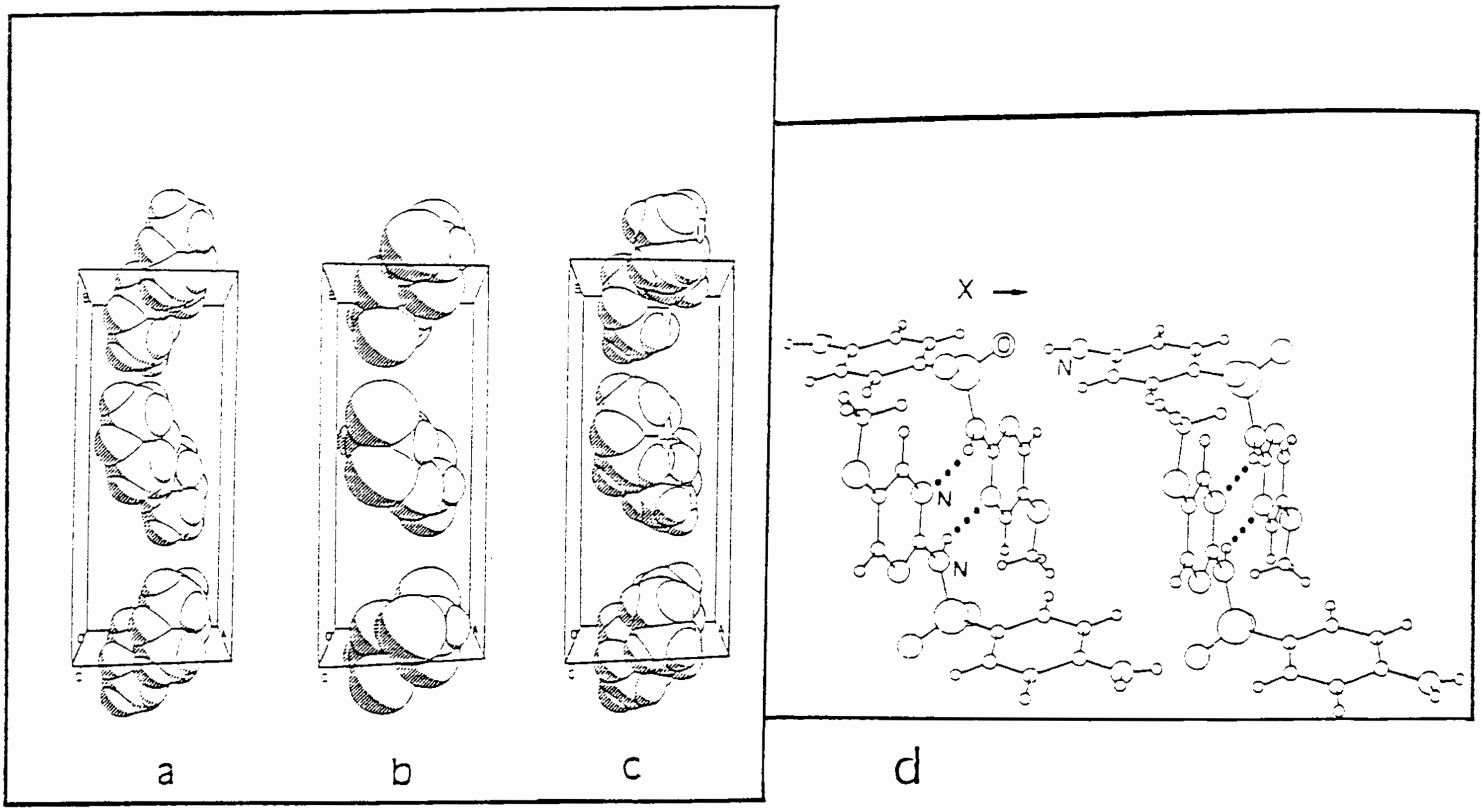

Figure 1.28 (a), (b) and (c) Dioxane, $CHCl_3$ and THF are cavitated within the crystalline framework of 5-methoxysulfadiazine respectively[34].

Figure 1.28 (d) Host dimerization via H-bonding (dotted lines) creates suitable guest cavities[34].

This study represents a typical investigation of the solid-state behaviour of drug substances using X-ray analysis and thermoanalytical methods in line with the overall subject of this project.

1.5.5 SUCCINYLSULFATHIAZOLE AND SULFATHIAZOLE

SUCCINYLSULFATHIAZOLE *[4^1-(2-thiazolylsulfamoyl)succinanilic acid]* (Figure 1.25) is a bacteriostatic that is poorly absorbed and has a long duration of pharmacological action. The latter owes to the slow liberation of the drug during hydrolysis in the bowel[85]. It is reported to exist in six anhydrous forms and three polymorphic monohydrates, (see **Figure 1.29 (a)** and **(b)**) as well as the acetone and n-butanol adducts[86].

Of interest is the crystal structure analysis of the monohydrate[87] indicated as HI in **Figure 1.29 (b)**. It is monoclinic, space group $P2_1/b$, a=16.28(1), b=19.49(1), c=5.143(4)Å with γ=94.10(4)° and Z=4. The structure in **Figure 1.29 (c)** features an interesting network of hydrogen bonds and it gives an idea of the stabilizing role played by water molecules in the system. This information enables a sensible interpretation of the thermodynamic data. For example, abormally high enthalpies (ΔH) and temperatures of desolvation may be explained in terms of the strength of host-guest binding.

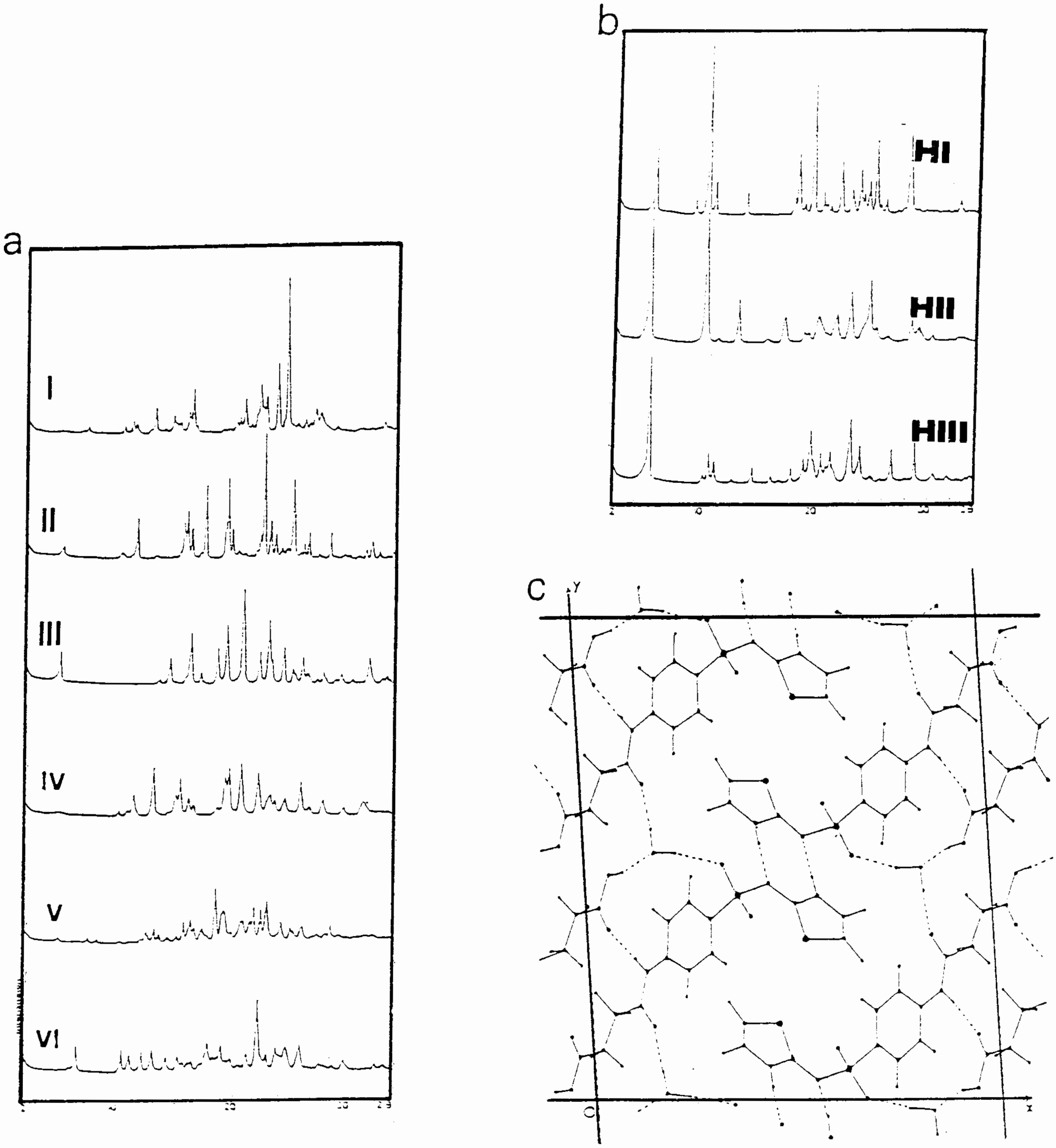

Figure 1.29 X-ray diffractograms of (a) six anhydrous forms, (b) three polymorphic monohydrates[86] and (c) the monohydrate crystal structure[87].

SULFATHIAZOLE ***[4-amino-N-2-thiazolylbenzenesulfonamide]*** **(Figure 1.26)** like succinylsulfathiazole, is also an antimicrobial agent. The complicated polymorphic behaviour of this drug has attracted a number of researchers to focus their attention on it[88-94]. Based on the more recent characterization studies it can now be said that sulfathiazole exists in at least four polymorphic forms[95] designated I, II, III and IV respectively as indicated in **Figure 1.30.** While it was easier to characterize forms I and II by TGA-DSC and XRD techniques, it proved quite difficult to discriminate between forms III and IV by the same techniques. The approach adopted in this project, namely crystallization of solvates, presents another important alternative route to achieving polymorphic modification of solid drug substances.

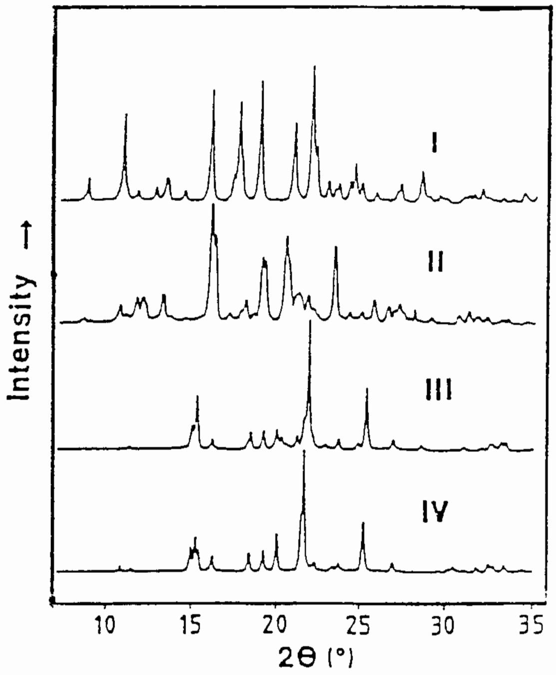

Figure 1.30 XRD patterns of polymorphs I, II, III and IV of sulfathiazole[95].

While the polymorphism of sulfathiazole has been studied in detail, the formation and properties of its solvates have not been discussed in the pharmaceutical literature. Only several research workers aiming to achieve diverse goals such as drug particle size reduction, polymorphic modification and investigation of structure-activity relationships have investigated this compound[96-99]. These studies have had little to do with the clathrate properties of the resulting adducts and hence, not much attempt has been made to hypothesize on the desolvation mechanisms.

REFERENCES

1. J.E.D. Davies, W. Kemula, H.M. Powell, N.O. Smith: *J.Incl.Phenom.,* **1,** 3, (1983).

2. C. Schafhäutl: *J.Prakt.Chem.,* 21, 129, (1841).

3. F. Wohler: *Ann.Chem.Liebigs,* **69,** 297 (1849).

4. A. Villiers: *C. R.Hebd.Sceances Acad.Sci.,* **112,** 536, (1891).

5. K.A. Hofmann, F. Küspert: *Z.Anorg.Allg.Chem.*, **15,** 204, (1897).

6. H. Hartley, N.G. Thomas: *J.Chem.Soc.,* 1013, (1906).

7. R. Spallino, G. Provenzal: *Gazz.Chim.Ital.,* **39,** 325, (1909).

8. A.P.Dianin: *J. Soc.Phys.Chem.Russe.,* **46,** 1310, (1914).

9. H. Wieland, H Sorge: *Z.Phisiol.Chem.Hoppe-Seyler's*, **97,** 1, (1916).

10. M.F. Bengen, German Patent Application, OZ 123438 (March 18, 1940).

11. E. Terres, W. Vollmer: *Z.Petroleum,* **31,** 1, (1935).

12. E. Weber: "Clathrate Chemistry Today - Some Problems and Reflections", in "Topics in Chemistry", **vol.140,** (1987).

13. E. Weber, H.P. Josel: *J.Incl.Phenom.,* **1,** 79, (1983).

14. I. Goldberg, in "Inclusion Compounds": 2, (1984); Atwood, Davies and MacNicol, eds, Academic Press, London, Chap.9, p.261.

15. D.D. MacNicol, J.J. McKendrick, D.R. Wilson: *Chem.Soc.Rev.* **7,** 65, (1978).

16. J.L. Spencer, E.H. Flynn, R.W. Roeske, F.Y.Siu, R.R. Chauvette: *J.Med.Chem.,* **9,** 746, (1966).

17. C.W. Ryan, R.L. Simon, E.M. Van Heyningen: *ibid.,* **12,** 310, (1969).

18. J. Haleblian, W. McCrone: *J.Pharm.Sci.,* **58,** 911, (1969).

19. O. Kennard, D.G. Watson: "Molecular Structures and Dimensions", International Union of Crystallography, **vols 1-8,** (1962-1978).

20. J.R. Clark: *Rev.Pure Appl.Chem.,* **13,** 50, (1963).

21. J. Shell: *Anal.Chem.,* **27,** 1665, (1955).

22. H.A. Rose, R.J. Hinch, W.C. McCrone: *Anal.Chem.,* **25**, 993, (1953).

23. E. Shefter, T. Higuchi: *J.Pharm.Sci.,* **52**, 781, (1963).

24. K. Austin, A.C. Marshall, H.Smith: *Nature (London),* **208**, 999, (1965).

25. J. Chapman, J.Page, A. Parker, D. Rogers, C.J. Sharp, S.E. Staniforth: *J.Pharm.Pharmacol.,* **20**, 418, (1968).

26. I.Himuro, Y.Tsuda, K. Sekiguchi, I. Horikoshi, M. Kanke: *Chem.Pharm.Bull.,* **19**, 1034, (1971).

27. H. Lin: *Diss.Abstr.Int.,* **B31**, 4703B, (1972).

28. L. Borka, P. Kristiansen, K. Backe-Hansen: *Acta Pharm.Suec.,* **9**, 573, (1972).

29. S.R. Byrn: "Solid-State Chemistry of Drugs", Academic Press, (1982).

30. M.R. Caira, R. Mohamed: *Acta Cryst.,* **B49**, 760, (1993).

31. S.A. Botha, M.R. Caira, J.K. Guillory, A.P. Lötter: *J.Pharm.Sci.,* **78**, 28, (1989).

32. S.A. Botha, M.R. Caira, J.K. Guillory, A.P. Lötter: *J.Pharm.Sci.,* **77**, **444**, (1988).

33. M.R. Caira, L.R. Nassimbeni, B. van Oudtshoorn: *J.Pharm.Sci.,* **82**, 1006, (1993).

34. M.R. Caira, R.Mohamed: *Supramolecular Chemistry,* **2**, 201, (1993).

35. F. Vögtle: "Supramolecular Chemistry", John Wiley and Sons, Chichester, (1991).

36. M.R. Caira, V.J. Griffith, L.R. Nassimbeni, B van Oudtshoorn: *J.Incl.Phenom., 17,* 187, (1994).

37. J. Szejtli, "Cyclodextrin Technology", Kluwer Academic Press, Dordrecht, (1988).

38. M. Kuhnert-Brandstatter, "Thermomicroscopy in the Analysis of Pharmaceuticals", Pergamon Press, New York, (1971).

39. B.H. O'Connor, E.N. Maslen: *Acta Cryst.,* **18**, 363, (1965).

40. G. Ghielmetti, T. Bruzzesse, T. Bianchi, F. Recusani: *J.Pharm.Sci.,* **65**, 905, (1976).

41. M. Kuhnert-Brandstatter, P. Gasser: *Microchem.J.,* **16**, 590, (1971).

42. R.P. Bouche, M. Draguet-Brughmans: *J.Pharm.Belg.,* 32, 23, (1977).

43. N.K. Jain, M.N. Mohammedi: *Indian Drugs,* **23**, 315, (1986).

44. S.H. Curry, K.M. Thakker: "Physicochemical Principles", in "Comprehensive Medicinal Chemistry", **vol.5**, 545, (1990).

45. J.J. Gerber, M.R. Caira, A.P. Lötter: *J.Crystallogr.Spectrosc. Res.,* **23**, 863, (1993).

46. J. Dabrowski: *Spectrochim.Acta,* **19**, (1963).

47. J. Dabrowski, U. Dabrowski: *Rocz.Chem.,* **32**, 821, (1958).

48. H.P. Schad: *Helv.Chim.Acta.,* **38**, 1117, (1955).

49. G.O. Dudek, G.P. Volpp: *J.Am.Chem.Soc.,* **85**, 2697, (1963).

50. M. Kuhnert-Brandstatter, F. Proll: *Mikrochim. Acta,* **2**, 463, (1983).

51. S. Niazi: *J.Pharm.Sci.,* **67**, 488, (1978).

52. F. Kozjek, L. Golic, P. Zupet, E. Palka, P. Vodopivec, M. Japelj: *Acta Pharm.Jugosl.,* **35**, 275, (1985).

53. E.G. Salole, F.A. Al-Sarraj: *Drug.Dev.Ind.Pharm.,* **11**, 855, (1985).

54. R.R. Pfeiffer, K.S. Yang, M.J. Tucker: *J.Pharm.Sci.,* **59**, 1809, (1970).

55. P.R. Perrier, S.R. Byrn: *J.Org.Chem.,* **47**, 4671, (1982).

56. A.P. Gray: "Progress in Quantitative Differential Thermal Analysis" in *Amer.Lab.,* **3**, 43, (1971).

57. L. Johnson: PhD Thesis, University of Cape Town, p.101, (1992).

58. F. Rodriguez-Caabeiro, A. Criado-Fornelio, A. Jimenez-Gonzalez, L. Guzman, A. Igual, A. Perez, M. Pujol: *Chemotherapy*, **33**, 266, (1987).

59. G.M. Brown: "The Biosynthesis of Folic Acid. II-Inhibition by Sulphonamides", *Journal of Biological Chemistry,* **237**, 536, (1962).

60. S.R.M. Bushby, G.H. Hitchings: "Trimethoprim, A Sulfonamide Potentiator", *British Journal of Pharmacology and Therapeutics,* **33**, 72, (1968).

61. D.O. Woods "The Biochemical Mode of Action of the Sulfonamide Drugs", *Journal of General Microbiology,* **29**, 687, (1962).

62. G. Domagk: *Dtsch.Med.Wochenschr.,* **61**, 250, (1935).

63. J. Trefouel, F. Nitti, D. Bovet, C.R. Seances: *Soc.Biol.Ses. Fil.,* **120**, 756, (1935).

64. A.D. Welch, C.A. Nichol: *Annu.Rev.Biochem.,* **21**, 633, (1952).

65. D.D. Woods in "Chemistry and Biology of Pteridines", Ciba Foundation Symposium Proceedings, Little, Brown, Boston, 1954, p.220.

66 R.L. Blakley: "The Biochemistry of Folic Acid & Related Pteridines", Ciba Foundation Proceedings, Little, Brown, Boston, 1954, p.220.

67. E. Haslam: "The Shikimate Pathway", Butterworths, London (1974).

68. T. Shiota, M.N. Disraely, M.P. McCann: *J.Biochem.,* **239**, 326, (1964).

69. G.A.H. Buttle, W.H.Grey, D. Stephenson: *Lancet,* **1**, 1286, (1936).

70. D.D. Woods: *Br.J.Exp.Pathol.,* **21**, 74, (1940).

71. P.G. Sammes: "Sulfonamides & Sulfones" in Comprehensive Medicinal Chemistry, **vol.2**, 255, 1990.

72. K.H. Bayer, J.E. Baer: *Pharmacol.Rev.,* **13**, 517, (1961).

73. O.B.T. Nielsen, H. Bruun, C. Bretting, P.W. Feit: *J.Med.Chem.,* **18**, 41, (1975).

74. A. Loubatieres: in "Oral Hypoglycaemic Agents", ed. G.D. Campbell, Academic Press, New York, 1, (1969).

75. T.H. Maren: *Drug.Dev.Res.,* **10**, 255, (1987).

76. P.G. Benedetti, M.C. Menziani, C. Frassinetti: *Quant.Struct.Act.Relat.Pharmacol.Chem.Biol.,* **4**, 23, (1985).

77 M.A. Moustafa, A.R. Ebian, S.A. Khalil, M.M. Motawi: *J.Pharm.Pharmacol.,* **23**, 868, (1971).

78. M.A. Moustafa, S.A. Khalil, A.R. Ebian, M.M. Motawi: *J.Pharm.Pharmacol.,* **24**, 921, (1972).

79. S.S. Yang, J.K. Guillory: *J.Pharm.Sci.,* **61**, 26, 1972.

80. O. Abdallar, S.A. El-Fattah: *Pharm.Ind.,* 970, (1984).

81. J. Rambaud, S. Alberola, H. Grignon, J. Masse, F. Sabon: *Trav.Soc.Pharm.Montpellier,* **34**, 293, (1974).

82. T. Yokoyama, T. Umeda, K. Kuroda, A. Watanabe: *Chem.Pharm.Bull.*, **26**, 1044, (1978).

83. G.P. Bettinetti, F. Giordano, A. La Manna, G. Giuseppetti: *Il Farmaco.Ed.Prat.,* **29**, 493, (1974).

84. A. Burger, R. Ramberger, K. Shulte: *Arch.Pharm.*(Weinheim), **313**, 1020, (1980).

85. R.A.D. Williams, Z.L. Kruk in "The Biochemistry and Pharmacology of Antibacterial Agents", Croom Helm, Biology in Medicine Series, London, p.28, (1981).

86. A. Burger, U.J. Grieber: *Sci.Pharm.,* **57**, 293, (1989).

87. N. Rodier, A. Chauvet, J. Masse: *Acta Cryst.,* **34**, 218, (1978).

88. G. Milosovich: *J.Pharm.Sci.,* **53**, 484, (1964).

89. J.K. Guillory: *J.Pharm.Sci.,* **56**, 72, (1967).

90. W.I. Higuchi, P.D. Bernardo, S.C. Mehta: *J.Pharm.Sci.,* **56**, 200, (1967).

91. L.S. Shenouda: *J.Pharm.Sci.,* **59**, 785, (1970).

92. R.J. Mesley: *J.Pharm.Pharmacol.*, **23**, 687, (1971).

93. G.J. Kruger, G. Gafner: *Acta Cryst.,* **B27**, 326, (1971).

94. G.J. Kruger, G. Gafner: *Acta Cryst.,* **B28**, 272, (1972).

95. A. Jamshed, S.E. Tarling, P. Barnes: *J.Pharm.Sci.,* **78**, 337, (1989).

96. K. Shirotani, E. Suzuki, K. Sekiguchi: *Chem.Pharm.Bull.,* **31**, 2085, (1983).

97. F.V. Babilev, V.K. Bel'skii, A.Yu Simonov: *Khim-Farm.Zh.,* 21(9), 1143, (1987).

98. M.C. Meyer, D.E. Guttman: *J.Pharm.Sci.,* **57**, 898, (1968).

99. E. Shefter, P.Sackman: *J.Pharm.Sci.,* **60**, 282, (1971).

CHAPTER 2

SUBCONTENTS

THE MAIN OBJECTIVES AND SCOPE OF THIS WORK

The pharmaceutical industry is constantly seeking ways and means of developing safer and more effective solid drug products. In the course of attempting to fulfil this global objective, the skills and expertise of well-trained solid-state chemists become indispensable.

The broad areas of physical and industrial pharmacy encompass powder technology and drug formulation which require astute knowledge about the stability of solids, kinetics of solid-state reactions and other molecular details. It is on that basis that in this project an attempt is made, so to say, of building a comprehensive architecture of facts and findings about the solid-state behaviour of two antimicrobials, namely succinylsulfathiazole and sulfathiazole. The four basic routes followed are:-

- solvate-formation by recrystallization from suitable solvents,
- structure analysis by X-ray diffraction and correlation with thermodynamic data,
- desolvation mechanisms and kinetics thereof, and
- identification of the resulting polymorphs.

2.1 RECRYSTALLIZATION FROM SUITABLE SOLVENTS

A wide range of common and readily available organic solvents were chosen based on their chain or aromatic structures, donor-acceptor electronic properties and bulky substituents which are likely to influence crystal packing.

In a series of experiments hereinafter CLASS A, **SST** (see glossary) was recrystallized from 1-butanol, 1-pentanol and 1,4-dioxane. In another series (CLASS B), **ST** was recrystallized from pyridine, 2-methylpyridine (α-picoline), 4-methylpyridine (γ-picoline), 3-methylpyridine (ß-picoline) and 2,6-dimethylpyridine (2,6 lutidine) with the crystallizing conditions well-recorded. These crystallizations were performed with the view to detect the existence of trends in the inclusion behaviour of the two drugs. The properties of solvents used and their chemical formulae are shown in **Figure 2.1**.

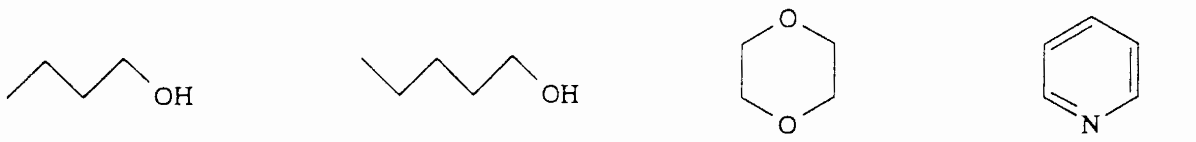

n-butanol
b.p. 118°C

n-pentanol
b.p. 133-139°C

1,4-dioxane
b.p. 101.1°C

pyridine
b.p. 115.2-115.3°C
pKa 5.19

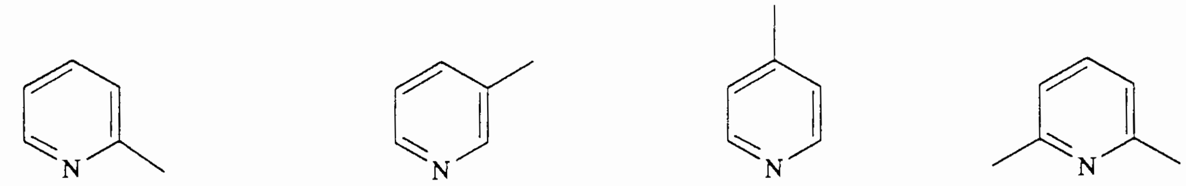

2-methylpyridine
(α-picoline)
b.p. 128-129°C
pKa 5.97

3-methylpyridine
(β-picoline)
b.p. 143-144°C
pKa 5.68

4-methylpyridine
(γ-picoline)
b.p. 145°C
pKa 6.02

2,6-dimethylpyridine
(2,6-lutidine)
b.p. 144°C

Note:- Physical constants were obtained from standard texts[100-102].

Figure 2.1 Structural formulae of organic solvents used in recrystallization experiments.

2.2 DETERMINATION OF STOICHIOMETRIC COMPOSITIONS

In the light of conflicting reports about the stoichiometry of the 1-butanol solvate of succinylsulfathiazole[86], it was decided to solve the crystal structures of all solvates crystallized and determine the host-guest ratios by thermal gravimetry, microanalysis and structure determination.

2.3 THE TOPOLOGY OF SOLVENT INCLUSION

The investigation of crystal packing modes, channel versus cavity occupation of solvents as well as the role of hydrogen bonding interactions between host and guest molecules was facilitated by X-ray diffraction studies.

2.4 CONFORMATIONS OF HOST MOLECULES

The analysis of torsion angles and molecular planes enabled the identification of the preferred conformational states of the drug molecules in the solid state.

2.5 DESOLVATION REACTIONS INVESTIGATED

Dynamic TGA was of great utility in the study of the desolvation processes. The kinetic and thermodynamic data obtained were then correlated with structural results.

2.6 IDENTIFICATION OF POLYMORPHS

Temperature-mediated desolvation was the route to achieving different polymorphic products. Subsequent to desorption, XRD patterns and melting point determinations (DSC) were used to identify the resulting polymorphs.

2.7 SELECTIVITY

Industrial separation processes do sometimes involve clathrates in the separation of close structural isomers[103]. Without detracting from the main theme of pseudopolymorphism, an attempt was made to ascertain the selective inclusion of 1-butanol versus 1-pentanol by succinylsulfathiazole. Recrystallization from mixtures followed by a series of GLC experiments were performed in order to investigate this phenomenon.

REFERENCES

100. C.W. Weast, M.J. Astel, W.H. Beyer: "CRC Handbook of Chemistry and Physics", 66th Edition, CRC Press, (1985-1986).

101. G.W.C. Kaye, T.H. Laby: "Tables of Physical and Chemical Constants and some Mathematical Functions", 14th Edition, Longman London and New York, 1973.

102. R.H. Perry, D Green: "Perry's Chemical Engineers' Handbook", McGraw-Hill International Editions, Chemical Engineering Series, 6th Edition, 1988.

103. S.A. Bourne, L.R. Nassimbeni, K. Skobridis: *J. Chem. Soc., Chem. Commun.* 282 (1991).

CHAPTER 3

SUBCONTENTS

3 EXPERIMENTAL PROCEDURES

3. EXPERIMENTAL PROCEDURES

3.1 CHARACTERIZATION OF SSTHYD AND ST

The raw materials were purchased as Sigma product S-8752 Lot 109F0017 for monohydrate **SSTHYD** and ALDRICH DY Lot 01208CY for anhydrous **ST**. In each case approximately 200mg of compound were weighed into a clean glass vial and reserved for preliminary characterizations by the methods to be discussed shortly.

3.2 PREPARATION OF HOST COMPOUND - SSTANHYD

Since the commercial product is a monohydrate, the host compound was obtained by dehydration. 500mg were weighed using a Mettler PE360 electronic balance and heated in an oven for *ca* 17 hours. at 105 °C
To ensure a complete and efficient dehydration, a further drying step was carried out in a vacuum drier Büchi TO-51 linked to a vacuum pump for *ca* 5 hours. The compound was then stored in a sealed glass vial to prevent absorption of atmospheric water vapour. It was important to fully dehydrate **SSTHYD** before carrying out the recrystallization experiments from organic solvents.
This is in order to avoid possible formation of ternary species.

3.3 PREPARATION OF SOLVATES

3.3.1 Crystal Growth

1-Butanol and 1-pentanol solvates were crystallized by slow cooling. In both cases 200mg of host compound were dissolved in *ca* 40 ml of solvent slowly added with vigorous stirring and gentle heating on a IKA-KOMBIMAG RCH hot plate.

The solutions were then heated to just below the b.p.'s of 1-butanol and 1-pentanol (118°C and 133-139°C)[120] respectively. After the solutions became clear, indicating complete dissolution, several drops of solvent were added to reduce the level of supersaturation. On the other hand **ST** (*ca* 2.4g in 100 ml of pyridine) required more vigorous stirring at the boiling points of pyridine solvents i.e. 101.1-144°C[100]. It was noted that the drug became highly soluble in substituted pyridines requiring 9.0g in 100 ml of solvent, almost four times the mass required to dissolve in the unsubstituted pyridine. In 2-methylpyridine 14.2g of **ST** were consumed per 100 ml of solvent.

In each case, the solution was filtered using a syringe and a 0.45μm MILLEX-LCR filter unit to remove dust particles and other insoluble impurities likely to affect the crystallization process. Upon standing for *ca* 24 hours in water initially at 100°C in a Dewar flask, high quality crystals precipitated.

Only the 1,4-dioxane solvate of **SST** defied this procedure, in which case the slow evaporation method was adopted[104].

3.3.2 MICROANALYSES

Despite the technical difficulties associated with determining microanalytical compositions of solvated substances, especially volatile host-guest compounds, the solvates were still submitted for this purpose. An instrument EA 1108 Elementar Analyser, Model CHNS-O[105] was used to ascertain the microanalytical compositions of raw materials and solvates. About 10 mg samples were weighed and analysed for C,H,N and S content.

3.3.3 DENSITY MEASUREMENTS

Clear and prismatic crystals were suspended in a mixture of saturated aqueous KI solution and de-ionized water. The advantage of fairly stable compounds was evident in the highly reproducible density measurements using an Anton Paar digital DMA 35 density meter. Quadruplicate determinations were obtained for each compound.

3.4 THERMOANALYTICAL CHARACTERIZATIONS

3.4.1 Thermomicroscopy

The behaviour of crystals upon heating could be observed visually by placing several good clear crystals on a Linkam Hotstage TH 600 coupled to a Linkam CO 600 Controller. Slowly increasing the temperature at a constant rate enabled the guest crystals and the melting of the polymorphs to be observed.

Subtle changes in the appearance of the crystals were photographed using a built-in Nikon Microflex AFX-II Photomicrographic attachment.

3.4.2 Stability Tests

The solvates were dabbed dry and then left standing at room temperature. After *ca* 2 hours, crystals of some of the solvates went opaque and showed obvious signs of deterioration. Stable crystals yielded high quality crystal data during X-ray intensity-data collection without too many problems.

3.4.3 TGA and DSC

The samples, *ca* 10 mg, were dabbed dry, crushed to roughly homogeneous particle sizes and then placed in a platinum bucket which was heated at a rate of 10°C/min from 30-250°C under constant positive N_2 flow. The experiment was conducted on a Perkin-Elmer PC7-Series consisting of a PE TGA7 Thermogravimetric Analyser automated by an Epson PCAX2 computer and a Hewlett-Packard Color Proplotter. Instrument calibration was performed according to the method described in references 106-107.

Differential Scanning Calorimetric measurements were performed on a Perkin-Elmer PC7-Series with a similar set-up to TGA. Samples *ca* 10 mg were weighed on a Sartorius Microbalance 1802 and then sealed in a vented aluminium pan using a Perkin Elmer Universal Sealing Press. A heating rate of 10°C/min was maintained throughout between 30 and 250°C. Instrument calibration was performed every day according to the procedure detailed in the relevant literature [108].

3.5 KINETICS OF DESORPTION BY DYNAMIC TGA

Samples were dabbed dry to remove surface solvent and then crushed to achieve nearly homogeneous particle sizes. They were then placed in a platinum pan as described in **section 3.4.3** above. Each time *ca* 10 mg samples were weighed as the method is affected by serious inconsistencies in particle geometry and sample size. Samples were sieved (< 100 μm) in order to achieve homogeneity in particle size. Four to five TGA measurements were done consecutively in the range of heating rates between 1 and 25°C/min.

3.6 X-RAY POWDER DIFFRACTION TECHNIQUES

The solvates were dried to remove surface solvent and then crushed into fine powder. They were then packed compactly in aluminium sample trays.

Using a Philips vertical goniometer PW 1050/80 with a Philips PW 1394 motor control and PW 1390 channel control, samples were step-scanned for 4 seconds every 0.01° 2Θ over the range $6^\circ \leq 2\Theta \leq 40^\circ$. Sensitivity range used was 1×10^4 - 4×10^4 counts/sec.

X-rays were generated by a Philips PW 1130/90 model generator at 30 mA and 40 kV. Nickel-filtered copper radiation, (CuKα, λ = 1.5418Å) was used with divergence and receiving slits of 1° each.

3.7 SINGLE CRYSTAL X-RAY DIFFRACTION

High quality single crystals were selected on the basis of uniform extinction of plane polarized light when they were examined under the optical microscope.

They were then cut to a nearly equant shape and size before they were lodged into a 0.3 or 0.5 mm Lindemann capillary tube containing mother liquor. To avoid the drying up of mother liquor the tube was sealed with wax at both ends and then it was attached to a brass pin ready for data collection.

Data were collected at 294K using an Enraf-Nonius CAD4 diffractometer with graphite-monochromated MoKα radiation (λ=0.7107Å) generated by a Philips PW 1730 model operating at ~~20~~30mA, 50kV. Accurate unit cell parameters were obtained by least-squares analysis of 24 reflections measured in the range $16^\circ < \Theta < 17^\circ$. More details of data collections appear in tables **7a** and **13a**. During data collection, three standard reflections were measured every 3600s to monitor the crystal stability and orientation control was performed every 200 reflections.

Lorentz-polarization and absorption corrections were applied to all the data collections. For some crystals, corrections for crystal decay were applied to the data (see tables 7a and 13a).

3.8 COMPUTATIONS

3.8.1 Computations for SST solvates

Only a general description of computations and programs used is outlined in this section. In view of the limited number of common programs that were invoked in solving the structures of **SST** solvates, it was decided to incorporate all the computational details pertaining to this series of compounds in this section.
On the other hand, the complications that were encountered with polar space groups in the **ST** series of compounds meant that different programs should be invoked in dealing with these compounds. Thus, it was decided to treat the details of computations for this series independently in **CHAPTER** 13.

All computations were performed using a remote VAX-VMS computer at the Computer Centre of the University of Cape Town. Most structures were solved by Patterson and Fourier methods using the program SHELX 76[109] except for the structures of the compounds **STPY1** and **STPY** which were solved by direct methods using the program SHELX 86[110]. The refinements were carried out using a program system which uses atomic radii calculated by Pauling[111]. Complex neutral atom scattering factors for non-hydrogen atoms were those of Cromer and Mann[112], those of hydrogen atoms were taken from Stewart *et al*[113]. Dispersion corrections were taken from Cromer and Liberman[114]. Agreement between the observed (F_O) and calculated (F_C) structure factors is expressed in terms of the residual factor, R, which is defined as:-

$$R = \frac{\Sigma \left| |F_o| - |F_c| \right|}{\Sigma |F_o|}$$

$$= \frac{\Sigma |\Delta F|}{\Sigma |F_o|}$$

Alternatively, the weighted residual factor, R_W is used,

$$R_W = \frac{\Sigma w^{\frac{1}{2}} |\Delta F|}{\Sigma w^{\frac{1}{2}} |F_o|}$$

$$\text{where } w = \frac{1}{\sigma^2(F_o) + gF_o^2}$$

In cases where it is necessary to discriminate between absolute structures, the generalized residual factor R_G is used for the application of the Hamilton test.

$$R_G = \frac{R_W |\Delta F|^2}{\Sigma |F_o|^2}$$

For **SSTPE** and **SSTDI**, a 3-dimensional Patterson map was computed and interpreted in terms of the space group $P\bar{1}$, since intensity statistics indicated the presence of a centre of symmetry. The positions of both sulphur atoms of the **SST** molecule were obtained from the map and these positions were used as the initial phasing model. The remaining atoms were located from the subsequent difference Fourier maps.

The close similarity between the unit cell parameters of **SSTBU** and **SSTPE**, both occurring in space group $P\bar{1}$, suggested that these structures were very closely related. As a trial model for **SSTBU**, the non-hydrogen atoms of the **SST** molecule obtained from the **SSTPE** crystal structure analysis were successfully used. For structure refinement, the least-squares technique was used in which $\Sigma w\|F_o| - |F_c\|^2$ was minimised and weights were chosen to give an even distribution of $\Sigma w(\Delta F)^2$ with $(\sin\Theta/\lambda)$ and $(F_O/F_{max})^{\frac{1}{2}}$. Hydrogen atoms were located from difference Fourier maps. Most of them were added in idealized positions in a riding model with different isotropic temperature factors for different groups of atoms. Non-hydrogen atoms were treated anisotropically. For **SSTPE** and **SSTBU** anomalous distances between some atoms of the included solvent molecules were observed on refinement, indicating some degree of disorder.

Suitable bond length constraints were applied to the C-C and C-O bond distances as 1.50Å (σ=0.002Å) and 1.40Å (σ=0.002Å) respectively.

For **SSTDI** possible disorder for one of the dioxane molecules was evident but no attempt was made to model this phenomenon. Details of intensity-data collections and refinements are listed in Table 7a.

For the geometrical molecular parameters, calculations were performed using the program PARST [115]. The IBM PC version of the program PLUTO[116] was used to produce the crystal and molecular packing diagrams.

Investigation of channels and cavities in crystals was conducted using program MOLMAP[117]. Input to this program consists of atomic coordinates, unit cell data, and space group data. Atoms are assigned van der Waals radii[118] and the program displays the intersections of the atoms with any desired section of the unit cell. If guest atoms are omitted from the input, occupation by the host molecules alone is revealed, allowing visualisation of channels or voids created by the host molecules.

Simulated X-ray powder patterns were computed using program LAZY PULVERIX[119] which requires the same input as described above for MOLMAP. Patterns were computed for CuKα-radiation (λ=1.5418Å) in the Θ-range 6°-40°.

3.9 SELECTIVITY EXPERIMENTS BY GLC

Varying mixtures of 1-butanol and 1-pentanol solutions were prepared in the range (0.0-1.0) mole fractions, x_b for 1-butanol and x_p for 1-pentanol.
This was followed by recrystallization of SST from these mixtures yielding crystals by the usual 24-hour slow cooling process. Crystals were then isolated from their mother liquors, dabbed dry and then transferred into tiny bottles followed by sealing with septum-containing lids. The bottles with their contents were then placed on a heating metal block at 145°C, for about one minute taking into account the independent desolvation temperatures of **SSTBU** and **SSTPE**. The condensed product of desorption was then withdrawn by means of a 5μl syringe and mixed with 25μl of methanol which was found to be a suitable calibration standard. After thorough mixing, this solution was then injected into the GLC column at 170°C. The instrument and column conditions were as follows:-

A Philips Pye Unicam PU 4500 Chromatograph equipped with a PM 8251 Single Pen Recorder was used in this experiment.

A 1.5m x 4 mm glass column was loaded with a 10% $^{w}/w$ stationary phase prepared by dissolving 9g of CHROMSORB$^{(R)}$-103 mixed with 1g of 20M CARBOWAX in chloroform. The dry mixture, having been rotavaped for six hours to expel all the chloroform, was packed into the glass column by means of suction and electric vibration to achieve uniform packing.

In order to optimize the flow-rate of gases the column (at 170°C) was flushed with N_2 at 30ml/min, H_2 at 33ml/min and synthetic medical air at 300ml/min for a few days. A number of trial runs on the GLC were tested while varying either the column temperature or N_2 flow-rate until consistent retention times were obtained for the 1-butanol and 1-pentanol chromatographic peaks.

REFERENCES

104. J.D. Wright in "Molecular Crystals": Cambridge University Press, Cambridge, (1987).

105. Instruction Manual EA 1108 Elementar Analyser, Fisons Instruments.

106. W.W.M. Wendlandt: *Analytica Chimica Acta,* **27**, 309, (1962).

107. W.W.M. Wendlandt, P.J. Elving, J.D. Winefordner, I.M. Kolthoff: *Chemical Analysis,* **vol 19**, Wiley Intersciences Publishers, N.Y.

108. "Operators' Manual", Du Pont Instruments, *Differential Scanning Calorimeter* 910, Du Pont Co., Instrument Systems, Wilmington, (1985).

109. G.M. Sheldrick: SHELX-76 Program for Crystal Structure Determination, University of Cambridge, Cambridge, England, (1976).

110. G.M. Sheldrick in "Crystallographic Computing 3", G.M. Sheldrick, C.Kruger and R. Goddard (Eds), Oxford University Press, 175, (1985).

111. L. Pauling in "The Nature of the Chemical Bond", Cornell University Press, Ithaca, New York (1965).

112. D.T. Cromer, J.B. Mann: *Acta Cryst.,* **A24**, 321, (1986).

113. R.F. Stewart, E.R. Davidson, W.T. Simpson: *J.Chem.Soc.*, **42**, 3175, (1965).

114. D.T. Cromer, D. Liberman: *J.Chem.Soc.*, **53**, 1891, (1970).

115. M. Nardelli, *Comput.Chem.,* **7**, 95, (1983).

116. W.D.S. Motherwell in "PLUTO and PLUTO-programs for plotting molecular and crystal structures", Cambridge University, England, unpublished. Modified by E.J. Dodson and G.D. Smith, further modified by N. Webster and E.J. Gabe, NRC, Canada, 1985.

117. L.J. Barbour: MOLMAP Program (unpublished), University of Cape Town.

118. R.C. Weast: Handbook of Chemistry and Physics, 55th Edition, CRC Press, Inc., (1974).

119. K. Yvon, W. Jeitschko, E. Parthe: *J.Appl. Cryst.,* **10**, 73, (1977).

CHAPTER 4

PRELIMINARY RESULTS OF INCLUSION
(SST AND ST COMPOUNDS)

SUBCONTENTS

4.1 THERMOMICROSCOPY AND CRYSTAL STABILITIES

4.1.1 GENERAL COMMENT

The commonly observed feature in most host-guest compounds, drug inclusion compounds included, is that of volatility. The process of guest release sometimes occurs at room temperature and under other mild conditions. This is often accompanied by visually obvious symptoms of crystal deterioration such as crystals turning opaque in a matter of seconds. Therefore preliminary investigations of H:G ratios and crystal stabilities are conducted on crystals in order to ensure that the subsequent quantitative characterization measurements can be performed safely to yield reliable results.

4.1.2 CRYSTAL STABILITIES

The compounds **SSTDI**, **SSTBU** and **SSTPE** were found to be fairly stable and hence amenable to investigation by TGA-DSC and X-ray diffraction techniques. The crystals of **SSTBU** and **SSTPE** remained solvated for *ca* 2 hours upon standing in ordinary room atmosphere~~s~~. On the other hand, the crystals of **SSTDI** started showing obvious signs of deterioration after *ca* 1 hour upon standing. Deterioration was characterized by a transformation from clear and prismatic crystallinity to plain opacity. It was found that defect sites such as chipped corners quickened the deterioration process.

The compounds of **ST** did not show comparable crystal stabilities. They survived ambient temperatures for only about 15 to 20 minutes. **STPY** was the most stable of them all, taking about 20 minutes to undergo decomposition.

Crystal developing opacity at 110°C

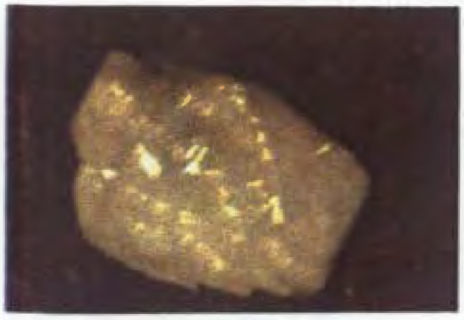

After the two-step loss of solvent at 121.1°C and 169°C respectively

Pure polymorph having melted at 201°C

Figure 4.1 (a) The crystal appearance (morphology) of SSTDI at various stages of a carefully-controlled heating process.

4.1.3 HOTSTAGE THERMOMICROSCOPY

Thermomicroscopy is a powerful visual means of observing thermal events with subtle changes being recorded as guest components are escaping.

In the case of the raw powder materials, **SSTHYD, SSTANHYD** and **ST,** wide melting temperature ranges were confirmed as according to the literature reports[86,95,120].

In the case of solvates, vigorous bubbling was noted as a confirmatory sign of the process of guest release, followed by rupturing and ultimately, the melting of the crystal as the temperature was slowly increased.

The case of **SSTDI** was a particularly interesting one. A clear prismatic crystal was mounted on the hostage and heated very slowly. The sharp edges of the crystal started developing opacity at about 110°C (see **Figure** 4.1 (a)) and it stayed opaque up to about 140°C. Thereafter, at 155°C more bubbling took place as evidence of the second guest release. The melting of the pure form (polymorph) of **SSTDI** took place at 201°C. From this observation a two-step loss of solvent was inferred.

The evidence of guest release for **SSTBU** and **SSTPE** was observed only at about 110°C and 120°C respectively, thus indicating a one-step decomposition.

Similarly all the compounds of **ST** indicated a one-step desolvation process at appropriate temperatures (see Tables **11.4.1** and **11.4.2** later).

It was possible to conclude at least two things from these observations namely:

(1) Whether or not inclusion had taken place,

and

(2) Whether a two-step or a single-step mechanism had been followed.

4.2 CRYSTAL DENSITIES

The molar masses and host:guest ratios, were determinable from measurements of crystal densities using the following equation:

$$Z_hM_h + Z_gM_g = D_mVN_A$$

where;

Z_h : number of host molecules per unit cell

Z_g : number of guest molecules per unit cell

M_h : molecular mass of host

M_g : molecular mass of guest

D_m : the measured (experimental) crystal density

V : the crystallographically-determined unit cell volume

N_A : 6.0220×10^{23} mol^{-1} Avogadro constant, Z_h and Z_g are integral values from which the prediction of H:G ratios is often possible.

Table 4.2.1 Tabulation of Measured and Calculated Densities

COMPOUND	D_m (gcm^{-3})	D_c (gcm^{-3})	H:G	V/Å^3
SSTDI	1.51(1)	1.498	1:1.0	978.0(6)
SSTBU	1.36(3)	1.302	1:1.0	1050(5)
SSTPE	1.37(1)	1.311	1:1.0	1077.9(3)
STPY	1.42(5)	1.423	1:0.98	1560(1)
STPY1	1.36(1)	1.361	1:0.99	1701.0(5)
STPY2	1.35(2)	1.350	1:0.99	1714(5)
STPY2	1.33(3)	1.366	1:0.94	3566(3)

Apparently, as indicated in **Table 4.2.1** there exists a close agreement between calculated and measured densities. This is an indication that compounds do not volatilize upon flotation in $H_2O/KI^{sat'd}$ solution, thus confirming the thermomicroscopic evidence that **SSTDI**, **SSTBU**, **SSTPE** and **ST** compounds are relatively stable. Furthermore, these density measurements also shed light on the stoichiometric compositions of the solvates.

4.3 MICROANALYSES

In principle, a close agreement between calculated (expected) and experimental %C, %H, %N, %S should be obtained. While it was easier to obtain reproducible microanalytical results for the raw drug materials **SSTHYD**, **SSTANHYD** and **ST**, it took many repeated experimental runs to obtain consistent results for solvated materials.

The reason for this was attributed to the unduly long periods between removal of crystals from mother liquor and the actual performance of the experiment which led to possible decompositions prior to the experiment being conducted.

Nevertheless, the results of microanalysis (see **Table 4.3.1**) still confirmed the 1:1 H:G inclusion, thus, complementing the TGA and density results.

Table 4.3.1 Tabulation of Microanalytical Results

CODE NAME	%C	%H	%N	%S	%O (by diff.)
SSTHYD					
calc.	41.8	4.1	11.3	19.1	23.7
obs.	42.0	4.2	11.5	18.8	23.5
SSTANHYD					
calc.	43.9	3.7	11.8	17.1	23.5
obs.	43.9	3.8	12.3	17.3	22.7
SSTDI					
calc.	46.0	4.7	25.3	9.5	14.5
obs.	45.8	4.9	24.9	9.2	15.2
SSTBU					
calc.	47.5	5.4	23.4	14.9	8.8
obs.	46.9	5.2	23.4	14.8	9.7
SSTPE					
calc.	46.4	5.8	21.4	14.2	12.2
obs.	44.9	4.8	20.1	13.3	16.9
STPY					
calc.	50.2	4.2	16.7	19.1	9.8
obs.	50.6	4.2	16.9	19.3	9.0
STPY1					
calc.	51.7	4.3	16.1	18.4	9.5
obs.	52.0	4.6	16.2	18.1	9.1
STPY2					
calc.	51.7	4.3	16.1	18.4	9.5
obs.	52.0	4.6	16.2	18.3	8.9
STPY26					
calc.	53.0	5.0	15.4	17.7	8.9
obs.	53.0	4.9	15.3	17.2	9.6

REFERENCES

120. "The Merck Index", Centennial Edition, 11th Edition, (1989).

CLASS A

(SUCCINYLSULFATHIAZOLE SOLVATES)

CHAPTER 5

SUBCONTENTS

5.1 THERMOANALYTICAL METHODS (TGA-DSC)

5.1.1 GENERAL COMMENT

Thermogravimetry (TG) and Differential Scanning Calorimetry (DSC) offer a complementary advantage of studying the physical properties of a substance as a function of temperature. The TGA-DSC dual measurements yield crucial information about mass, temperature, thermal energies and phase transformations. These data serve as a useful probe in interpreting inclusion behaviour since they are collected under the same thermal conditions. No attempt will be made to give detailed theoretical background on these techniques, but only the superficial theory is explained and the rest is left to the reader to consult authoritative sources[106-108].

5.1.2 THERMOGRAVIMETRIC ANALYSIS

TGA involves heating a sample at a predetermined linear heating rate and plotting the weight change as a function of temperature.

A thermobalance is a combination of a suitable electronic microbalance with a furnace and a temperature programmer. Typically, a maximum load of 1g with a sensitivity of 1 μg is required.

Depending on the heating rate, the geometry of the system and gases flowing through it, there is usually a temperature lag T_f-T_s between the temperature of the sample, T_s, and that of the furnace, T_f. This lag can sometimes be as high as 30°C. Proper calibration of the system is required in order to minimise this effect.

5.1.3 THE TGA EXPERIMENTS

The TGA experiment consists of an open system in which a sample is placed in a platinum pan and suspended from the balance **(Fig. 5.1.3 a)**. The system is then purged with a continuous stream of dry N_2 gas in order to flush out the gaseous products likely to affect the results and to avoid condensation of such gaseous products. Furthermore, the continuous N_2 purge provides a cooling mechanism for the thermobalance. As indicated in Fig. 5.1.3 b), a multi-step thermal degradation profile of $CuSO_4.5H_2O$ yields the stoichiometry of the reaction[121].

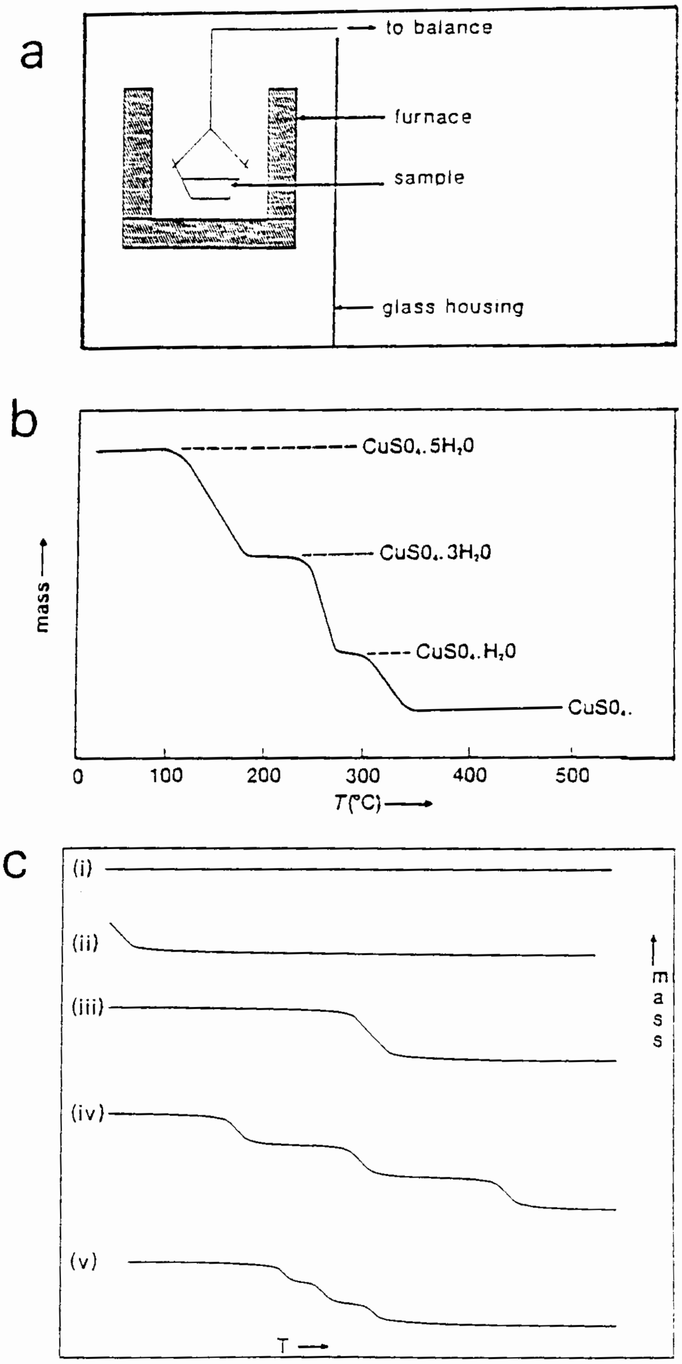

Figure 5.1.3 (a) Simple sketch of the TGA sample in the furnace[122].
(b) TG multi-step thermal degradation profile of $CuSO_4.5H_2O$[121].
(c) Different types of TG curves[124].

On the other hand, non-stoichiometric TG curves are also common, for example **(Fig. 5.1.3 c)** gives a listing of several main TG curve types as follows:-

(i) sample does not decompose.

(ii) desorption of surface solvent only (drying).

(iii) a one-step decomposition e.g. $CaCO_3 \rightarrow CaO + CO_2\uparrow$

(vi) multi-step decomposition with stable intermediates yielding stoichiometric information, e.g.

$NiX_2B_4 \rightarrow NiX_2B_2 \rightarrow NiX_2$

where X = (NCS-), B = (C_7H_7N) with $CHCl_3$ as guest[123].

(v) multi-step decomposition in which unstable intermediates are formed. This case is often difficult to analyse and it requires the heating rate to be decreased.

5.2 DIFFERENTIAL SCANNING CALORIMETRY

In Differential Scanning Calorimetry (DSC), the sample and reference are maintained at the same temperature where $\Delta T = T_s - T_f = 0$; T_s and T_f represent sample and furnace temperatures respectively. The energy difference in the independent supplies to sample and reference are recorded against temperature. The area under the curve is proportional to the enthalpy change.

$$\Delta H = \frac{\text{Area x K}}{\text{mass of sample}}$$

K is the calibration factor, fixed for DSC but temperature-dependent for Differential Thermal Analysis (DTA).

The instrument used in this project was the Perkin-Elmer DSC7 which operates on the principle that the energy absorbed or evolved by the sample is compensated by adding or subtracting an equivalent amount of energy to a heater that is located in the sample holder. Any detectable thermal event such as loss of guest component is manifested as deviation from the baseline. Such deviation makes the direct measurement of power in milliwatts possible from peak areas.

By convention, peaks appearing above the DSC baseline are taken to represent *endothermic* events, whereas *exothermic* events are evident from peaks occurring below the baseline **(Fig. 5.2 a)**.

By the same token as in TGA, the multi-step thermal decomposition of $CuSO_4.5H_2O$ is shown in **(Fig. 5.2 b)** measured in terms of the DSC technique.

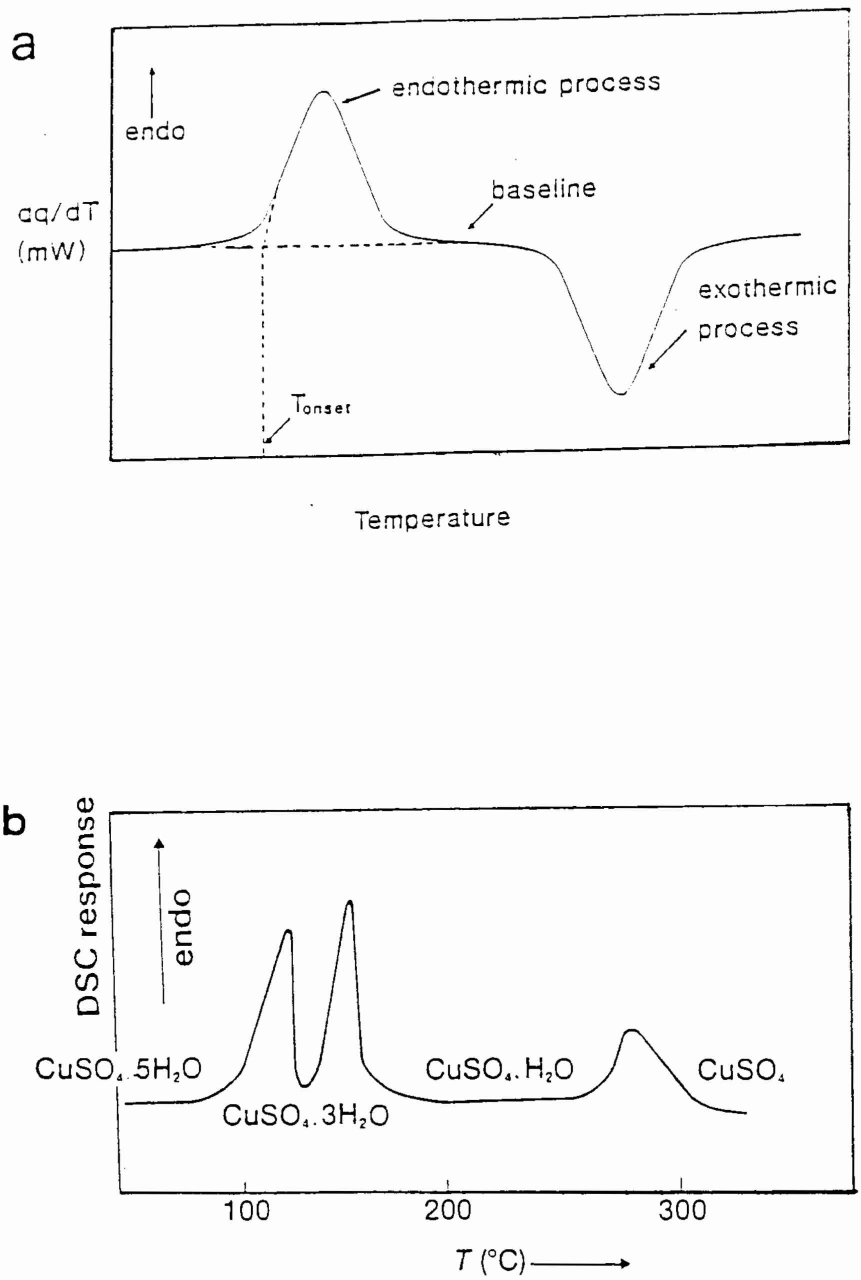

Figure 5.2 (a) Sketch of a typical DSC curve with its main features[125].
(b) DSC thermogram of $CuSO_4.5H_2O$ representing its thermal decomposition[122].

5.2.1 THE DSC EXPERIMENTS

In DSC, samples were heated at a predetermined heating rate of 10°C/min and the sample temperature compared with the reference temperature as a function of increasing furnace temperature. The drying and crushing of samples were the same as for TGA, after which samples were sealed in vented aluminium pans. An empty pan was used as a reference. Samples were run with continuous N_2 purge in order to get rid of unwanted vapours.

Of utmost importance in the DSC experiments was the maintenance of a stable baseline which was run under the same thermal conditions as those of actual samples. Typically, TGA and DSC thermograms were plotted on the same temperature axes for each compound in order to facilitate the complementary study of thermal behaviour.

5.3 TGA-DSC THERMOGRAMS OF THE COMPOUNDS STUDIED

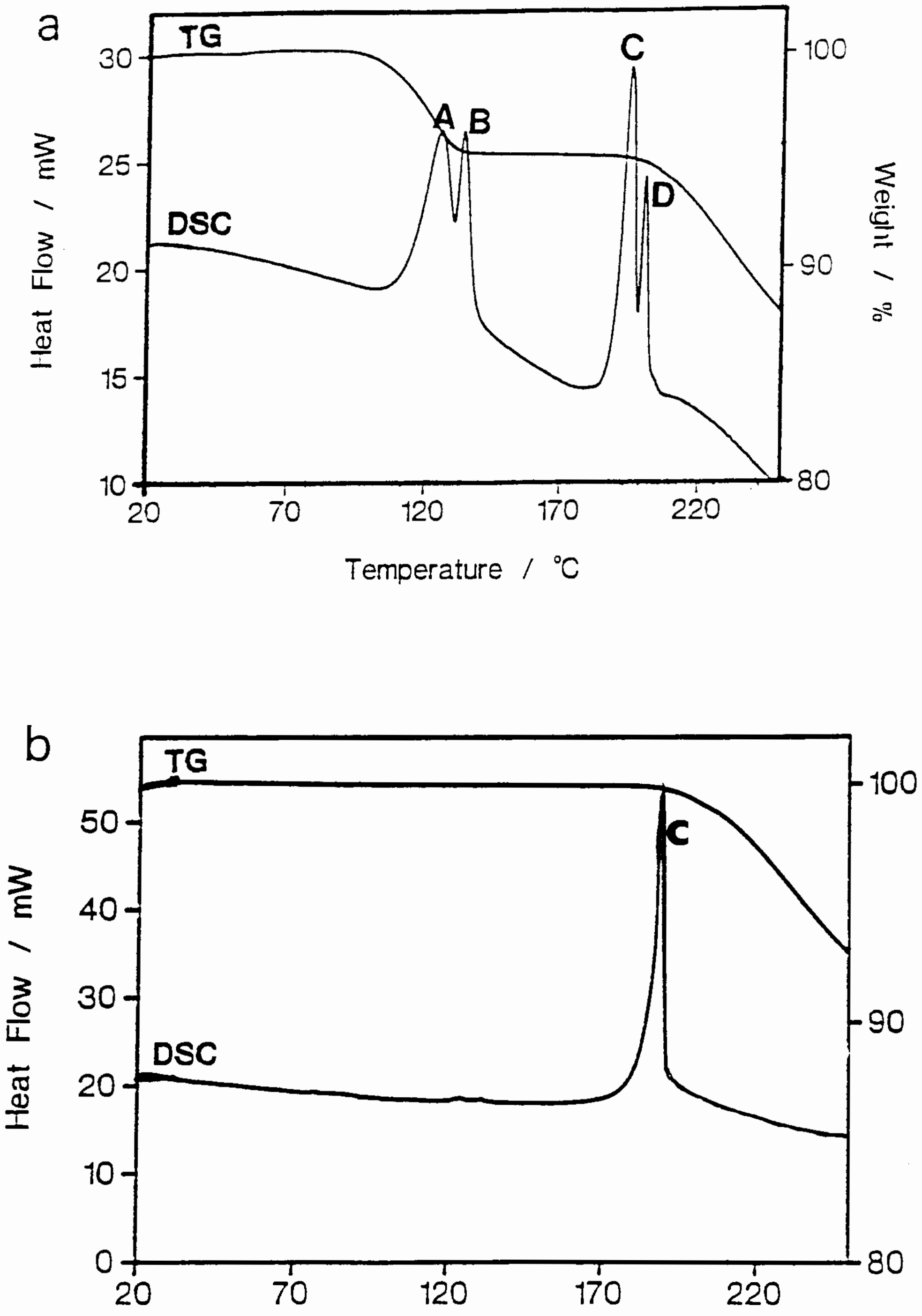

Figure 5.3 (a) TGA-DSC thermograms for **SSTHYD**
(b) TGA-DSC thermograms for **SSTANHYD**

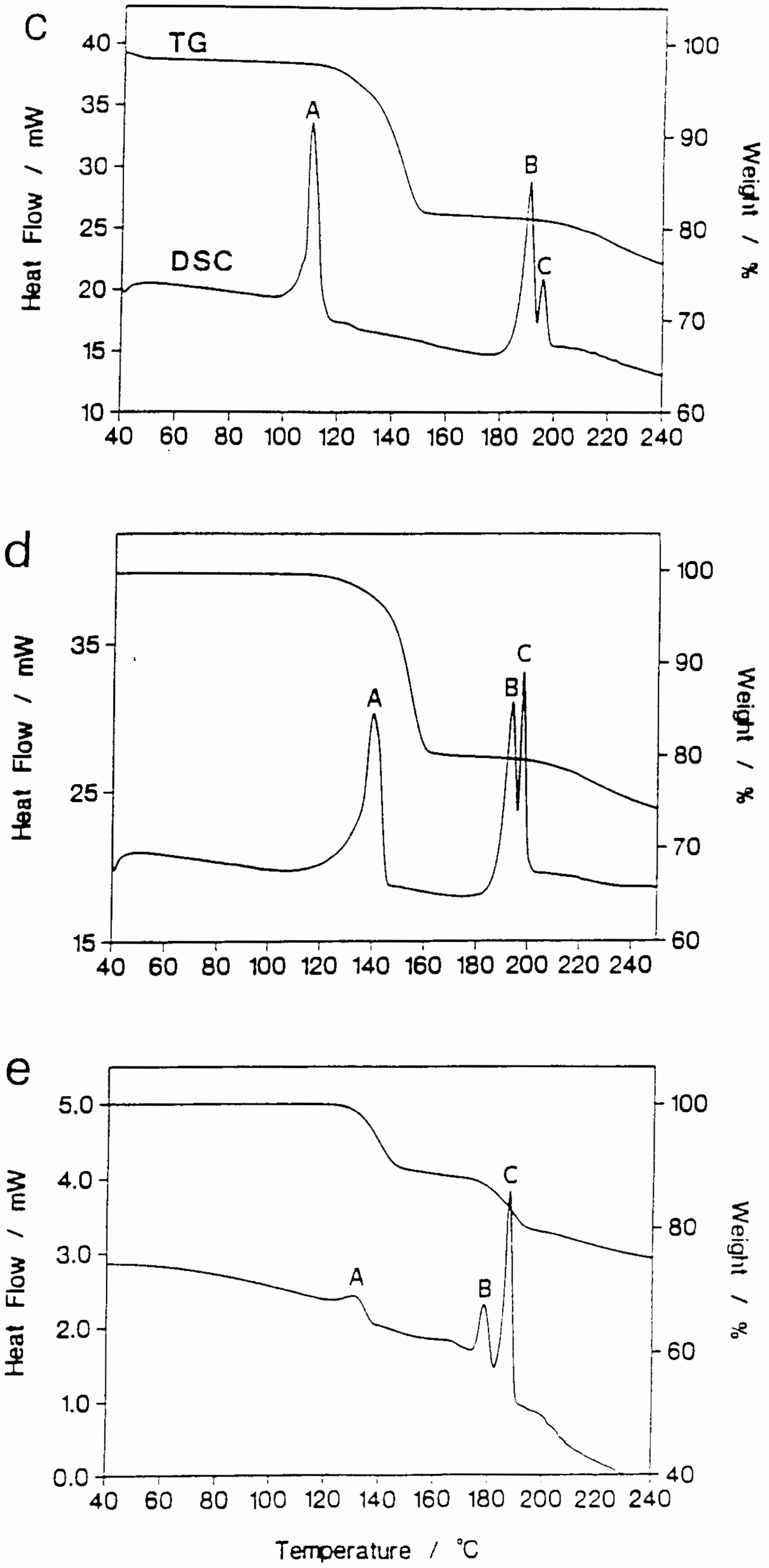

Figure 5.3 (c) TGA-DSC thermograms for **SSTBU**.
(d) TGA-DSC thermograms for **SSTPE**.
(e) TGA-DSC thermograms for **SSTDI**.

5.4 TABULATION OF THERMAL RESULTS

5.4.1 TGA Table of Results

	STEP 1		STEP 2		OVERALL CALC.WEIGHT LOSS (%).
CODE NAME	T_{ons}(°C)	ΔW(%)	T_{ons}(°C)	ΔW(%)	FOR 1:1 H:G RATIOS
SSTHYD	69.6	4.9	-	-	4.8
SSTANHYD	-	-	-	-	-
SSTBU	109.1	17.0	-	-	17.3
SSTPE	120.4	19.7	-	-	19.9
SSTDI	110.5	10.8	152.9	10.3	19.9

5.4.2 DSC Table of Results

	PEAK A		PEAK B		PEAK C	
CODE NAME	T_{ons}(°C)	ΔH ($kJmol^{-1}$)	T_{ons}(°C)	ΔH ($kJmol^{-1}$)	T_{ons}(°C)	ΔH ($kJmol^{-1}$)
SSTHYD	106.7	9.9	121.6	26.5	187.9	35.0
SSTANHYD	-	-	-	-	182.4	31.3
SSTBU	109.1	37.9	181.8	44.1	-	-
SSTPE	134.6	60.0	180.6	42.3	-	-
SSTDI	121.1	14.8	169.0	6.6	178.4	16.4

5.5 INTERPRETATION OF TGA-DSC RESULTS

(i) **SSTHYD** and **SSTANHYD** in **Figures** 5.3 **(a)** and **(b)**

Since the raw commercial material was in a monohydrate form, it was imperative to execute complete dehydration prior to solvate preparation. This task was made easier once the temperature region became known (as evident in **Figure** 5.3 **(a)** = 115 - 120˘C) over which H_2O bleeds off the crystalline system. Without this step being effectively carried out, no crystallization of **SST** from organic solvents would have been possible. The DSC reveals a peak B which is almost unresolved with the solvent-release peak A. Peak B was assigned to some polymorphic phase change which might be ocurring directly after dehydration. This was not considered a superficial suggestion given the abundance of the polymorphic forms of succinylsulfathiazole as reported earlier in this text.

Peak C is probably due to another phase change occurring just prior to the melting of **SST**. Peak D (which is indicated in **Figure** 5.3 **(a)** but its data are not recorded in **Table 5.4.2**) was assigned to the melting of **SST** with the onset temperature and ethalpy evaluated as 198˘ and 27 $kJmol^{-1}$ respectively.

To test for complete dehydration the sample was heated again by TGA (**Figure** 5.3 **(b)**) which resulted in the disappearance of the peak corresponding to solvent release at about 107˘C.

(ii) **SSTBU** and **SSTPE** in **Figures** 5.3 (c) and 5.3 (d).

A one-step desolvation process was indicated for both **SSTBU** and **SSTPE** at the DSC onset temperatures of 109.1 and 134.6°C respectively. The reason for quoting onset temperatures instead of the thermodynamic parameter ΔH is because of the relatively high reproducibility of onset temperatures compared to enthalpies. A further anomaly observed in all thermograms is the apparent out-of-step appearance of the TGA peaks with their corresponding DSC counterparts. This observation has been implied in **sections 5.1.2, 5.1.3** and **5.2** where it was made clear that while the thermal conditions may have been kept the same in TGA-DSC experiments, the systems are however different. TGA is an open system whereas DSC is a closed system and that results in this apparent inconsistency. Besides this anomaly, some useful data from TGA measurements did unequivocally indicate 1:1 H:G stoichiometry in both compounds, which was a reinforcement on earlier tentative indications based on microanalysis and density measurements.

(ii) **SSTDI** as represented in **Figure 5.3 (e)**

Thermal observations on **SSTDI** became an object of curiosity, not only because it is a new and hitherto unknown compound but also because of the neatly resolved two-step loss of dioxane at the DSC onset temperatures of 121.1°C and 169.0°C. Without placing too much emphasis on enthalpies, yet another curious point is the fact that

in moving from the first guest release the enthalpy is almost halved from 14.8 to 6.6 $kJmol^{-1}$. A number of practical suggestions were advanced here.
To mention but one of them:-
The crystal could undergo structural rearrangement upon losing the first half a mole of dioxane. This new structural arrangement may cause loosening of the entire host-guest aggregate so that loss of the second half a mole of dioxane demands less energy than the earlier guest-release process.

However, this postulation should be treated with caution considering the earlier comment on poor reproducibility of DSC enthalpies.

REFERENCES

121. H.G. Wiedemann: *J.Thermal Anal.* **12**, 147, (1977).

122. M.E. Brown: in "Introduction to Thermal Analysis - Techniques and Applications. Chapman and Hall, NY, (1988).

123. M.H. Moore, L.R. Nassimbeni, M.L. Niven: *Inorganica Chimica Acta,* **131**, 45, (1987).

124. W.W.M. Wendlandt: in "Thermal Analysis", 3rd Edition, New York, 118, (1986).

125. B. Wunderlich: in "Thermal Analysis", Academic Press (1990).

CHAPTER 6

SUBCONTENTS

6.1 DESOLVATION KINETICS BY DYNAMIC TGA

6.1.1 GENERAL

In their paper, *"A Quick, Direct Method for the Determination of Activation Energy from Thermogravimetric Data"*, J.H. Flynn and L.A. Wall presented a suitable and fairly straightforward technique of evaluating kinetic data using dynamic TGA[126]. This approach, though lacking in rigour is quite useful when comparing desolvation behaviour of a series of compounds. Furthermore, it works very well for compounds which display simple stoichiometric one-step desolvation process, typical of **SSTBU** and **SSTPE (see 5.3(c) and (d)**).

Otherwise, a number of cumbersome curve-fitting techniques based on single TGA curves exist. For the purpose of obtaining more rigorous kinetic results most workers resort to isothermal techniques. However, Flynn *et al* are adamant that 'disastrous results' are likely to be obtained in cases where a simple reaction order "n" cannot be rationalized which is the case with most inclusion compounds.

6.1.2 THE PHYSICAL CHEMISTRY OF THE TECHNIQUE

C - is defined as the degree of conversion such that 1-C = weight of material lost divided by the total weight loss as T or $t \rightarrow \infty$,

then $dC/dT \quad = \quad (A/\beta)\ f(C)\exp(-Ea/RT)$---(1)

where,

T - absolute temperature (K)

ß - predetermined heating rate

A - collision factor (Arrhenius)

Ea - activation energy ($Jmol^{-1}$)

R - gas constant ($8.314JK^{-1}mol^{-1}$)

f(C) - a function of degree of conversion i.e. weight loss

The mathematically simplifying assumptions are:-

(i) f(C), A and Ea are independent of T, and

(ii) A and Ea are independent of C.

By the method of separation of variables equation (2) can be integrated to obtain equation (3).

$$F(C) = \int_{0}^{C} dC/f(C) = (A/\beta)\int_{T_0}^{T} \exp(-Ea/RT)dT \quad \text{---} \ (2)$$

$$d \log\beta / d\,(1/T) \approx (0.457/R)Ea \quad \text{---} \ (3)$$

Equation (3) allows for the determination of Ea from weight loss versus temperature thermograms at several heating rates. The activation energy is obtained from the slope of a plot of log ß versus 1/T. In order to obtain constant Ea with respect to C and T, several more curves should be plotted ~~runs should be repeated~~ at different 1-C values. It was noted in this project that these procedures should be limited to low 1-C for desirable Ea values. Furthermore, high ß values i.e. above 30°Cmin^{-1} were found to produce non-linear curves.

6.2 THE MODES OF DESOLVATION

Probably the single most difficult task in the study of inclusion compounds is to postulate their decomposition mechanisms. The attempt by Byrn[29] to describe the phenomenon still does not leave one with a clear picture about the actual sequence of events during decomposition. Qualitative descriptions are often put forward. In general, an inclusion compound often referred to as the ß-phase can decompose via several pathways as illustrated in **Figure 6.2.1**.

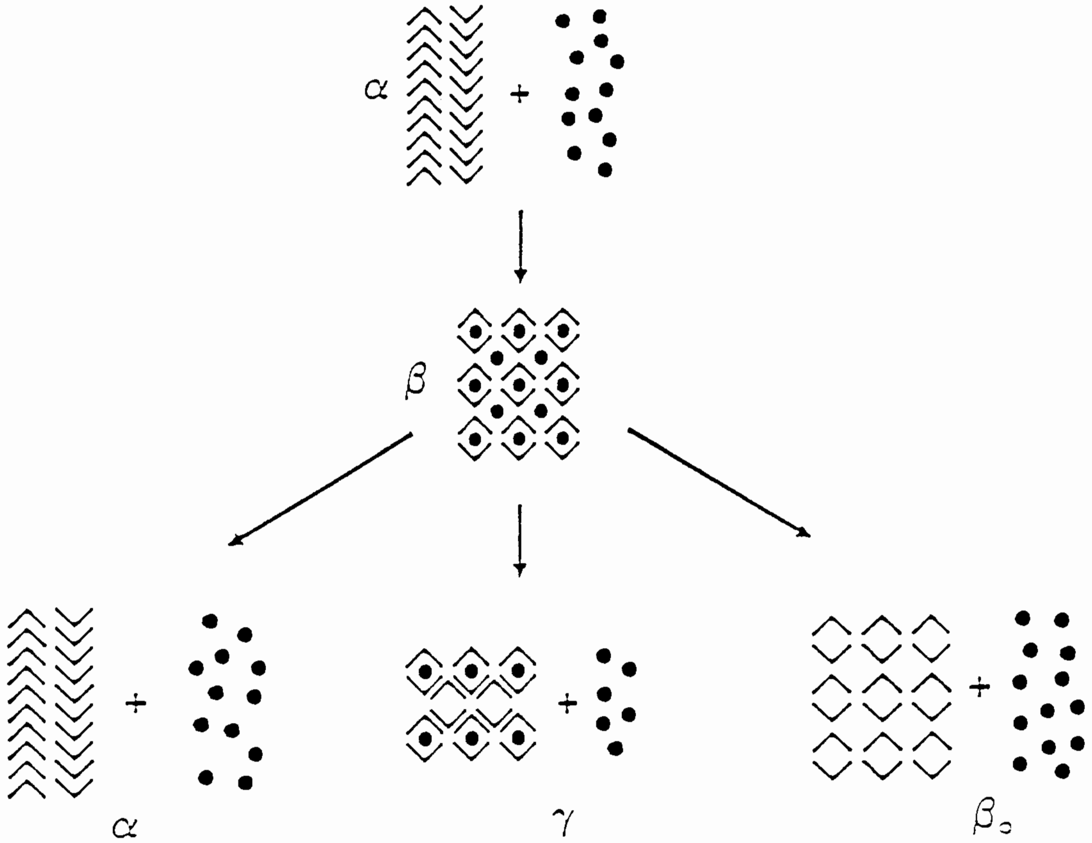

Figure 6.2.1 A schematic representation of how inclusion compounds undergo decomposition[127].

The ß-phase can decompose in such a way that the resulting host framework resembles its unsolvated form, α-form. On the other hand, an intermediate phase which resembles neither α- nor ß-phases can result from molecular re-arrangement during decomposition. This stable crystalline intermediate is referred to as a γ-phase. A third possibility is that on losing guest, the host crystal structure is maintained giving rise to an empty $ß_0$ structural framework. In this series of compounds, **SSTDI** desolvates only partially with a DSC evidence that structural rearrangement does take place. It was thoroughly emphasized in chapter one that the phenomenon of phase changes, i.e. *(polymorphism/pseudopolymorphism)* is very common in drug compounds.

6.3 THE TGA KINETIC EXPERIMENT

The purpose of these experiments was to compare Ea values and use the kinetic data in conjunction with the structural data to hypothesize on the mode of desolvation. Particle size homogenization by crushing and the maintenance of fairly constant sample masses were strictly observed in the preparation step. It was noted that high heating rates (ß) and high extents of decomposition (1-C) tended to produce uninterpretable results such as non-linear -logß versus 1/T curves, therefore these factors were taken cognisance of. It was decided not to study **SSTDI** by this technique since a two-step loss would lead to complicated kinetic results.

6.4 THE TGA KINETIC RESULTS

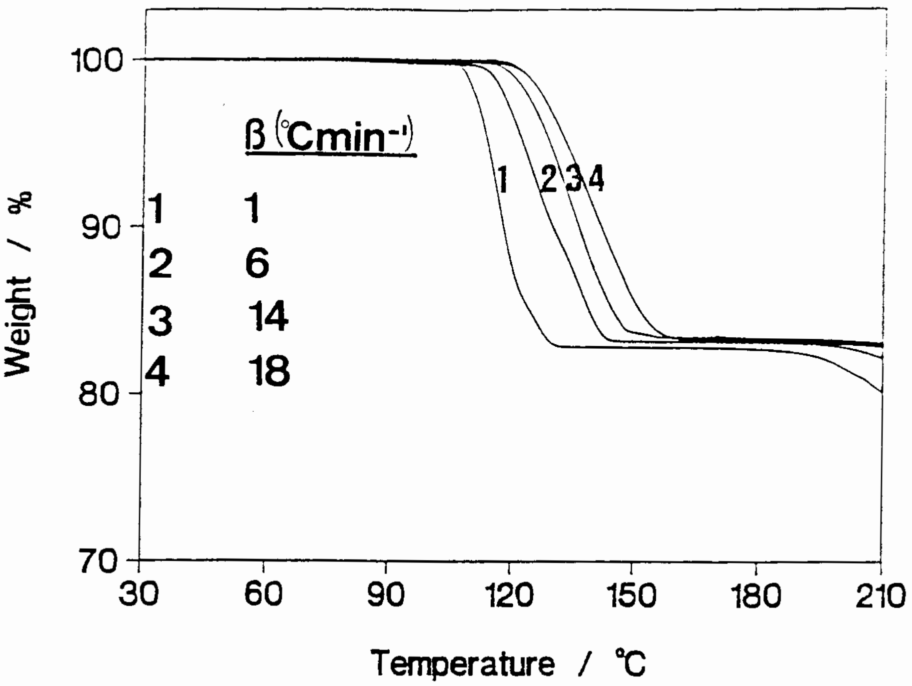

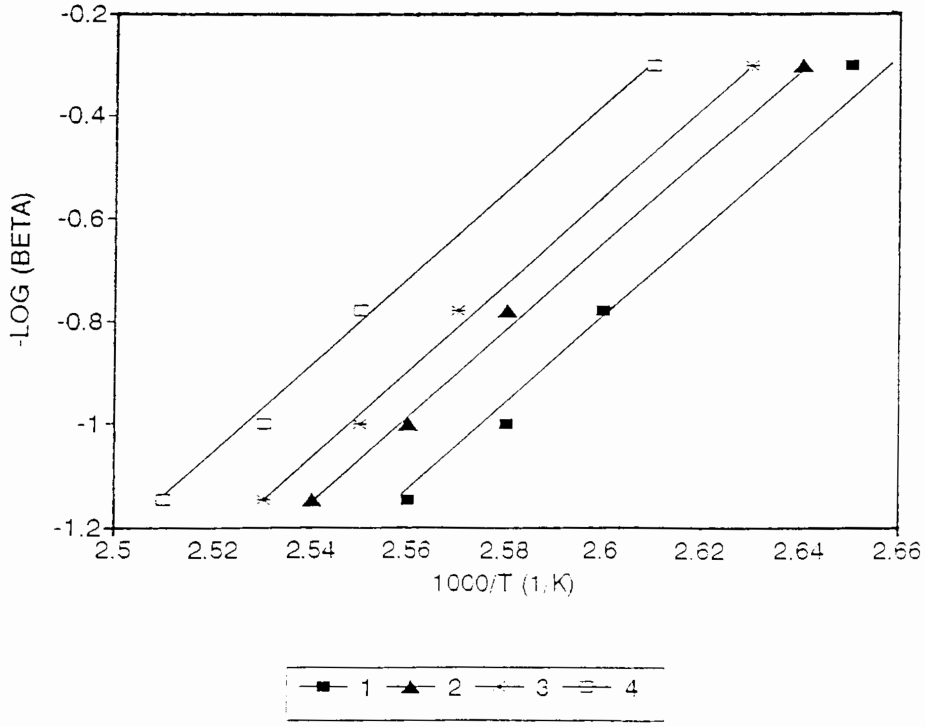

Figure 6.4.1 SSTBU kinetic curves yielding $Ea = 155$ $kJmol^{-1}$

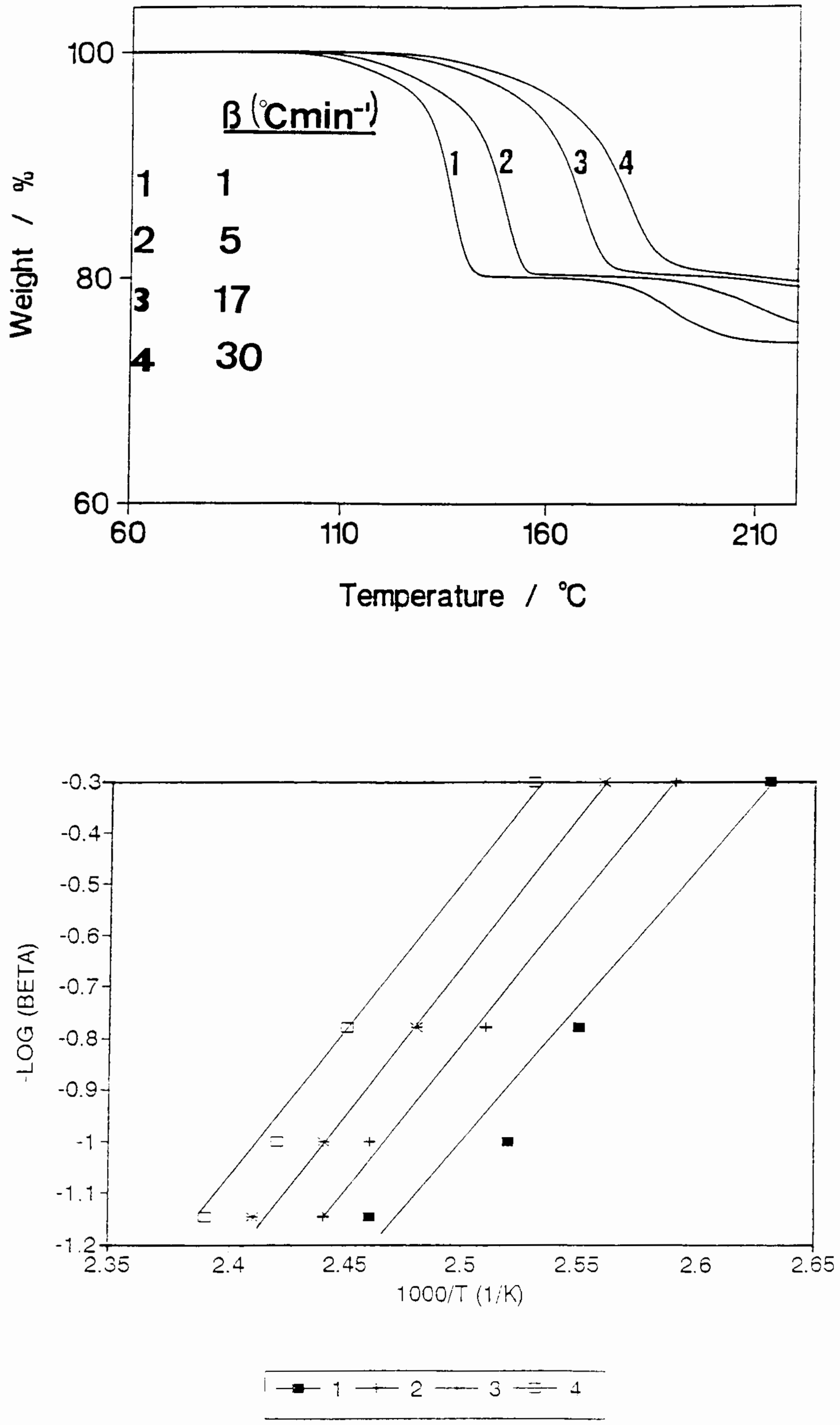

Figure 6.4.2 SSTPE kinetic curves yielding Ea = 149.0 kJmol^{-1}

6.5 INTERPRETATION OF KINETIC RESULTS

Interpretation was facilitated after the single crystal X-ray analyses of **SSTBU** and **SSTPE** were performed (see **Chapter** 7). These analyses showed that these solvates are isormophous. It was thus considered reasonable that the Ea values for solvent loss from these compounds should be similar. In general, Ea = 149-155 $kJmol^{-1}$ are quite large which might be due to strong hydrogen bonding interactions between host and guest components.

It may be commented at this point that the validity of applying the Arrhenius equation to heterogeneous reactions has been questioned, but the parameter Ea does have practical value even if its theoretical interpretation is difficult[122].

REFERENCES

126. J.H. Flynn, L.A. Wall: *Polymer Letters,* **4**, 323, (1966).

127. D.R Bond, M.R. Caira, G.A. Harvey, L.R. Nassimbeni, F. Toda: *Acta Cryst.* **B46,** 771, (1990)

CHAPTER 7

SUBCONTENTS

7.1 CRYSTAL STRUCTURE ANALYSES

7.1.1 GENERAL LAYOUT OF THIS CHAPTER

7.1.2 INTRODUCTION

7.1.3 THE HOST MOLECULE

7.1.4 CONFORMATION OF SST IN THE SOLVATES

7.2 STRUCTURES OF SOLVATES

7.a - e TABLES OF STRUCTURAL DATA

7.1 CRYSTAL STRUCTURE ANALYSES

7.1.1 GENERAL LAYOUT OF THIS CHAPTER

The purpose of this general outline is to assist the reader in locating the crucial information pertaining to the structures.

The following tables have been included for the sole convenience of quick cross-referencing.

The tables are presented according to the order in which the structures have been presented i.e. **SSTDI**, **SSTBU** and **SSTPE.**

TABLE 7 a	Intensity Data Collection and Structure Refinements.
TABLE 7 b	Listing of Hydrogen Bonds
TABLE 7 c	**(i)** Fractional Atomic Coordinates,
	(ii) Thermal Parameters for all atoms,
	(iii) Bond Lengths (Å),
	(iv) Bond Angles (°), and
	(v) Torsion Angles (°) for compound **SSTDI.**

Corresponding **TABLES 7d (i)-(v)** for compound **SSTBU**, and **TABLES** 7e **(i)-(v)** for compound **SSTPE.**

The structure factor tables have been appended in the computer diskette **(see Appendix 1)**. Besides permitting ease of cross-referencing, the contents of these tables have been constantly referred to in the present text. With regard to actual crystal structures, the presentation style adopted is that of presenting a summary of the essential crystallographic data alongside with a diagram of the asymmetric unit and its atom numbering.

7.1.2 INTRODUCTION

The presence of S atoms in the host compound **SST** made all three compounds, namely **SSTDI, SSTBU** and **SSTPE** amenable to solution by the heavy-atom method. Centrosymmetry was indicated in all three structures by the intensity-statistics of initial runs. Space group $P\bar{1}$ was indicated in all structures.

7.1.3 THE HOST MOLECULE

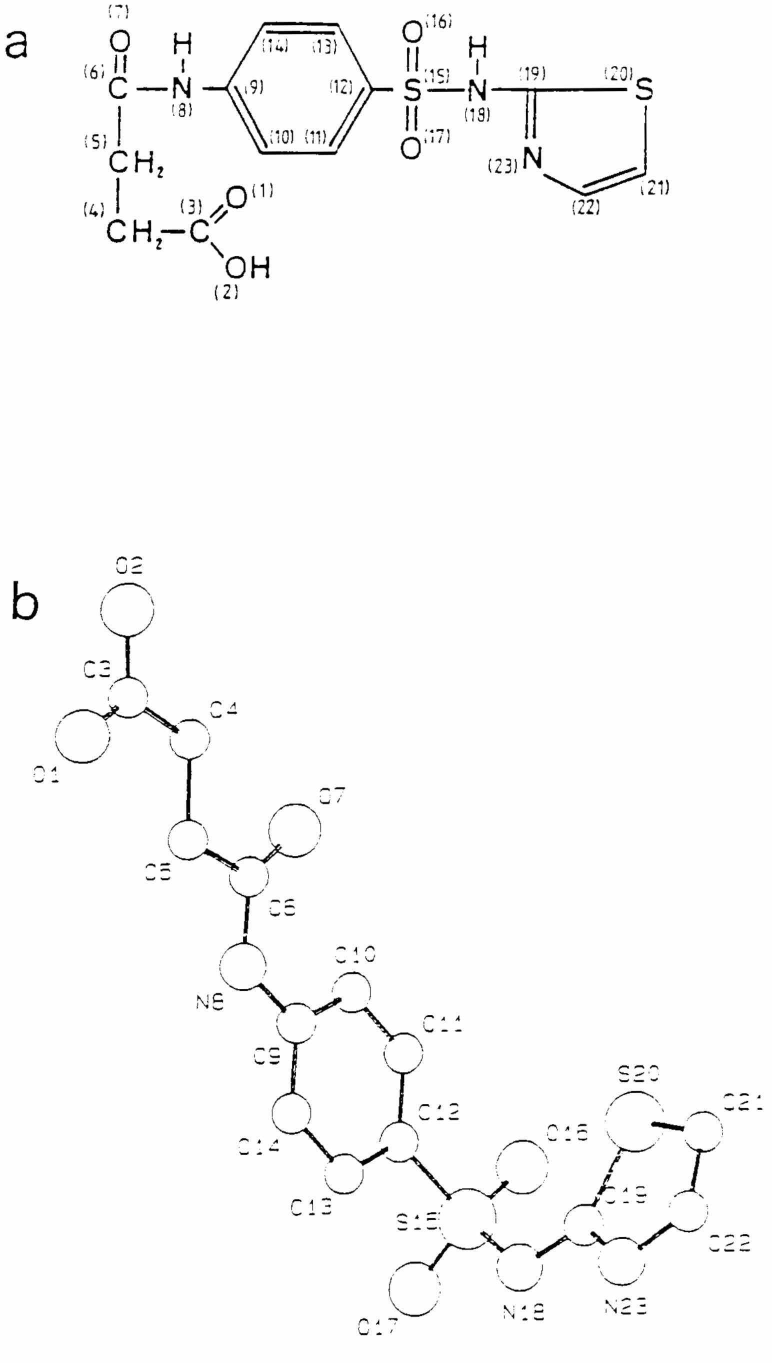

Figure 7.1.3 (a) Structural diagram of SST and, (b) Typical conformation in the solid state shown here for SSTDI;both indicate the atom numbering scheme adopted in the study of SST solvates.

In all three crystal structures that were solved the arbitrary numbering scheme indicated above (see **Figure 7.1.3** (a)) was adopted.

7.1.4 THE CONFORMATION OF THE SST MOLECULE IN THE SOLVATES

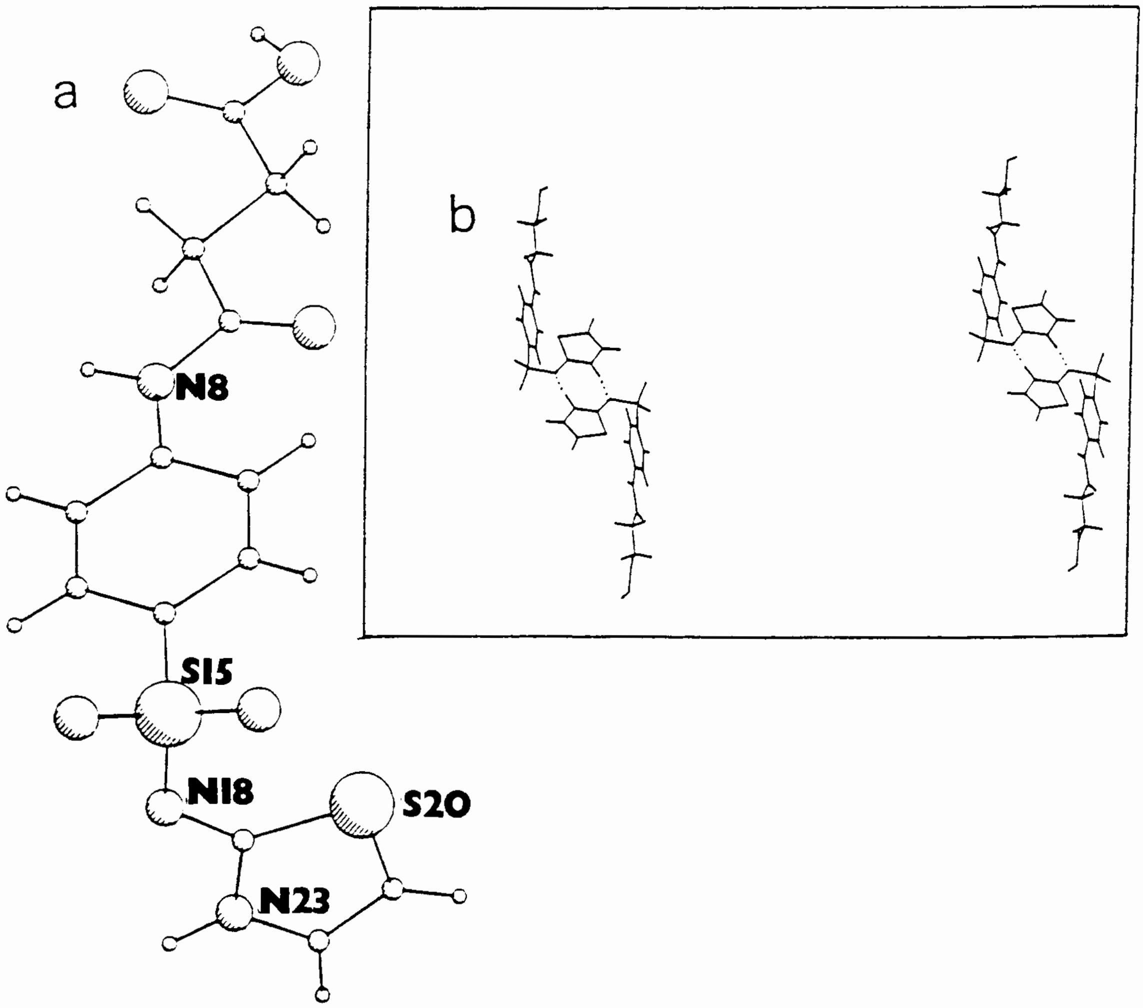

Figure 7.1.4 (a) A representative conformer of SST obtained from SSTBU.
(b) Stereoview of the centrosymmetric and hydrogen-bonded dimers of SST in the solvates.

One common feature in all three solvates is the "syn" arrangement of the sulphur atoms in **SST**, namely the sulphur atom in the sulfonamide group and its counterpart in the thiazolyl ring.

Another common feature is the presence of the imido tautomeric form throughout. In this form N(23) instead of N(18) bears the hydrogen atom, thus making the latter atom available for participation in the hydrogen bonding scheme shown in **Figure 7.1.4 (b).**

(c)

Torsion Angle	SSTBU	SSTPE	SSTDI
O(1)–C(3)–C(4)–C(5)	17.3(8)	11(2)	-3.8(7)
C(3)–C(4)–C(5)–C(6)	-178.2(4)	-179(1)	-178.0(4)
C(4)–C(5)–C(6)–N(8)	-176.7(4)	-177(1)	173.3(4)
C(5)–C(6)–N(8)–C(9)	179.5(5)	180(1)	173.1(4)
C(6)–N(8)–C(9)–C(10)	-176.9(5)	-173(1)	-165.8(5)
C(11)–C(12)–S(15)–N(18)	73.2(5)	73(1)	55.3(4)
C(12)–S(15)–N(18)–C(19)	79.9(4)	80(1)	74.0(4)
S(15)–N(18)–C(19)–S(20)	7.1(7)	4(2)	9.5(6)

Table 7.1.4 (c) Torsion Angles (°) defining the conformation adopted by the **SST** molecule in the solvates.

The torsion angles tabulated above have been obtained from **Tables 7 c(v), d(v) and e(v).**

It is worth noting that the typical dihedral angle C(12) - S(15) - N(18) - C(19) is remarkably similar in **SSTBU** being 79.9(4)° and **SSTPE**, 80(1)°. However, it is slightly different in **SSTDI**, 74.0(4)°.

A close inspection of other typical dihedral angles in the table above reveals the same trend. This is not surprising in view of the distinct structural differences between the isomorphous pair **SSTBU** and **SSTPE**, and **SSTDI**. Furthermore, the centrosymmetric dimerization of the host molecules is persistent in all structures. This phenomenon (see **Figure 7.1.4 (b)**) was also observed in the monohydrate crystal structure of **SST**[87].

An analogous case of dimerization was encountered in the work with the *coordinato clathrates* of the drug, 5-methoxysulfadiazine also referred to earlier in **Figure 1.28 (d)**. In the present case of **SST** the dimeric repeating motif contains identical N(23)-H(23)...N(18) hydrogen bonds. It was thus suggested that this particular arrangement in these compounds is probably the most stable one.

7.2 STRUCTURES OF SOLVATES

7.2.1 1,4-Dioxane Solvate of Succinylsulfathiazole (SSTDI)

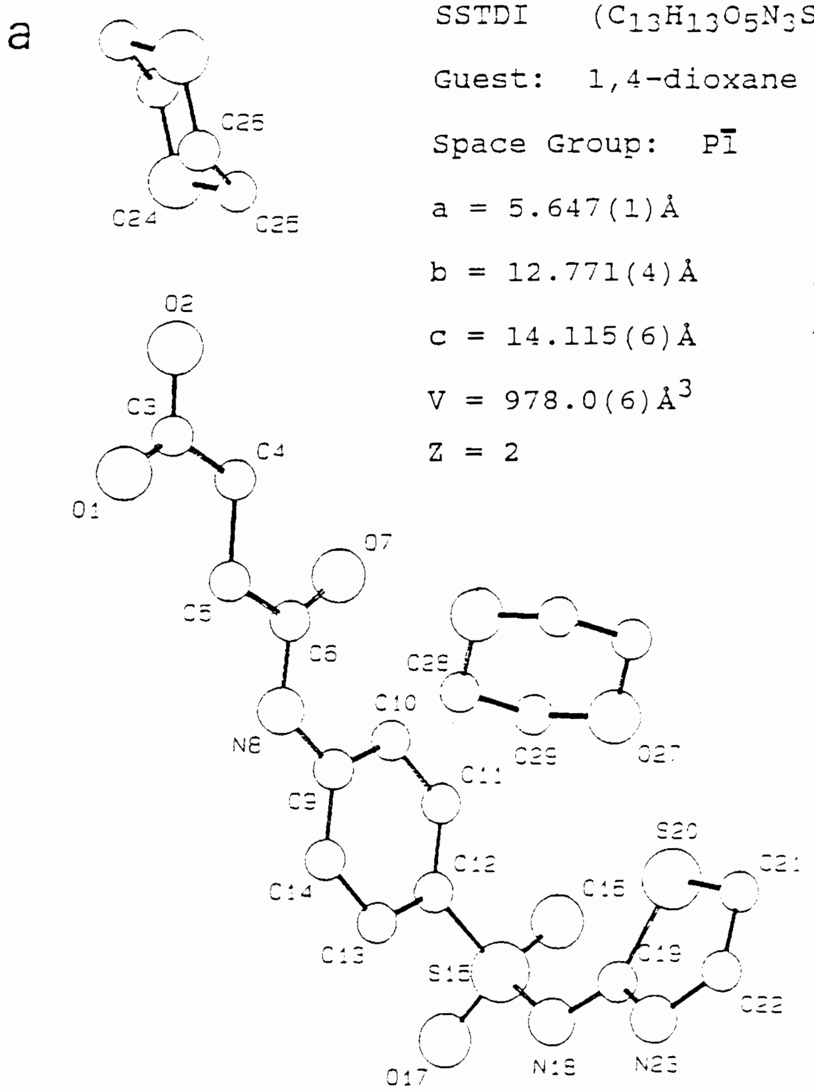

SSTDI ($C_{13}H_{13}O_5N_3S_2 . C_4H_8O_2$)

Guest: 1,4-dioxane

Space Group: $P\bar{1}$

a = 5.647(1)Å α = 94.48(3)°

b = 12.771(4)Å β = 100.92(3)°

c = 14.115(6)Å γ = 99.96(2)°

V = 978.0(6)$Å^3$

Z = 2

Figure 7.2.1 (a) The asymmetric unit of **SSTDI** consisting of one **SST** molecule and one half (labelled) of each of the dioxane molecules in a 1:1 ratio.

The 1:1 stoichiometric ratio was deduced from the crystal density, microanalysis and the TG data. Upon structure solution the two dioxane molecules were found to occupy independent crystallographic sites of symmetry $\bar{1}$ within the host-guest aggregate (see **Figure 7.2.1 (b)**).
One of these molecules refined with somewhat normal U_{iso} values of 0.054-0.063Å^2 and acceptable geometry whereas the other solvent molecule~~s~~ refined with unusually high U_{iso} values of 0.11-0.13Å^2 and somewhat abnormal geometry. This necessitated the imposition of a C-C distance constraint of 1.510Å (σ=0.002Å) for C(28)-C(29) in order to obtain the geometry matching that of the well-behaved dioxane molecule. The hydrogen atoms were located in $\Delta\rho$ maps and added in idealized positions at 1.00Å from their parent atoms. All non-hydrogen atoms were treated anisotropically in the final refinement.

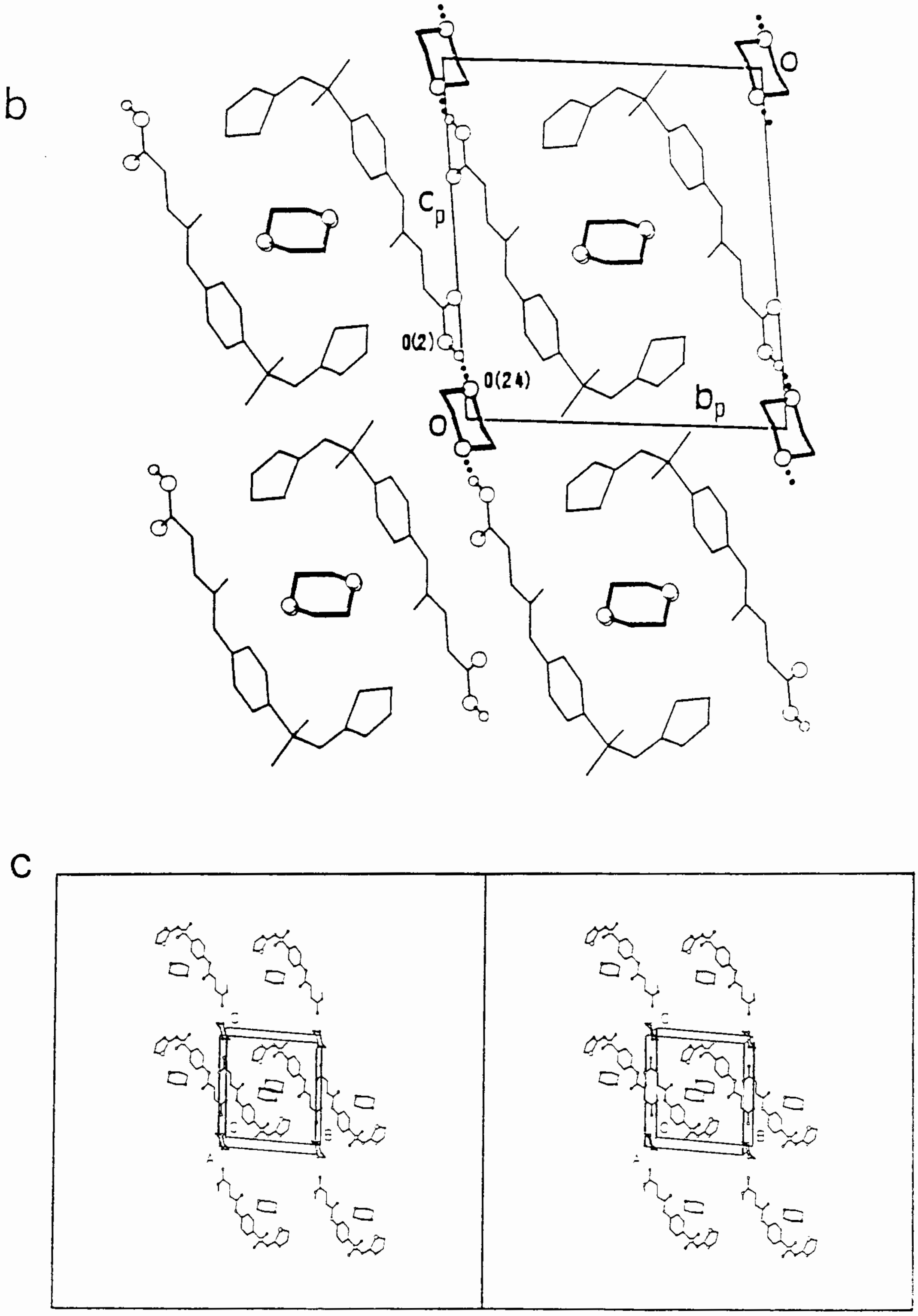

Figure 7.2.1 (b) (100) Projection of the structure of SSTDI showing two crystallographically-independent solvent molecules.

(c) Stereoview of molecular packing.

(d)

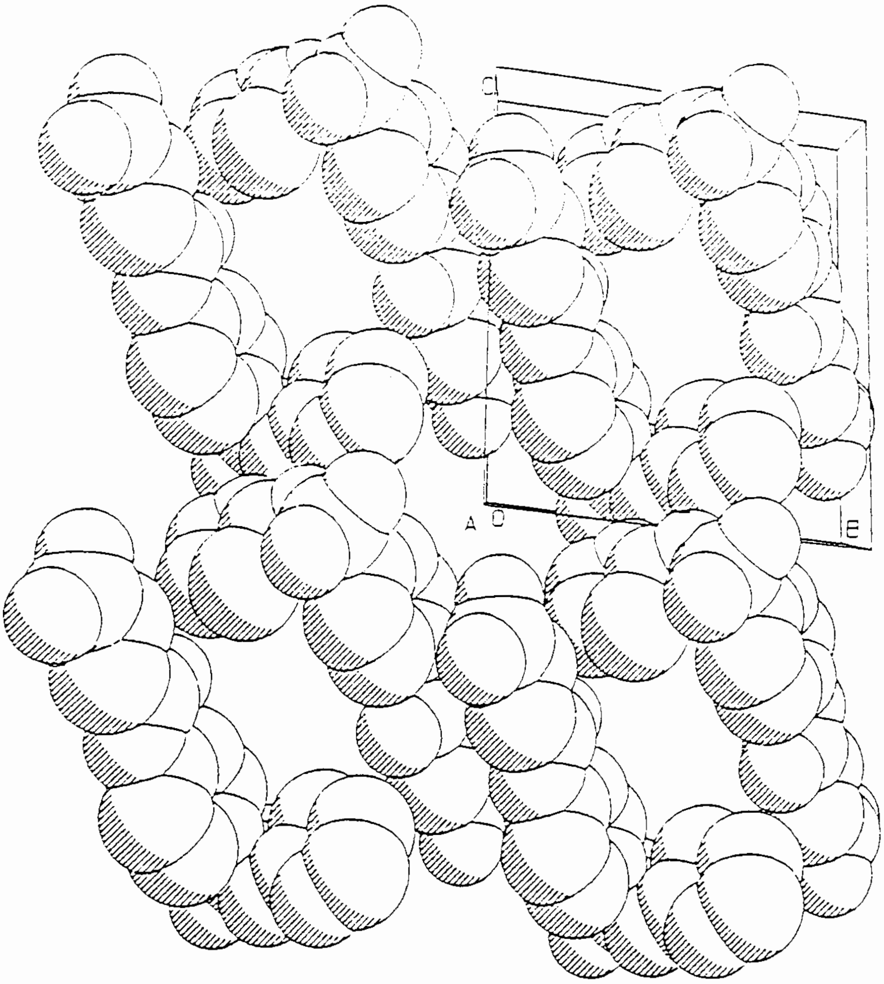

Figure 7.2.1 (c) Channel-occupation by the solvent molecules in **SSTDI** is indicated as voids when only the host molecules are represented.

Salient ~~molecular~~ structural features were evident in the nature of host-guest interactions in this compound. The dioxane molecule which refined with normal U_{iso} values (located at 0,0,0) is held tightly by hydrogen bonding while the other dioxane which refined with high values of U_{iso} values (located at $0,\frac{1}{2},\frac{1}{2}$) is not hydrogen-bonded. This latter observation is consistent with the appearance of two distinct events in the TG-DSC thermograms associated with solvent release **(see Figure 5.3 (e))**.

7.2.2 1-Butanol Solvate of Succinylsulfathiazole (SSTBU)

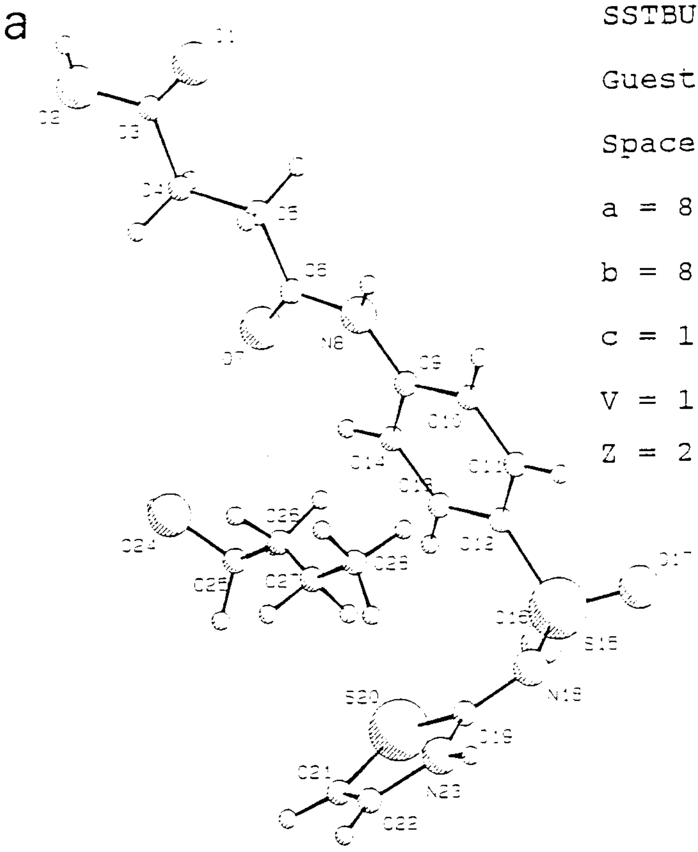

SSTBU ($C_{13}H_{13}O_5N_3S_2 \cdot C_4H_{10}O$)

Guest: 1-butanol

Space Group: P$\bar{1}$

a = 8.642(2)Å α = 82.33(3)°

b = 8.931(3)Å β = 78.40(3)°

c = 14.026(4)Å γ = 89.40(3)°

V = 1050.8(5)Å^3

Z = 2

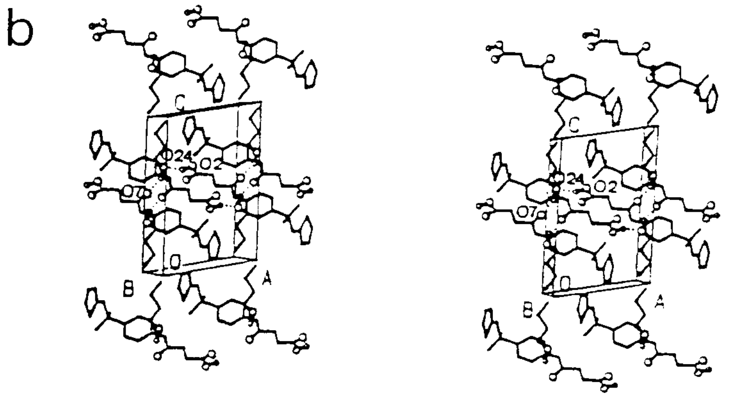

Figure 7.2.2 **(a)** The asymmetric unit of **SSTBU** consisting of a 1:1 H:G entity.
(b) Stereoview of crystal and molecular packing in **SSTBU** with hydrogen bonding indicated as dotted lines.

Confirmatory characterization of **SSTBU** was carried out with the objective to assess the validity of the 1 : 0.89 H:G composition which was reported earlier[86].

Microanalysis, density measurements and TG yielded unambiguously a more common 1:1 stoichiometry. The space group symmetry of $\bar{1}$ prescribes that the two H:G units be situated within the cell and be related to each other by the centre of symmetry. The stereo diagram in **7.2.2 (b)** illustrates the mode of association between the host and the guest whereby the guest molecules are imprisoned in cavities created by the host lattice (see **Figure 7.2.2 (c)**) and engage in hydrogen bonding with the host. Hence, **SSTBU** and **SSTPE** were accordingly described as *coordinato clathrates*. The hydroxyl group of the solvent is both a hydrogen bond donor and acceptor. Atom O(24) of the solvent molecule accepts a hydrogen bond, O(2)-H(2)...O(24), from the carboxylic group of one **SST** molecule and donates its H-atom in a hydrogen bond, O(24)-H(24)...O(7'), to a carbonyl O atom of a second **SST** molecule related to the first by unit translation along x.

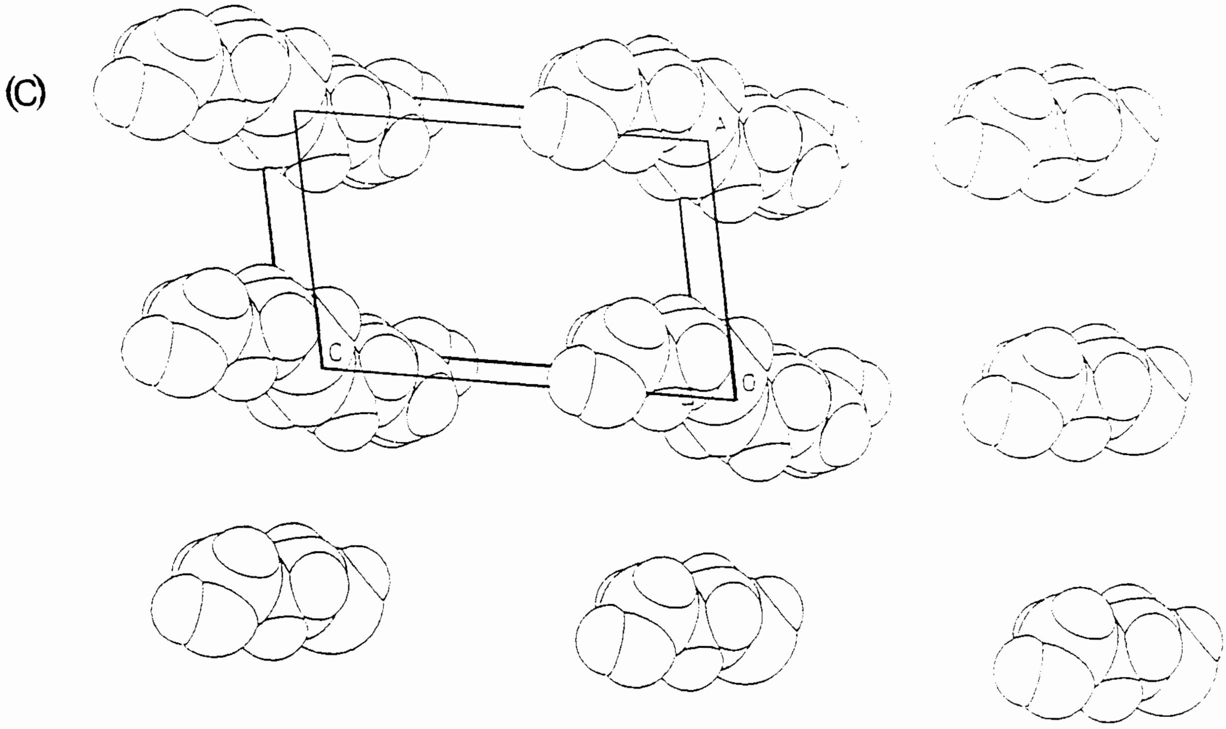

Figure 7.2.2 (c) The spatial arrangement of 1-butanol molecules indicate the cavity occupation.

7.2.3 1-Pentanol Solvate of Succinylsulfathiazole (SSTPE)

SSTPE ($C_{13}H_{13}O_5N_3S_2.C_5H_{12}O$)

Guest: 1-pentanol

Space Group: $P\bar{1}$

$a = 8.665(2)Å$ $\alpha = 82.72(1)°$

$b = 9.008(1)Å$ $\beta = 78.68(1))°$

$c = 14.198(2)Å$ $\gamma = 88.30(2)°$

$V = 1077.9(3)Å^3$

$Z = 2$

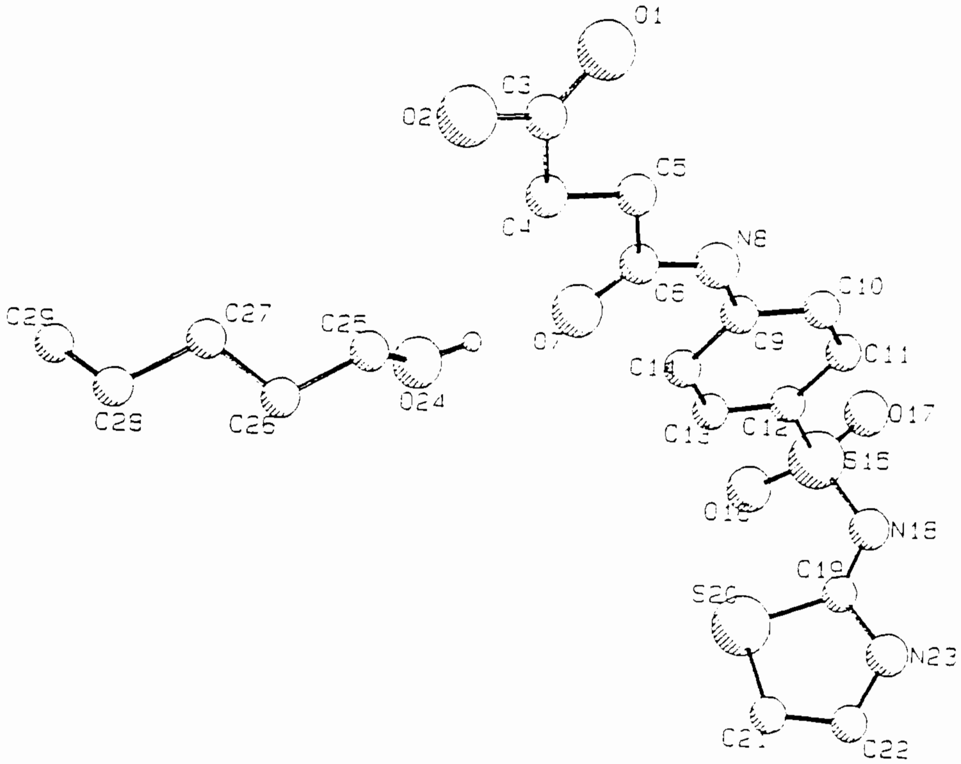

Figure 7.2.3 (a) The asymmetric unit of **SSTPE** consisting of a 1:1 H:G entity analogous to **SSTBU**.

The structures of **SSTBU** and **SSTPE** are isomorphous with respect to the host molecules and have solvent molecules occupying crystallographically-equivalent sites in each case.

In general, the structures solved well except for the solvent molecules which were characterized by high thermal motions. A literature review revealed that the phenomenon of abormal thermal motion is not uncommon in compounds whose guests contain hydrocarbon chains[128-131]. At some stage certain difficulties were experienced with what appeared to be disordered guest molecules. However the imposition of distance constraints yielded satisfactory results.

TABLE 7.a Details of Intensity Data Collections and Structure Refinements

COMPOUND	SSTPE	SSTBU	SSTDI
Molecular formula	$C_{13}H_{13}O_5N_3S_2.C_5H_{12}O$	$C_{13}H_{13}O_5N_3S_2.C_4H_{10}O$	$C_{13}H_{13}O_5N_3S_2.C_4H_8O_2$
Guest	n-pentanol	n-butanol	dioxane
H:G Ratio	1:1	1:1	1:1
Crystal system	triclinic	triclinic	triclinic
Space group	$P\bar{1}$	$P\bar{1}$	$P\bar{1}$
a/Å	8.665(2)	8.642(2)	5.647(1)
b/Å	9.008(1)	8.931(3)	12.771(4)
c/Å	14.198(2)	14.026(4)	14.115(6)
α/°	82.72(1)	82.33(3)	94.48(3)
β/°	78.68(1)	78.40(3)	100.92(3)
γ/°	88.30(2)	89.40(3)	99.96(2)
V/Å^3	1077.9(3)	1050.8(5)	978.0(6)
Z	2	2	2
Dc/gcm^{-3}	1.367	1.358	1.506
F(000)	468	452	464
μ(MoKα)/cm^{-1}	2.73	2.78	3.04
Crystal size/mm	.50x.50x.25	.65x.65x.75	.20x.35x.40
Range scanned,θ/°	1-25	1-25	1-25
Index range	0,10;-10,10;-16,16	0,10;-10,10;-16,16	-6,6;-15,15;0,16
Scan width,x/°	0.85+0.35tanθ	0.85+0.35tanθ	0.85+0.35tanθ
Aperture width/mm	1.12+1.05tanθ	1.12+1.05tanθ	1.12+1.05tanθ
No.of reflections collected	4055	3966	3606
No. of unique reflections	3228	3411	2999
No.of reflections observed ($I_o>2\sigma(I_o)$)	2481	3031	2393
No.of parameters refined	281	275	275
R	0.092	0.064	0.052
Rw	0.090	0.064	0.051
Maximum shift/esd	0.05	0.05	0.02
Absorption correction factor range	0.9627 - 0.9996	0.7920 - 0.9989	0.9756 - 0.9995
Crystal stability (%)	-12.5	-0.5	-18.9
Δρ:maximum, min/eÅ^{-3}	+0.48; -0.51	+0.67; -0.59	+0.40; -0.50

Table 7 b–Distances (Å) and angles (°) for Hydrogen Bonds

Donor-H		Donor-Acceptor		H...Acceptor		Donor-H...Acceptor Angle	
SSTBU							
O(2)-H(2)	1.00(2)	O(2)...O(24)^{a}	2.624(6)	H(2)...O(24)^{a}	1.69(2)	O(2)-H(2)...O(24)^{a}	153(3)
O(24)-H(24)	1.00(4)	O(24)...O(7)^{b}	2.830(7)	H(24)...O(7)^{b}	2.00(7)	O(24)-H(24)...O(7)^{b}	138(3)
N(8)-H(8)	1.00(1)	N(8)...O(16)^{c}	3.103(6)	H(8)...O(16)^{c}	2.12(1)	N(8)-H(8)...O(16)^{c}	166(1)
N(23)-H(23)	1.00(1)	N(23)...N(18)^{d}	2.825(5)	H(23)...N(18)^{d}	1.84(1)	N(23)-H(23)...N(18)^{d}	167(1)
SSTPE							
O(2)-H(2)	1.00(1)	O(2)...O(24)^{a}	2.68(2)	H(2)...O(24)^{a}	1.69(1)	O(2)-H(2)...O(24)^{a}	169(1)
O(24)-H(24)	1.0(1)	O(24)...O(7)^{b}	2.83(2)	H(24)...O(7)^{b}	1.8(2)	O(24)-H(24)...O(7)^{b}	167(12)
N(8)-H(8)	1.00(2)	N(8)...O(16)^{c}	3.12(1)	H(8)...O(16)^{c}	2.17(1)	N(8)-H(8)...O(16)^{c}	158(1)
N(23)-H(23)	1.00(1)	N(23)...N(18)^{d}	2.84(1)	H(23)...N(18)^{d}	1.87(1)	N(23)-H(23)...N(18)^{d}	164(1)
SSTDI							
O(2)-H(2)	1.00(4)	O(2)...O(24)^{e}	2.651(5)	H(2)...O(24)^{e}	1.70(4)	O(2)-H(2)...O(24)^{e}	159(4)
N(8)-H(8)	1.00(1)	N(8)...O(1)^{f}	2.992(6)	H(8)...O(1)^{f}	2.00(1)	N(8)-H(8)...O(1)^{f}	171(1)
N(23)-H(23)	1.00(5)	N(23)...N(18)^{g}	2.862(5)	H(23)...N(18)^{g}	1.87(1)	N(23)-H(23)...N(18)^{g}	173(1)

Equivalent positions:

^{a} 3-x,1-y,1-z ^{b} 2-x,1-y,1-z ^{c} 1+x,y,z ^{d} 1-x,1-y,2-z

^{e} 2-x,-y,2-z ^{f} 2-x,-y,1-z ^{g} 1-x,1-y,-z

TABLE 7 c (i) Fractional atomic coordinates (x 10^4)
and Thermal Parameters (Å^2 x 10^3)
with e.s.d.'s in parentheses for **SSTDI**

Atom	x/a	y/b	z/c	Uiso/Uequiv(*)
O(1)	11265(6)	75(3)	6731(2)	63(2) *
O(2)	9541(6)	462(3)	7960(2)	58(1) *
C(3)	9765(8)	466(3)	7052(3)	41(2) *
C(4)	7947(8)	1047(4)	6495(3)	45(2) *
C(5)	8035(8)	1045(4)	5432(3)	47(2) *
C(6)	6102(8)	1606(4)	4913(3)	45(2) *
O(7)	4803(7)	2054(3)	5334(2)	67(2) *
N(8)	5934(6)	1525(3)	3939(2)	43(1) *
C(9)	4517(8)	2037(3)	3255(3)	38(2) *
C(10)	2674(8)	2552(4)	3455(3)	46(2) *
C(11)	1449(8)	3070(4)	2746(3)	46(2) *
C(12)	2018(7)	3071(3)	1854(3)	38(2) *
C(13)	3834(8)	2545(4)	1639(3)	47(2) *
C(14)	5064(8)	2023(3)	2340(3)	44(2) *
S(15)	510(2)	3771(1)	964(1)	48(1) *
O(16)	-1096(6)	4310(3)	1417(2)	63(2) *
O(17)	-554(6)	3031(3)	110(2)	69(2) *
N(18)	2648(6)	4585(3)	670(2)	42(1) *
C(19)	3829(8)	5453(3)	1253(3)	38(2) *
S(20)	3190(3)	6011(1)	2318(1)	58(1) *
C(21)	5726(9)	7030(4)	2453(3)	57(2) *
C(22)	6889(9)	6936(4)	1723(3)	52(2) *
N(23)	5792(7)	6060(3)	1063(2)	42(1) *
O(24)	6934(6)	160(3)	10818(2)	55(1) *
C(25)	5103(9)	705(4)	9305(4)	61(2) *
C(26)	7365(9)	446(4)	9896(4)	65(2) *
O(27)	568(10)	6049(4)	5376(5)	127(3) *
C(28)	665(19)	4222(6)	5536(6)	140(6) *
C(29)	2154(13)	5333(7)	5596(8)	185(6) *

$$U_{eq} = (1/3)\sum_i \sum_j U_{ij}\, a_i^* a_j^*\, a_i \cdot a_j$$

Hydrogen atom coordinates (X 10^4) for SSTDI

Parent atom	H	x/a	y/b	z/c
O(2)	H(2)	10711(68)	61(33)	8330(30)
C(4)	H(41)	6256	699	6549
C(4)	H(42)	8306	1807	6797
C(5)	H(51)	7736	287	5128
C(5)	H(52)	9696	1421	5371
N(8)	H(8)	6931	1043	3671
C(10)	H(10)	2236	2551	4109
C(11)	H(11)	127	3447	2894
C(13)	H(13)	4262	2548	983
C(14)	H(14)	6347	1628	2182
C(21)	H(21)	6247	7615	3006
C(22)	H(22)	8400	7444	1664
N(23)	H(23)	6438	5889	468
C(25)	H(251)	5393	870	8651
C(25)	H(252)	4714	1346	9652
C(26)	H(261)	8752	1075	10003
C(26)	H(262)	7810	-173	9537
C(28)	H(281)	-502	4237	6010
C(28)	H(282)	1760	3707	5750
C(29)	H(291)	3360	5333	5164
C(29)	H(292)	3182	5563	6300

TABLE 7 c (ii) Anisotropic thermal paramaters for non-hydrogen atoms in SSTDI with e.s.d.'s in parentheses

Anisotropic atoms have thermal parameters ($\text{Å}^2 \times 10^3$) of the form :

$$T=\exp(-2\pi^2(U_{11}h^2a^{*2}+U_{22}k^2b^{*2}+U_{33}l^2c^{*2}+2U_{23}klb^*c^*+2U_{13}hla^*c^*+2U_{12}hka^*b^*)) \times 10^3.$$

Atom	U11	U22	U33	U23	U13	U12
O(1)	77(3)	86(3)	45(2)	19(2)	20(2)	55(2)
O(2)	68(2)	86(3)	33(2)	19(2)	11(2)	42(2)
C(3)	46(3)	42(3)	36(3)	7(2)	7(2)	12(2)
C(4)	48(3)	51(3)	37(3)	7(2)	2(2)	20(2)
C(5)	51(3)	56(3)	37(3)	12(2)	6(2)	23(2)
C(6)	50(3)	48(3)	40(3)	13(2)	7(2)	18(2)
O(7)	85(3)	99(3)	37(2)	20(2)	18(2)	62(2)
N(8)	55(2)	49(2)	31(2)	9(2)	7(2)	29(2)
C(9)	45(3)	39(3)	33(2)	9(2)	7(2)	16(2)
C(10)	51(3)	63(3)	37(3)	18(2)	18(2)	28(2)
C(11)	45(3)	60(3)	45(3)	17(2)	13(2)	30(2)
C(12)	33(2)	44(3)	39(3)	15(2)	4(2)	9(2)
C(13)	55(3)	57(3)	38(3)	15(2)	13(2)	25(3)
C(14)	52(3)	51(3)	38(3)	8(2)	11(2)	29(2)
S(15)	46(1)	57(1)	45(1)	24(1)	5(1)	17(1)
O(16)	45(2)	87(3)	76(3)	44(2)	25(2)	36(2)
O(17)	75(3)	62(2)	53(2)	15(2)	-18(2)	0(2)
N(18)	51(2)	44(2)	34(2)	10(2)	8(2)	15(2)
C(19)	45(3)	44(3)	32(2)	16(2)	9(2)	23(2)
S(20)	73(1)	69(1)	43(1)	4(1)	25(1)	28(1)
C(21)	70(4)	53(3)	47(3)	-4(3)	8(3)	21(3)
C(22)	62(3)	43(3)	52(3)	6(2)	5(3)	19(3)
N(23)	51(2)	44(2)	35(2)	4(2)	11(2)	17(2)
O(24)	55(2)	76(2)	38(2)	16(2)	1(2)	26(2)
C(25)	67(4)	77(4)	47(3)	31(3)	13(3)	28(3)
C(26)	68(4)	82(4)	54(3)	28(3)	13(3)	25(3)
O(27)	137(5)	83(4)	159(6)	-16(4)	21(4)	38(3)
C(28)	262(12)	134(8)	60(5)	27(5)	35(7)	124(8)
C(29)	75(5)	109(7)	326(14)	-73(8)	-56(7)	47(5)

TABLE 7 c (iii) Bond lengths (Angstrom) with e.s.d.'s in parentheses for SSTDI

O(1)	- C(3)	1.195(6)
O(2)	- C(3)	1.312(5)
C(3)	- C(4)	1.507(7)
C(4)	- C(5)	1.510(6)
C(5)	- C(6)	1.514(7)
C(6)	- O(7)	1.214(7)
C(6)	- N(8)	1.355(5)
N(8)	- C(9)	1.410(5)
C(9)	- C(10)	1.384(7)
C(9)	- C(14)	1.383(6)
C(10)	- C(11)	1.384(7)
C(11)	- C(12)	1.357(6)
C(12)	- C(13)	1.385(7)
C(12)	- S(15)	1.771(4)
C(13)	- C(14)	1.382(6)
S(15)	- O(16)	1.440(4)
S(15)	- O(17)	1.435(3)
S(15)	- N(18)	1.592(4)
N(18)	- C(19)	1.321(5)
C(19)	- S(20)	1.740(5)
C(19)	- N(23)	1.322(6)
S(20)	- C(21)	1.730(5)
C(21)	- C(22)	1.331(7)
C(22)	- N(23)	1.372(5)
O(24)	- C(26)	1.432(7)
C(25)	- C(26)	1.491(7)
C(25)	- $O(24)^{i}$	1.424(6)
O(27)	- C(29)	1.40(1)
C(28)	- C(29)	1.51(1)
C(28)	- $O(27)^{ii}$	1.33(1)

Symmetry code : (i) 1-x, -y, 2-z (ii) -x, 1-y, 1-z

TABLE 7 c (iv) Bond angles (degrees) with e.s.d.'s in parentheses for **SSTDI**

O(1)	- C(3)	- O(2)	123.4(5)
O(2)	- C(3)	- C(4)	111.1(4)
O(1)	- C(3)	- C(4)	125.6(4)
C(3)	- C(4)	- C(5)	113.9(4)
C(4)	- C(5)	- C(6)	110.9(4)
C(5)	- C(6)	- N(8)	113.0(4)
C(5)	- C(6)	- O(7)	122.7(4)
O(7)	- C(6)	- N(8)	124.2(5)
C(6)	- N(8)	- C(9)	127.7(4)
N(8)	- C(9)	- C(14)	116.7(4)
N(8)	- C(9)	- C(10)	123.9(4)
C(10)	- C(9)	- C(14)	119.5(4)
C(9)	- C(10)	- C(11)	119.6(4)
C(10)	- C(11)	- C(12)	120.9(5)
C(11)	- C(12)	- S(15)	120.5(4)
C(11)	- C(12)	- C(13)	120.2(4)
C(13)	- C(12)	- S(15)	119.3(4)
C(12)	- C(13)	- C(14)	119.5(4)
C(9)	- C(14)	- C(13)	120.4(5)
C(12)	- S(15)	- N(18)	105.2(2)
C(12)	- S(15)	- O(17)	108.1(3)
C(12)	- S(15)	- O(16)	106.8(2)
O(17)	- S(15)	- N(18)	105.4(2)
O(16)	- S(15)	- N(18)	112.4(3)
O(16)	- S(15)	- O(17)	118.2(3)
S(15)	- N(18)	- C(19)	121.5(3)
N(18)	- C(19)	- N(23)	121.4(4)
N(18)	- C(19)	- S(20)	129.6(4)
S(20)	- C(19)	- N(23)	109.0(3)
C(19)	- S(20)	- C(21)	90.8(3)
S(20)	- C(21)	- C(22)	111.2(4)
C(21)	- C(22)	- N(23)	112.5(5)
C(19)	- N(23)	- C(22)	116.5(4)
O(24)	- C(26)	- C(25)	110.4(5)
C(26)	- O(24)	- C(25)^{i}	110.7(4)
C(26)	- C(25)	- O(24)^{i}	111.5(5)
O(27)	- C(29)	- C(28)	109.3(7)
C(29)	- O(27)	- C(28)^{ii}	108.4(7)
C(29)	- C(28)	- O(27)^{ii}	107.5(7)

Symmetry code : (i) 1-x, -y, 2-z (ii) -x, 1-y, 1-z

TABLE 7 c (V) Torsion angles (degrees) with e.s.d.'s in parentheses for **SSTDI**

(RIGHT-HAND RULE,KLYNE & PRELOG.(1960).EXPERIENTIA,16,521)
(E.S.D.'S, FOLLOWING STANFORD & WASER,ACTA CRYST.(1972).A28,213)

O(2)	- C(3)	- C(4)	- C(5)	-177.7(4)
O(1)	- C(3)	- C(4)	- C(5)	3.8(7)
C(3)	- C(4)	- C(5)	- C(6)	178.0(4)
C(4)	- C(5)	- C(6)	- O(7)	4.7(7)
C(4)	- C(5)	- C(6)	- N(8)	-173.3(4)
C(5)	- C(6)	- N(8)	- C(9)	-173.1(4)
O(7)	- C(6)	- N(8)	- C(9)	9.0(8)
C(6)	- N(8)	- C(9)	- C(10)	-13.5(8)
C(6)	- N(8)	- C(9)	- C(14)	165.8(5)
N(8)	- C(9)	- C(14)	- C(13)	-177.3(4)
N(8)	- C(9)	- C(10)	- C(11)	177.5(5)
C(10)	- C(9)	- C(14)	- C(13)	2.0(7)
C(14)	- C(9)	- C(10)	- C(11)	-1.7(7)
C(9)	- C(10)	- C(11)	- C(12)	0.6(8)
C(10)	- C(11)	- C(12)	- C(13)	0.4(7)
C(10)	- C(11)	- C(12)	- S(15)	-178.0(4)
C(11)	- C(12)	- S(15)	- O(16)	3.5(5)
C(11)	- C(12)	- S(15)	- O(17)	-124.6(4)
C(11)	- C(12)	- S(15)	- N(18)	123.1(4)
C(11)	- C(12)	- C(13)	- C(14)	-0.2(7)
C(13)	- C(12)	- S(15)	- O(16)	-174.9(4)
C(13)	- C(12)	- S(15)	- O(17)	57.0(5)
C(13)	- C(12)	- S(15)	- N(18)	-55.3(4)
S(15)	- C(12)	- C(13)	- C(14)	178.2(4)
C(12)	- C(13)	- C(14)	- C(9)	-1.0(7)
C(12)	- S(15)	- N(18)	- C(19)	-74.0(4)
O(17)	- S(15)	- N(18)	- C(19)	171.8(4)
O(16)	- S(15)	- N(18)	- C(19)	41.8(5)
S(15)	- N(18)	- C(19)	- S(20)	-9.5(6)
S(15)	- N(18)	- C(19)	- N(23)	171.8(4)
N(18)	- C(19)	- N(23)	- C(22)	-179.4(4)
N(18)	- C(19)	- S(20)	- C(21)	179.6(5)
S(20)	- C(19)	- N(23)	- C(22)	1.7(5)
N(23)	- C(19)	- S(20)	- C(21)	-1.5(4)
C(19)	- S(20)	- C(21)	- C(22)	1.1(4)
S(20)	- C(21)	- C(22)	- N(23)	-0.4(6)
C(21)	- C(22)	- N(23)	- C(19)	-0.9(7)
C(25)	- C(26)	- O(24)	- C(25)^{i}	56.0(6)
O(24)	- C(26)	- C(25)	- O(24)^{i}	-56.5(6)
C(26)	- O(24)	- C(25)^{i}	- C(26)^{i}	-56.7(6)
C(28)	- C(29)	- O(27)	- C(28)^{ii}	-63.2(9)
O(27)	- C(29)	- C(28)	- O(27)^{ii}	62.6(9)
C(29)	- O(27)	- C(28)^{ii}	- C(29)^{ii}	62.0(9)

TABLE 7 d (i) Fractional atomic coordinates (x 10^4)
and Thermal Parameters ($Å^2$ x 10^3)
with E.s.d.'s in parentheses for **SSTBU**

Atom	x/a	y/b	z/c	Uiso/Uequiv(*)
O(1)	17227(5)	7505(6)	4270(4)	94(2) *
O(2)	17128(5)	9723(5)	3416(3)	79(2) *
C(3)	16468(6)	8545(6)	3990(4)	52(2) *
C(4)	14709(6)	8521(5)	4158(3)	45(2) *
C(5)	14053(6)	7246(6)	4974(4)	54(2) *
C(6)	12282(6)	7105(5)	5172(3)	46(2) *
O(7)	11444(4)	7889(5)	4719(3)	70(2) *
N(8)	11705(5)	6020(5)	5934(3)	49(1) *
C(9)	10148(6)	5582(6)	6329(3)	46(2) *
C(10)	9850(6)	4483(6)	7146(4)	55(2) *
C(11)	8370(6)	4021(6)	7588(3)	51(2) *
C(12)	7093(6)	4647(5)	7224(3)	40(2) *
C(13)	7368(6)	5711(6)	6397(3)	49(2) *
C(14)	8884(6)	6172(6)	5944(3)	51(2) *
S(15)	5161(1)	4130(1)	7814(1)	41(0) *
O(16)	4125(4)	4691(4)	7167(2)	53(1) *
O(17)	5125(4)	2548(4)	8159(2)	55(1) *
N(18)	4837(5)	4924(4)	8794(2)	41(1) *
C(19)	4470(5)	6359(5)	8796(3)	37(1) *
S(20)	4052(2)	7677(1)	7868(1)	52(1) *
C(21)	3802(7)	9055(6)	8642(4)	60(2) *
C(22)	3965(7)	8498(5)	9531(4)	53(2) *
N(23)	4357(5)	6991(4)	9614(3)	45(1) *
O(24)	9789(5)	475(7)	6825(4)	109(3) *
C(25)	8578(11)	-442(10)	7379(6)	109(3)
C(26)	9483(9)	-1292(15)	8120(7)	201(6)
C(27)	8321(12)	-1897(22)	9070(8)	319(12)
C(28)	9227(17)	-2782(16)	9798(7)	215(6)

$$U_{eq} = (1/3) \sum_i \sum_j U_{ij} a_i^* a_j^* a_i \cdot a_j$$

Hydrogen atom coordinates ($x10^4$)

Parent atom	H	x/a	y/b	z/c
O(2)	H(2)	18230(19)	9671(38)	3538(32)
C(4)	H(41)	14299	9510	4355
C(4)	H(42)	14369	8352	3540
C(5)	H(51)	14381	7445	5590
C(5)	H(52)	14510	6272	4780
N(8)	H(8)	12516	5461	6254
C(10)	H(10)	10760	4022	7414
C(11)	H(11)	8191	3230	8176
C(13)	H(13)	6456	6152	6124
C(14)	H(14)	9071	6932	5338
C(21)	H(21)	3564	10135	8439
C(22)	H(22)	3820	9104	10092
N(23)	H(23)	4542	6417	10242
O(24)	H(24)	9604(69)	617(102)	6135(22)
C(25)	H(251)	7677	146	7701
C(25)	H(252)	8171	-1152	6984
C(26)	H(261)	10228	-552	8292
C(26)	H(262)	10093	-2119	7830
C(27)	H(271)	7719	-1087	9363
C(27)	H(272)	7561	-2643	8894
C(28)	H(281)	8470	-3204	10408
C(28)	H(282)	9987	-2067	9967
C(28)	H(283)	9829	-3623	9498

TABLE 7 d (ii) Anisotropic thermal parameters for non-hydrogen atoms in **SSTBU** with e.s.d.'s in parentheses

Anisotropic atoms have thermal parameters ($Å^2 \times 10^3$) of the form

$$T=\exp(-2\pi^2(U_{11}h^2a^{*2}+U_{22}k^2b^{*2}+U_{33}l^2c^{*2}+2U_{23}klb^*c^*+2U_{13}hla^*c^*+2U_{12}hka^*b^*)) \times 10^3,$$

Atom	U11	U22	U33	U23	U13	U12
O(1)	48(2)	111(4)	108(3)	48(3)	-21(2)	17(2)
O(2)	46(2)	82(3)	99(3)	38(2)	-20(2)	4(2)
C(3)	42(3)	64(3)	49(3)	8(2)	-15(2)	13(2)
C(4)	42(3)	49(3)	46(2)	-3(2)	-13(2)	14(2)
C(5)	44(3)	61(3)	53(3)	9(2)	-12(2)	12(3)
C(6)	42(3)	53(3)	46(3)	0(2)	-15(2)	14(2)
O(7)	44(2)	77(3)	81(3)	29(2)	-22(2)	12(2)
N(8)	34(2)	61(3)	49(2)	8(2)	-9(2)	14(2)
C(9)	36(3)	58(3)	47(3)	-7(2)	-12(2)	17(2)
C(10)	43(3)	62(3)	57(3)	10(2)	-14(2)	21(3)
C(11)	49(3)	53(3)	50(3)	8(2)	-15(2)	16(2)
C(12)	44(3)	42(2)	36(2)	-3(2)	-12(2)	10(2)
C(13)	39(3)	63(3)	46(3)	6(2)	-18(2)	11(2)
C(14)	44(3)	64(3)	44(3)	14(2)	-17(2)	10(2)
S(15)	44(1)	40(1)	40(1)	-4(1)	-13(1)	6(1)
O(16)	45(2)	70(2)	49(2)	-7(2)	-20(2)	6(2)
O(17)	67(2)	37(2)	61(2)	-4(2)	-11(2)	2(2)
N(18)	49(2)	37(2)	38(2)	0(2)	-13(2)	13(2)
C(19)	33(2)	41(2)	39(2)	0(2)	-11(2)	6(2)
S(20)	65(1)	44(1)	47(1)	5(1)	-20(1)	15(1)
C(21)	74(4)	39(3)	67(3)	-5(2)	-18(3)	18(3)
C(22)	62(3)	38(3)	62(3)	-6(2)	-16(3)	13(2)
N(23)	53(3)	37(2)	46(2)	-3(2)	-13(2)	12(2)
O(24)	53(3)	133(5)	124(4)	52(4)	-27(3)	8(3)

TABLE 7 d (iii) Bond lengths (Angstrom) with E.s.d.'s in parentheses for **SSTBU**

O(1)	- C(3)	1.200(7)
O(2)	- C(3)	1.296(6)
C(3)	- C(4)	1.491(7)
C(4)	- C(5)	1.527(6)
C(5)	- C(6)	1.503(7)
C(6)	- O(7)	1.215(6)
C(6)	- N(8)	1.360(6)
N(8)	- C(9)	1.387(6)
C(9)	- C(10)	1.389(7)
C(9)	- C(14)	1.383(7)
C(10)	- C(11)	1.347(7)
C(11)	- C(12)	1.389(7)
C(12)	- C(13)	1.380(6)
C(12)	- S(15)	1.745(5)
C(13)	- C(14)	1.377(7)
S(15)	- O(16)	1.440(4)
S(15)	- O(17)	1.430(4)
S(15)	- N(18)	1.604(4)
N(18)	- C(19)	1.317(6)
C(19)	- S(20)	1.727(5)
C(19)	- N(23)	1.331(6)
S(20)	- C(21)	1.731(6)
C(21)	- C(22)	1.314(8)
C(22)	- N(23)	1.379(6)
O(24)	- C(25)	1.38(1)
C(25)	- C(26)	1.54(1)
C(26)	- C(27)	1.54(1)
C(27)	- C(28)	1.54(2)

TABLE 7 d (iv) Bond angles (degrees) with E.s.d.'s in parentheses for SSTBU

O(1)	- C(3)	- O(2)	121.9(6)
O(2)	- C(3)	- C(4)	114.1(5)
O(1)	- C(3)	- C(4)	123.6(5)
C(3)	- C(4)	- C(5)	109.5(5)
C(4)	- C(5)	- C(6)	113.2(5)
C(5)	- C(6)	- N(8)	112.7(5)
C(5)	- C(6)	- O(7)	124.2(5)
O(7)	- C(6)	- N(8)	123.2(5)
C(6)	- N(8)	- C(9)	129.0(5)
N(8)	- C(9)	- C(14)	123.3(4)
N(8)	- C(9)	- C(10)	118.2(5)
C(10)	- C(9)	- C(14)	118.6(5)
C(9)	- C(10)	- C(11)	121.9(5)
C(10)	- C(11)	- C(12)	119.8(5)
C(11)	- C(12)	- S(15)	120.7(4)
C(11)	- C(12)	- C(13)	119.1(5)
C(13)	- C(12)	- S(15)	120.1(4)
C(12)	- C(13)	- C(14)	120.9(5)
C(9)	- C(14)	- C(13)	119.7(4)
C(12)	- S(15)	- N(18)	105.6(2)
C(12)	- S(15)	- O(17)	108.1(3)
C(12)	- S(15)	- O(16)	108.0(2)
O(17)	- S(15)	- N(18)	104.5(2)
O(16)	- S(15)	- N(18)	111.3(2)
O(16)	- S(15)	- O(17)	118.6(3)
S(15)	- N(18)	- C(19)	122.8(3)
N(18)	- C(19)	- N(23)	120.1(4)
N(18)	- C(19)	- S(20)	130.3(3)
S(20)	- C(19)	- N(23)	109.6(3)
C(19)	- S(20)	- C(21)	90.8(3)
S(20)	- C(21)	- C(22)	111.2(4)
C(21)	- C(22)	- N(23)	113.2(5)
C(19)	- N(23)	- C(22)	115.1(4)
O(24)	- C(25)	- C(26)	98.8(7)
C(25)	- C(26)	- C(27)	109.9(8)
C(26)	- C(27)	- C(28)	109.6(9)

TABLE 7 d (v) Torsion angles (degrees) with E.s.d.'s in parentheses for SSTBU

(RIGHT-HAND RULE, KLYNE & PRELOG. (1960). EXPERIENTIA, 16, 521)
(E.s.d.'s, FOLLOWING STANFORD & WASER, ACTA CRYST. (1972). A28, 213)

O(2)	- C(3)	- C(4)	- C(5)	-170.2(5)
O(1)	- C(3)	- C(4)	- C(5)	17.3(8)
C(3)	- C(4)	- C(5)	- C(6)	-178.2(4)
C(4)	- C(5)	- C(6)	- O(7)	1.8(8)
C(4)	- C(5)	- C(6)	- N(8)	-176.7(4)
C(5)	- C(6)	- N(8)	- C(9)	179.5(5)
O(7)	- C(6)	- N(8)	- C(9)	0.9(9)
C(6)	- N(8)	- C(9)	- C(10)	-176.9(5)
C(6)	- N(8)	- C(9)	- C(14)	3.8(9)
N(8)	- C(9)	- C(14)	- C(13)	-178.1(5)
N(8)	- C(9)	- C(10)	- C(11)	178.4(5)
C(10)	- C(9)	- C(14)	- C(13)	2.6(8)
C(14)	- C(9)	- C(10)	- C(11)	-2.3(8)
C(9)	- C(10)	- C(11)	- C(12)	0.2(8)
C(10)	- C(11)	- C(12)	- C(13)	1.6(8)
C(10)	- C(11)	- C(12)	- S(15)	-177.2(4)
C(11)	- C(12)	- S(15)	- O(16)	-167.7(4)
C(11)	- C(12)	- S(15)	- O(17)	-38.2(5)
C(11)	- C(12)	- S(15)	- N(18)	73.2(5)
C(11)	- C(12)	- C(13)	- C(14)	-1.2(8)
C(13)	- C(12)	- S(15)	- O(16)	13.7(5)
C(13)	- C(12)	- S(15)	- O(17)	143.1(4)
C(13)	- C(12)	- S(15)	- N(18)	-105.5(4)
S(15)	- C(12)	- C(13)	- C(14)	177.6(4)
C(12)	- C(13)	- C(14)	- C(9)	-1.0(8)
C(12)	- S(15)	- N(18)	- C(19)	79.9(4)
O(17)	- S(15)	- N(18)	- C(19)	-166.2(4)
O(16)	- S(15)	- N(18)	- C(19)	-37.1(5)
S(15)	- N(18)	- C(19)	- S(20)	7.1(7)
S(15)	- N(18)	- C(19)	- N(23)	-173.8(4)
N(18)	- C(19)	- N(23)	- C(22)	-179.9(5)
N(18)	- C(19)	- S(20)	- C(21)	-179.1(5)
S(20)	- C(19)	- N(23)	- C(22)	-0.7(6)
N(23)	- C(19)	- S(20)	- C(21)	1.8(4)
C(19)	- S(20)	- C(21)	- C(22)	-2.5(5)
S(20)	- C(21)	- C(22)	- N(23)	2.6(7)
C(21)	- C(22)	- N(23)	- C(19)	-1.3(7)
O(24)	- C(25)	- C(26)	- C(27)	156.2(9)
C(25)	- C(26)	- C(27)	- C(28)	178.5(10)

TABLE 7 e (i) Fractional atomic coordinates (x 10^4) and Thermal Parameters (Å^2 x 10^3) with e.s.d.'s in parentheses for **SSTPE**

Atom	x/a	y/b	z/c	Uiso/Uequiv(*)
O(1)	17109(12)	7496(12)	4329(8)	111(6) *
O(2)	16927(11)	9643(11)	3450(7)	91(4) *
C(3)	16303(16)	8476(15)	4023(8)	60(5) *
C(4)	14579(14)	8467(13)	4201(8)	58(5) *
C(5)	13982(14)	7167(14)	4983(8)	61(5) *
C(6)	12211(15)	7059(15)	5192(8)	60(5) *
O(7)	11344(10)	7869(10)	4764(6)	81(4) *
N(8)	11688(12)	5940(11)	5923(7)	60(4) *
C(9)	10100(15)	5513(13)	6322(8)	53(5) *
C(10)	9848(16)	4430(12)	7146(8)	57(6) *
C(11)	8382(15)	3969(13)	7555(8)	53(5) *
C(12)	7088(14)	4637(12)	7208(7)	46(5) *
C(13)	7299(14)	5697(12)	6409(7)	48(5) *
C(14)	8768(15)	6154(13)	5965(8)	57(5) *
S(15)	5180(4)	4141(3)	7823(2)	47(1) *
O(16)	4116(9)	4726(8)	7197(5)	56(3) *
O(17)	5180(10)	2569(8)	8153(5)	59(3) *
N(18)	4915(11)	4906(9)	8782(6)	46(4) *
C(19)	4546(13)	6338(12)	8796(8)	47(5) *
S(20)	4140(4)	7689(3)	7870(2)	60(1) *
C(21)	3925(16)	9018(12)	8619(8)	66(5) *
C(22)	4052(15)	8457(12)	9503(9)	61(6) *
N(23)	4372(11)	7011(9)	9611(6)	47(4) *
O(24)	9940(13)	603(14)	6773(9)	119(6) *
C(25)	8752(25)	-320(20)	7155(11)	130(7)
C(26)	9357(27)	-1644(22)	7784(11)	212(12)
C(27)	8664(33)	-1542(24)	8858(10)	270(15)
C(28)	9072(32)	-2979(16)	9474(12)	215(12)
C(29)	9457(45)	-2575(29)	10424(16)	324(19)

$$U_{eq} = (1/3) \sum_i \sum_j U_{ij} a_i^* a_j^* a_i \cdot a_j$$

Hydrogen atom coordinates (x 10^4) for **SSTPE**

Parent atom	H	x/a	y/b	z/c
O(2)	H(2)	18096	9658	3406
C(4)	H(41)	14164	9435	4427
C(4)	H(42)	14216	8335	3591
C(5)	H(51)	14337	7323	5592
C(5)	H(52)	14437	6212	4758
N(8)	H(8)	12517	5353	6211
C(10)	H(10)	10762	4001	7426
C(11)	H(11)	8213	3149	8108
C(13)	H(13)	6365	6134	6154
C(14)	H(14)	8917	6933	5388
C(21)	H(21)	3723	10100	8418
C(22)	H(22)	3916	9077	10050
N(23)	H(23)	4479	6451	10250
O(24)	H(24)	9655(222)	1158(178)	6174(77)
C(25)	H(251)	7919	244	7559
C(25)	H(252)	8329	-663	6614
C(26)	H(261)	10511	-1655	7654
C(26)	H(262)	8958	-2597	7596
C(27)	H(271)	9152	-647	9044
C(27)	H(272)	7508	-1406	8952
C(28)	H(281)	10046	-3444	9108
C(28)	H(282)	8187	-3679	9596
C(29)	H(291)	9682	-3495	10832
C(29)	H(292)	8457	-2087	10786
C(29)	H(293)	10317	-1852	10299

TABLE 7 e (ii) Anisotropic thermal parameters for non-hydrogen atoms in **SSTPE**

Anisotropic atoms have thermal parameters $(A^2 \times 10^3)$ of the form :

$$T=\exp(-2\pi^2(U_{11}h^2a^{*2}+U_{22}k^2b^{*2}+U_{33}l^2c^{*2}+2U_{23}klb^*c^*+2U_{13}hla^*c^*+2U_{12}hka^*b^*)) \times 10^3,$$

Atom	U11	U22	U33	U23	U13	U12
O(1)	68(8)	116(9)	135(10)	55(7)	-29(7)	11(7)
O(2)	61(7)	102(7)	104(8)	40(6)	-29(6)	-15(6)
C(3)	57(10)	71(9)	47(7)	14(7)	-15(7)	2(8)
C(4)	47(9)	69(8)	57(8)	12(7)	-20(7)	-3(7)
C(5)	49(9)	78(9)	53(8)	14(7)	-13(7)	0(7)
C(6)	44(9)	92(10)	44(7)	7(7)	-16(7)	-5(8)
O(7)	55(6)	99(7)	79(6)	43(5)	-23(5)	5(5)
N(8)	56(8)	72(7)	49(6)	13(5)	-19(6)	4(6)
C(9)	54(9)	62(8)	42(7)	0(6)	-8(6)	-4(7)
C(10)	69(10)	48(7)	52(7)	0(6)	-15(7)	18(7)
C(11)	62(9)	54(8)	36(6)	5(6)	0(7)	11(7)
C(12)	51(8)	56(7)	38(6)	-9(6)	-16(6)	1(6)
C(13)	45(8)	59(8)	39(6)	0(6)	-12(6)	9(6)
C(14)	52(9)	75(9)	44(7)	13(6)	-22(7)	0(7)
S(15)	57(2)	45(2)	43(2)	-5(1)	-15(2)	-1(2)
O(16)	48(5)	67(5)	56(5)	-2(4)	-23(4)	-2(4)
O(17)	84(7)	43(4)	53(5)	-7(4)	-11(5)	-5(4)
N(18)	60(7)	36(5)	41(5)	5(4)	-15(5)	5(5)
C(19)	44(8)	47(7)	52(7)	14(6)	-20(6)	-9(6)
S(20)	77(3)	55(2)	50(2)	12(2)	-24(2)	4(2)
C(21)	91(11)	34(7)	68(9)	6(6)	-15(8)	15(7)
C(22)	84(11)	41(7)	65(8)	-18(6)	-22(8)	9(7)
N(23)	66(7)	41(5)	35(5)	-1(4)	-15(5)	9(5)
O(24)	62(7)	140(10)	140(10)	70(8)	-39(7)	-21(7)

TABLE 7 e (iii) Bond lengths (Angstrom) with e.s.d.'s in parentheses for **SSTPE**

O(1)	- C(3)	1.20(1)
O(2)	- C(3)	1.31(1)
C(3)	- C(4)	1.46(1)
C(4)	- C(5)	1.53(1)
C(5)	- C(6)	1.51(1)
C(6)	- O(7)	1.22(1)
C(6)	- N(8)	1.37(1)
N(8)	- C(9)	1.43(1)
C(9)	- C(10)	1.41(1)
C(9)	- C(14)	1.43(1)
C(10)	- C(11)	1.34(1)
C(11)	- C(12)	1.40(1)
C(12)	- C(13)	1.37(1)
C(12)	- S(15)	1.75(1)
C(13)	- C(14)	1.36(1)
S(15)	- O(16)	1.446(9)
S(15)	- O(17)	1.434(8)
S(15)	- N(18)	1.577(9)
N(18)	- C(19)	1.32(1)
C(19)	- S(20)	1.76(1)
C(19)	- N(23)	1.35(1)
S(20)	- C(21)	1.68(1)
C(21)	- C(22)	1.32(1)
C(22)	- N(23)	1.32(1)
O(24)	- C(25)	1.33(2)
C(25)	- C(26)	1.54(2)
C(26)	- C(27)	1.54(2)
C(27)	- C(28)	1.54(2)
C(28)	- C(29)	1.54(3)

TABLE 7 e (iv) Bond angles (degrees) with e.s.d.'s in parentheses for SSTPE

O(1)	- C(3)	- O(2)	121(1)
O(2)	- C(3)	- C(4)	114(1)
O(1)	- C(3)	- C(4)	125(1)
C(3)	- C(4)	- C(5)	109(1)
C(4)	- C(5)	- C(6)	112(1)
C(5)	- C(6)	- N(8)	112(1)
C(5)	- C(6)	- O(7)	124(1)
O(7)	- C(6)	- N(8)	124(1)
C(6)	- N(8)	- C(9)	128(1)
N(8)	- C(9)	- C(14)	124(1)
N(8)	- C(9)	- C(10)	117(1)
C(10)	- C(9)	- C(14)	119(1)
C(9)	- C(10)	- C(11)	120(1)
C(10)	- C(11)	- C(12)	120(1)
C(11)	- C(12)	- S(15)	119(1)
C(11)	- C(12)	- C(13)	121(1)
C(13)	- C(12)	- S(15)	120(1)
C(12)	- C(13)	- C(14)	120(1)
C(9)	- C(14)	- C(13)	120(1)
C(12)	- S(15)	- N(18)	106(1)
C(12)	- S(15)	- O(17)	108(1)
C(12)	- S(15)	- O(16)	107.0(5)
O(17)	- S(15)	- N(18)	104.2(4)
O(16)	- S(15)	- N(18)	111.9(5)
O(16)	- S(15)	- O(17)	119.4(5)
S(15)	- N(18)	- C(19)	122(1)
N(18)	- C(19)	- N(23)	122(1)
N(18)	- C(19)	- S(20)	130(1)
S(20)	- C(19)	- N(23)	107(1)
C(19)	- S(20)	- C(21)	91(1)
S(20)	- C(21)	- C(22)	112(1)
C(21)	- C(22)	- N(23)	115(1)
C(19)	- N(23)	- C(22)	115(1)
O(24)	- C(25)	- C(26)	109(2)
C(25)	- C(26)	- C(27)	110(2)
C(26)	- C(27)	- C(28)	109(1)
C(27)	- C(28)	- C(29)	109(1)

TABLE 7 e (V) Torsion angles (degrees) with e.s.d.'s in parentheses for SSTPE

(RIGHT-HAND RULE,KLYNE & PRELOG.(1960).EXPERIENTIA,16,521)
(E.S.D.'S, FOLLOWING STANFORD & WASER,ACTA CRYST.(1972).A28,213)

O(2)	- C(3)	- C(4)	- C(5)	-172(1)
O(1)	- C(3)	- C(4)	- C(5)	11(2)
C(3)	- C(4)	- C(5)	- C(6)	-179(1)
C(4)	- C(5)	- C(6)	- O(7)	3(2)
C(4)	- C(5)	- C(6)	- N(8)	-177(1)
C(5)	- C(6)	- N(8)	- C(9)	180(1)
O(7)	- C(6)	- N(8)	- C(9)	0(2)
C(6)	- N(8)	- C(9)	- C(10)	-173(1)
C(6)	- N(8)	- C(9)	- C(14)	4(2)
N(8)	- C(9)	- C(14)	- C(13)	-178(1)
N(8)	- C(9)	- C(10)	- C(11)	-180(1)
C(10)	- C(9)	- C(14)	- C(13)	-1(2)
C(14)	- C(9)	- C(10)	- C(11)	3(2)
C(9)	- C(10)	- C(11)	- C(12)	-5(2)
C(10)	- C(11)	- C(12)	- C(13)	4(2)
C(10)	- C(11)	- C(12)	- S(15)	-174(1)
C(11)	- C(12)	- S(15)	- O(16)	-167(1)
C(11)	- C(12)	- S(15)	- O(17)	-38(1)
C(11)	- C(12)	- S(15)	- N(18)	73(1)
C(11)	- C(12)	- C(13)	- C(14)	-3(2)
C(13)	- C(12)	- S(15)	- O(16)	14(1)
C(13)	- C(12)	- S(15)	- O(17)	144(1)
C(13)	- C(12)	- S(15)	- N(18)	-105(1)
S(15)	- C(12)	- C(13)	- C(14)	176(1)
C(12)	- C(13)	- C(14)	- C(9)	1(2)
C(12)	- S(15)	- N(18)	- C(19)	80(1)
O(17)	- S(15)	- N(18)	- C(19)	-167(1)
O(16)	- S(15)	- N(18)	- C(19)	-37(1)
S(15)	- N(18)	- C(19)	- S(20)	4(2)
S(15)	- N(18)	- C(19)	- N(23)	-178(1)
N(18)	- C(19)	- N(23)	- C(22)	178(1)
N(18)	- C(19)	- S(20)	- C(21)	-178(1)
S(20)	- C(19)	- N(23)	- C(22)	-4(1)
N(23)	- C(19)	- S(20)	- C(21)	4(1)
C(19)	- S(20)	- C(21)	- C(22)	-4(1)
S(20)	- C(21)	- C(22)	- N(23)	2(1)
C(21)	- C(22)	- N(23)	- C(19)	1(2)
O(24)	- C(25)	- C(26)	- C(27)	110(2)
C(25)	- C(26)	- C(27)	- C(28)	172(2)
C(26)	- C(27)	- C(28)	- C(29)	142(2)

REFERENCES

128. G.L. Blutt, L.W. Deady, M.F. McKay: *J. Heterocycl. Chem.*, **25**, 321, (1988).

129. F.J. Farris, G. Weber, C.C. Chiang, I.C. Paul: *J. Am. Chem. Soc.*, **100**, 4469, (1978).

130. C. Bianchini, D. Masi, C. Mealli: *Inorg. Chem.*, **23**, 2838, (1984).

131. C.L. Raston, G.L. Rowbottom, A.H. White: *J. Chem. Soc.*, Dalton Transactions, 1372 (1981).

CHAPTER 8

SUBCONTENTS

8. X-RAY POWDER DIFFRACTION

8.1 GENERAL

The powder diffraction patterns have played the single most important role in identifying the starting materials, the solvated forms and the products of desolvation i.e. polymorphs. For example, the pattern for the monohydrate shown below in **Figure 8.1 (a)** corresponds very closely with the published XRD pattern quoted earlier and shown in **Figure 1.29 (b).** The commercial product was accordingly identified as *H I* according to the nomenclature by Rodier *et al*[87]. Further confirmation of this was obtained by inserting the single crystal X-ray data of Rodier *et al* into the program LAZY PULVERIX and calculating the X-ray powder pattern. This pattern overlapped that of **Figure 8.1(a)**.

Similarly, the polymorph resulting from dehydration of H I was identified as *MOD III* of the six anhydrous forms characterized by Burger *et al*[86] (see **Figure 1.29 (a)**).

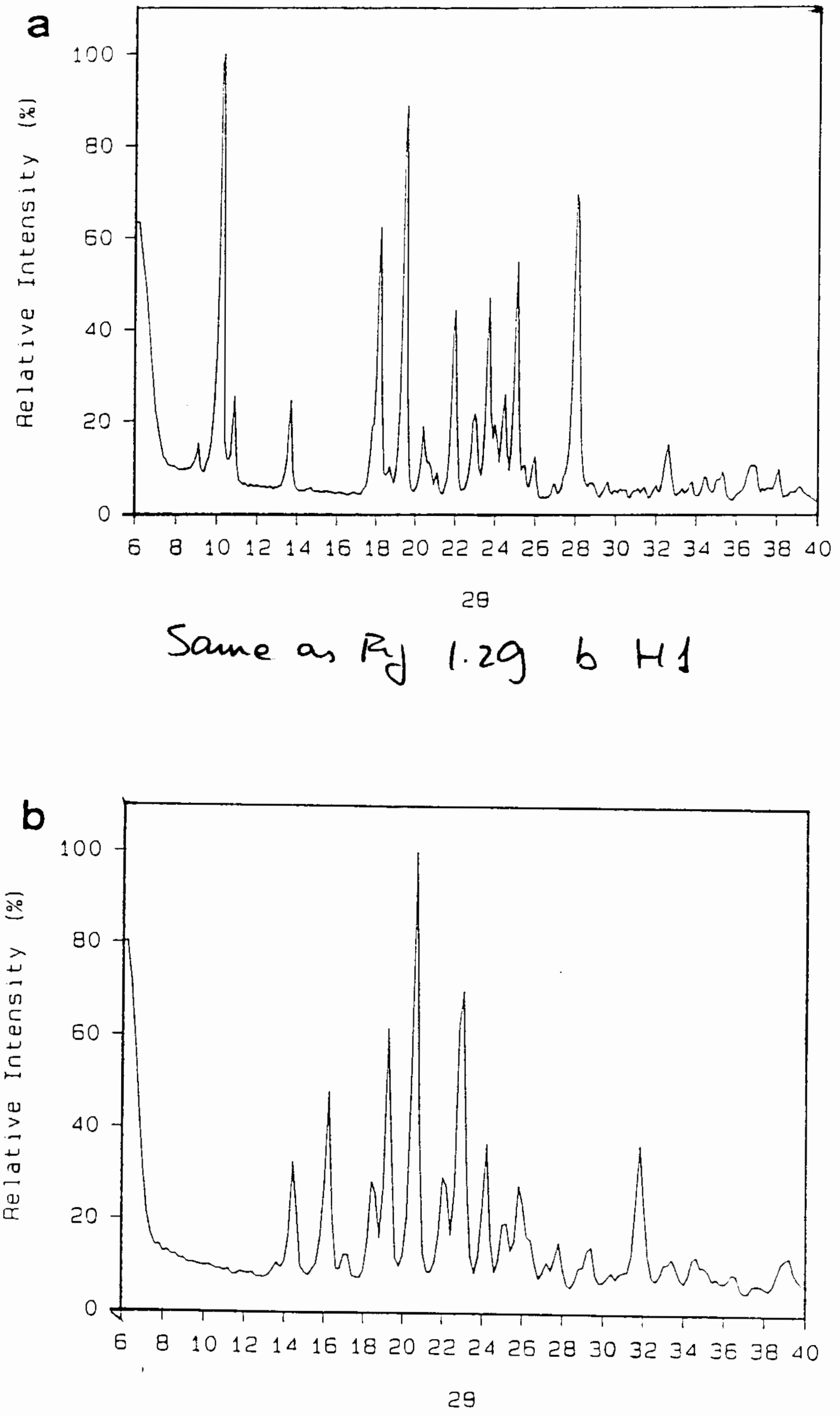

Same as Fig 1.29 b H1

Figure 8.1 (a) XRD pattern for the commercial product in the monohydrate form, **SSTHYD** and (b) the product of dehydration, **SSTANHYD**.

8.2 THE SOLVATES AND THEIR DESOLVATION PRODUCTS

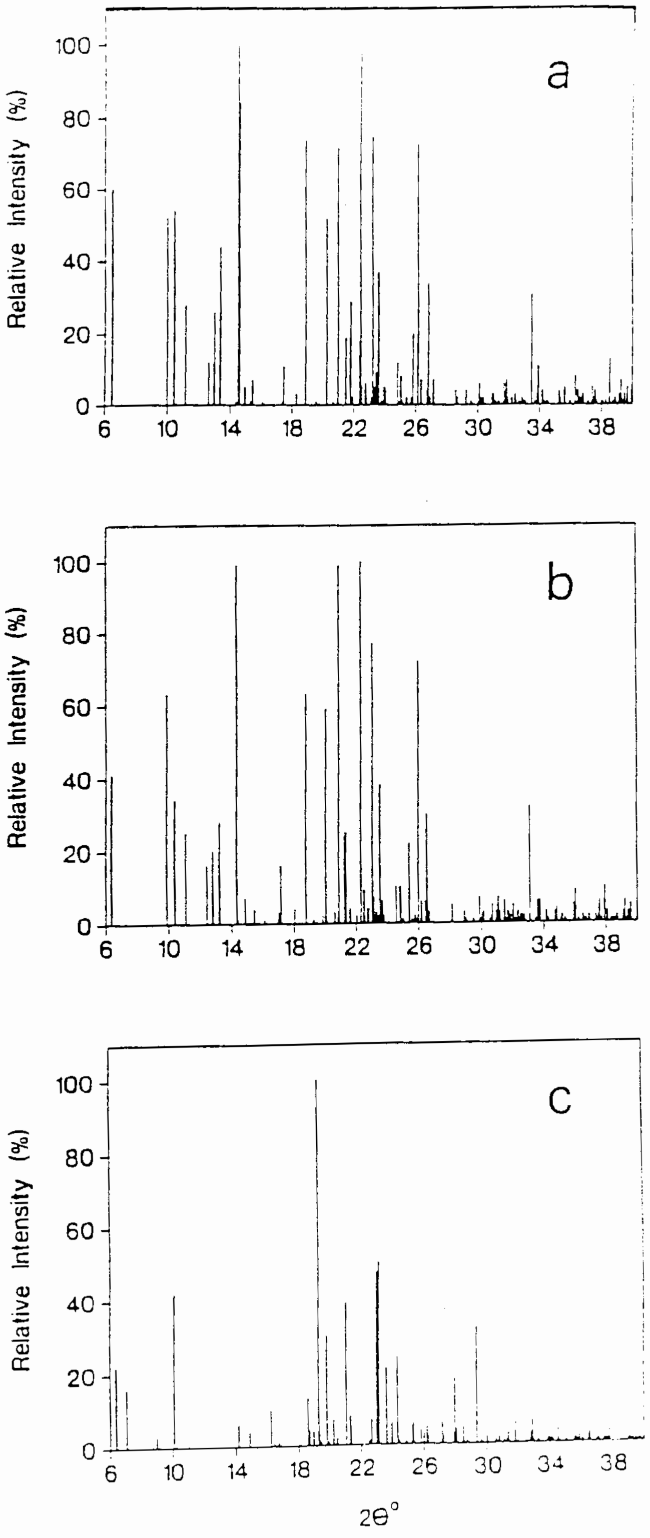

Figure 8.2 (a)-(c) The simulated XRD patterns for SST~~EI~~BU, SST~~BU~~PE and SST~~PE~~DI respectively.

8.3 DISCUSSION

It was commented earlier upon the fact that the outcome of the XRD experiments can be seriously affected by factors like the preferred crystal orientation of the micro crystallites. Another drawback in obtaining the truly representative powder patterns of polymorphic species is the grinding step that must be carried out prior to the experiment. The latter step may itself cause polymorphic transformation.

In the case of **SST** solvates some serious difficulties were experienced in obtaining reproducible powder patterns despite several repeated trials. In view of the large surface area exposed during the grinding step, possible volatilization was blamed for the inconsistency. Therefore, the final XRD patterns were obtained by computation from the single crystal data **(see Figure 8.2 a-c)**. This was done in accordance with the recommendation by Bar and Bernstein that the computed spectra represent the best model for the pure material[132]. On the basis of all the spectra obtained the near isomorphism of **SSTBU** and **SSTPE** was again evident in the remarkably similar XRD patterns while a different pattern was obtained for **SSTDI** **(Figure 8.2 a-c)**. Furthermore, the desolvation of **SSTBU** resulted in the solid whose powder pattern matches that of *MOD IV* published by Burger *et al*[86].

Thus an interesting sequence of reactions involving **SSTBU** was established starting with the raw material as follows:-

$$\mathit{H\ I} \xrightarrow[-H_2O]{\text{Heat}} \mathit{MOD\ III} \xrightarrow{\text{BuOH}} \textbf{SSTBU} \xrightarrow[-\text{BuOH}]{\text{Heat}} \mathit{MOD\ IV}$$

This type of polymorphic interconversion scheme could be of great utility to the pharmaceutical chemist wishing to follow a simple route to achieve a specific polymorphic product.

On the other hand the desolvation of **SSTPE** yielded a powder pattern matching none of the published ones. However, many of the observed peaks had counterparts in the patterns for MODS II-IV, thus indicating that the desolvation of **SSTPE** probably yields a mixture of these polymorphs.

It was not possible to obtain powder patterns for the desolvation product of **SSTDI** since the final desolvation step in this species happens almost simultaneously with the host melting (see **Figure** 5.3(e)).

REFERENCES

132. I.Bar, J. Bernstein: *J.Pharm.Sci.*, **74**, 255, (1985).

CHAPTER 9

SUBCONTENTS

9. SELECTIVITY

9.1 GENERAL

In some cases a host compound can be economically very attractive if it displays some selectivity towards one particular isomer in a mixture. Host compounds often discriminate between isomers on the basis of the very subtle features such as molecular shapes, sizes and electronic properties thus acting as highly specific molecular filters. This phenomenon has received wide attention from a number of research workers[133-135]. Zeolites, a large family of aluminosilicates are industrially attractive due to their applications in shape-selective catalysis, molecular sieving and their uses as storage media for certain types of nuclear waste. The secret of their selective binding abilities lies in the intricate networks of cavities and channels within their highly stable structures[1,136-137].

9.2 THE GLC EXPERIMENT

This experiment was meant to investigate whether SST would discriminate between 1-butanol and 1-pentanol given their aliphatic and homologous chain structures.

The solutions were prepared according to the method described in **section** 3.~~7~~9 of **"EXPERIMENTAL PROCEDURES"**. (sealed vials) The choice, preparation of the column as well as the optimization of the chromatographic conditions were performed according to the literature[138-140].

9.3 THE GLC RESULTS

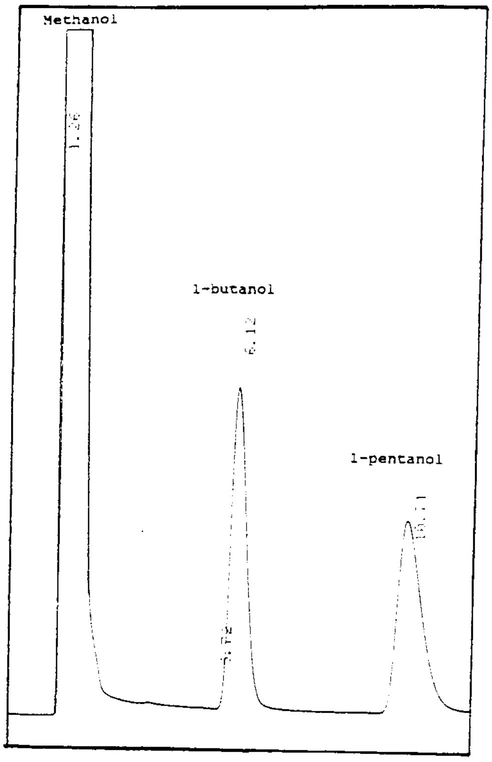

9.3 (a) A Typical trace obtained using a Spectra-Physics SP4290 Integrator.

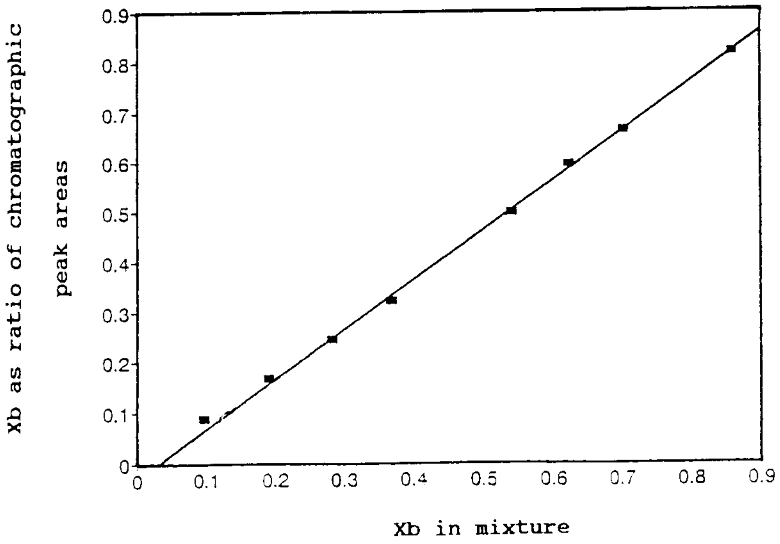

(b) A plot of Calibration Curve for 1-butanol. This curve indicates that the column and other chromatographic conditions that were optimized produce a linear response for 1-butanol.

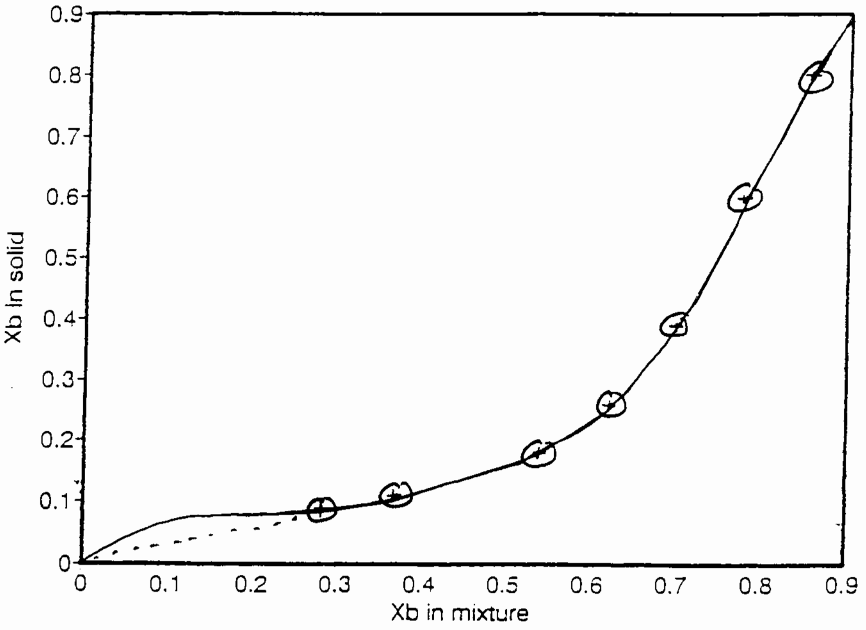

9.3 (c) A plot of Selectivity Curve for 1-butanol in crystal *versus* 1-butanol in mixture.

9.4 DISCUSSION

It is evident from the calibration curve in **Figure 9.3 (b)** that the detector used i.e. Flame Ionization Detector (FID) produces a linear response for this system.

From the selectivity curve it is evident that **SST** does not discriminate between 1-butanol and 1-pentanol in mixtures of low mole fraction $X_b(X_b \leq 0.10)$. However, in the case of equimolar proportions of solvents the drug displays a strong preference for 1-pentanol and this preference varies in the range of $0.10 \leq X_b \leq 0.90$. This result is somewhat curious given the isostructural nature of the two solvents. It would seem that the extension of the chain structure by one methylene group is strongly detectable by the nature of voids in the SST host structure.

REFERENCES

133. P. Strazewski, J. Lipkowski: *Pol.J.Chem.,* **53**, 1869, (1979).

134. F. Toda: "Isolation and Optical Resolution of Materials Utilizing Inclusion Crystallization" in "Topics in Chemistry". **140**, 43, Springer-Verlag, Berlin Heidelberg, (1987).

135. M. Newcombe, J.L. Toner, R.C. Helgeson, D.J. Cram: *J.Am.Chem.Soc.,* **101**, 4941, (1979).

136. T. Way: *Roy.Soc.,* **11**, 313, (1850).

137. C.Li-feng, L.V.C. Rees: *Zeolites.,* **8**, 310, (1988).

138. H.M. McNair, E.J. Bonelli in "Basic Gas Chromatography", p.158, Walnut Creek, CA:Varian Aerograph, (1978).

139. C.F. Poole, S.A. Schuette: "Contemporary Practice of Chromatography", p.60, Elsevier, (1984).

140. G.H. Jeffrey, J. Bassett, J. Mendham, R.C. Denney: "Vogel's Textbook of Quantitative Chemical Analysis", Longman Scientific and Technical, Fifth Ed., (1989).

CHAPTER 10

THE OVERALL CONCLUSION ON SST SOLVATES

10. THE OVERALL CONCLUSION ON SST SOLVATES

A comprehensive picture has emerged from the characterization studies of **SST** solvates. Based on their topological characteristics and modes of molecular associations it was possible to classify them as *"coordinato clathrates in a coordination-assisted host lattice"*.

The 1:1 H:G stoichiometries were evaluated and confirmed by TGA, microanalysis, density measurements and crystal structure solutions. The thermal behaviour of these compounds indicated that they are fairly stable clathrates. Clearly, there are hardly any discrepancies between the structural and thermodynamic results. ~~On the contrary, the success and lack of ambiguity in characterizing these compounds were attributed to a high degree of correlation between structure and thermodynamics.~~

Satisfactory results were obtained from the kinetic investigation of at least two of these compounds, namely **SSTBU** and **SSTPE**. The unusually high and similar activation energies for desolvation were rationalized in terms of both the extensive hydrogen bonding network found within these compounds as well as their isomorphous structures.

Of prime importance is the success with which polymorphism and pseudopolymorphism of **SST** was investigated. In particular, the interesting polymorphic interconversion scheme that was established for the desolvation of **SSTBU** can be regarded as a crucial probe in confirming the existence of the six polymorphs of **SST**. The success of pharmaceutical manoeuvering with **SST** in the solid state lies in the confidence and reproducibility with which its polymorphs can be manufactured. An example of this fact may be drawn from the polymorphs of the drug mebendazole quoted earlier in **CHAPTER 1**, where polymorphs should be properly characterized in order to clear the way for ensuring correct choice of the desired polymorph.

A potential industrial application of this study was tapped by the way of the competition experiments which provoked further academic questions about the phenomenon of inclusion in general i.e. *exactly which factors determine the selective inclusion of specific types of guest molecules?*

Hence, this study can be regarded as a contribution to the solid-state chemistry of the drug, succinylsulfathiazole.

CLASS B

(SULFATHIAZOLE SOLVATES)

CHAPTER 11

SUBCONTENTS

11. THERMAL ANALYSIS AND THE KINETICS OF DESOLVATION

11.1 GENERAL BACKGROUND

In pursuing the polymorphic and pseudopolymorphic study with sulfathiazole (**ST**), pyridine and its substituted derivatives were chosen as solvents of crystallization. This choice was made with the view to obtaining information about a more systematic inclusion trend. The rationale behind this was based on their structural and chemical characteristics such as planarity, the presence of a hetero-N atom and its basicity to act as a probe for possible host:guest coordination and the influence of the methyl substituents at different positions on the H:G binding strength. Several research workers have investigated the above factors with a variety of host compounds[141-145].

The only series of sulfathiazole solvates studied, namely those involving ketones, did not include single crystal X-ray studies[96]. So far, the only the crystal structure reported is that of the 1,4-dioxane solvate[97]. This scenario creates grounds for further scholarly inquiry into the inclusion behaviour of sulfathiazole.

11.2 THE LAYOUT OF THIS CHAPTER

In essence, the compounds discussed here are those which were fully characterized, namely the **ST** solvates of pyridine, 2-methylpyridine (α-picoline) and

3-methylpyridine (ß-picoline). Problems of severe crystal decay were experienced during an attempt to collect the intensity data for **STPY26**; thus, only the thermal and XRD data are presented for this compound. On the other hand, the solvate of 4-methylpyridine yielded very poor quality thermal and XRD data and it was subsequently abandoned.

The thermal and kinetic data for all four compounds are presented and discussed simultaneously. For the compounds **STPY2** and **STPY26**, only the thermal data are presented and discussed since no kinetic data were obtained for them.

11.3 TGA-DSC THERMOGRAMS AND THE KINETIC CURVES FOR STPY AND STPY1

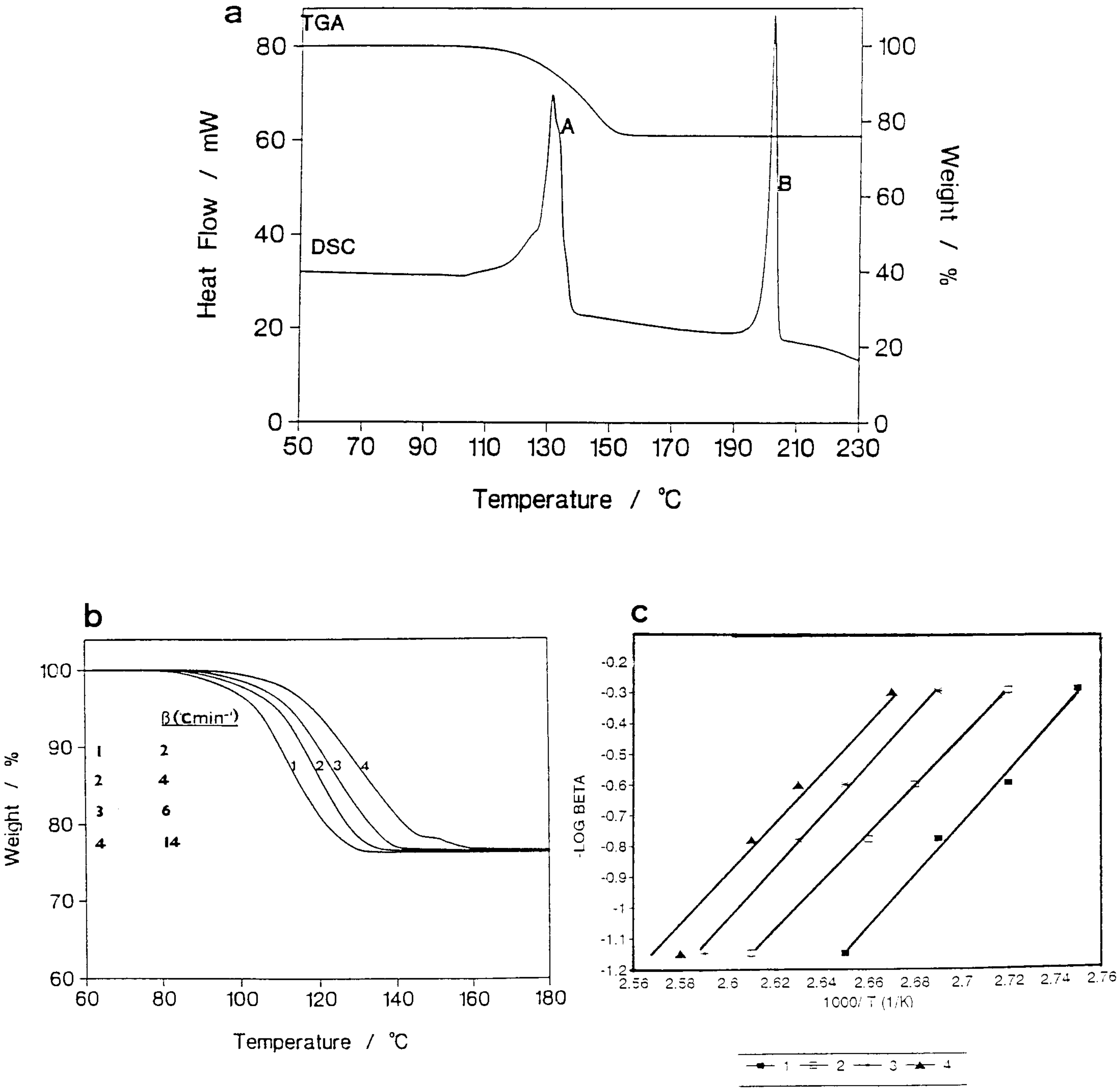

Figure 11.3.1 (a) TGA-DSC thermograms for STPY.
(b)-(c) Kinetic curves for STPY yielding Ea=150-170 $kJmol^{-1}$.

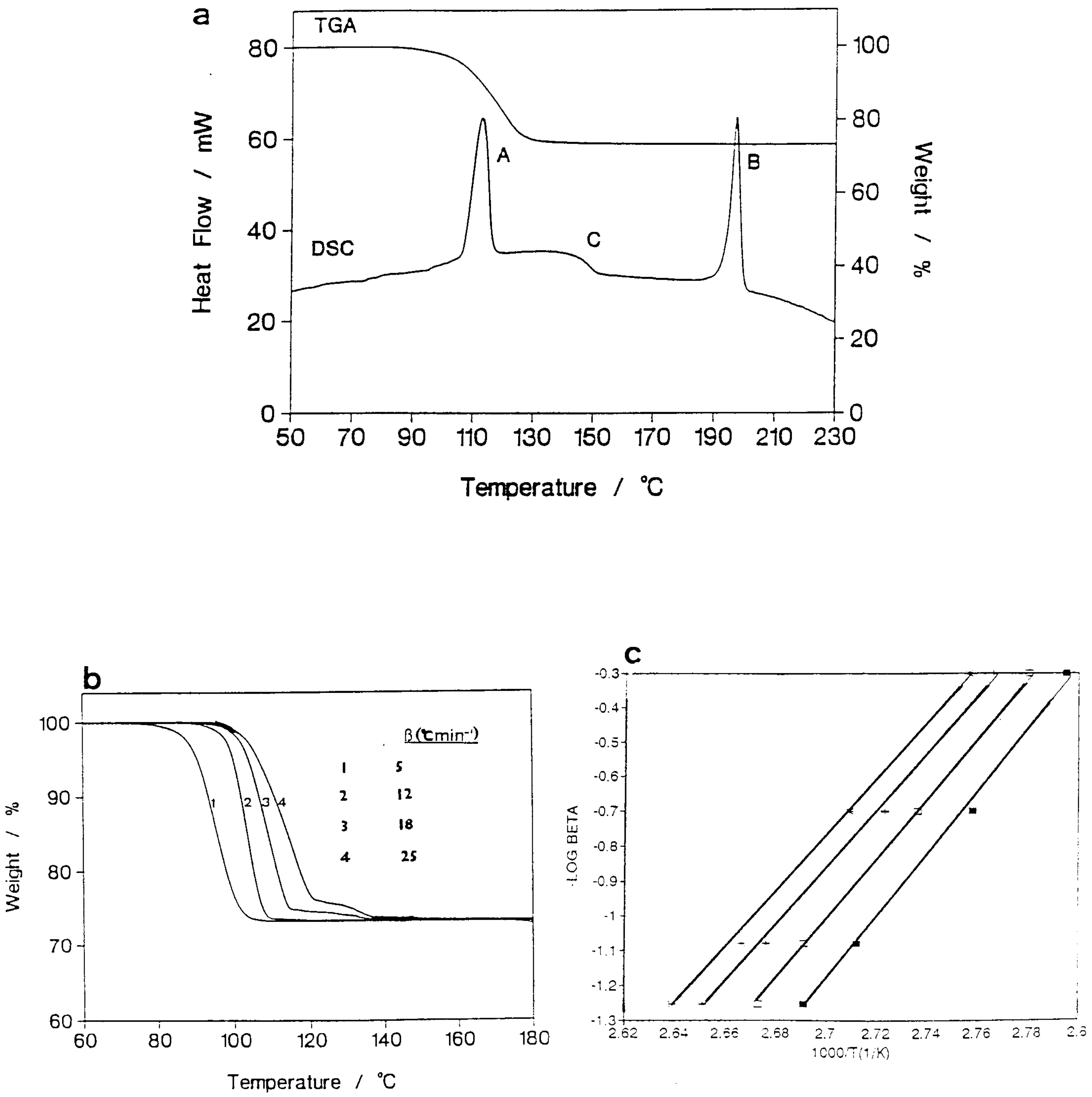

Figure 11.3.2 (a) TGA-DSC Thermograms for **STPY1**
(b)-(c) Kinetic curves for **STPY1** yielding
Ea=147-165 kJmol^{-1}.

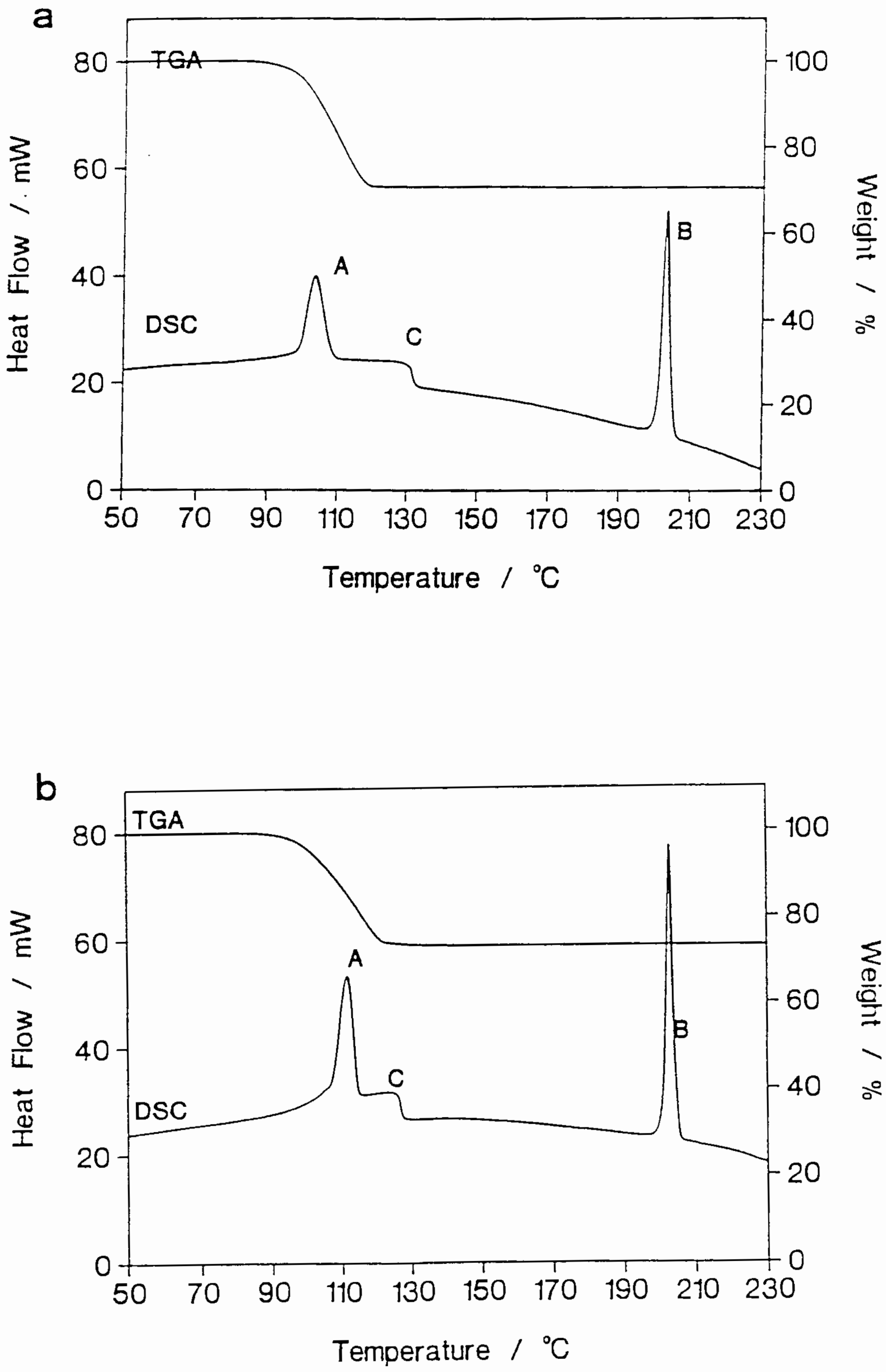

Figure 11.3.3 b (~~a~~) TGA-DSC thermograms for STPY2
a (~~b~~) TGA-DSC thermograms for STPY26.

11.4 TABULATION OF THERMAL AND KINETIC RESULTS

11.4.1 TGA Table of Results

	ONSET TEMP. AND OVERALL CALC WEIGHT LOSS FOR 1:1 H:G RATIO		DYNAMIC TGA KINETIC RESULTS
CODE NAME	T_{ons}(°C)	ΔW(%)	Ea (kJmol^{-1})
STPY	116.0	23.7	149-170
STPY1	99.0	26.5	147-165
STPY2	100.1	26.5	-
STPY26	90.0	29.6	-

11.4.2 DSC Table of Results

	PEAK A		PEAK B	
CODE NAME	T_{ons}(°C)	ΔH (kJmol^{-1})	T_{ons}(°C)	ΔH (kJmol^{-1})
STPY	124.0	41.5	200.0	23.4
STPY1	107.0	24.6	201.0	25.0
STPY2	105.4	26.7	193.9	22.0
STPY26	99.2	13.8	200.9	18.5

11.5 INTERPRETATION OF THERMAL AND KINETIC RESULTS

(i) STPY and STPY1 in Figures 11.3.1 (a)-(c) and 11.3.2 (a)-(c)

The single step desolvation and 1:1 H:G stoichiometries have been confirmed by TGA as follows:-

The expected weight losses (%) for 1:1 H:G ratios are 23.7 and 26.5 for **STPY** and **STPY1** respectively. Thus, the experimentally-determined values of 23.5 and 26.5% which are obviously in excellent agreement with the theoretical values did confirm a 1:1 inclusion.

For **STPY** the DSC onset temperature corresponding to solvent release (T_{ons}=124.0°C, see **Table 11.4.2**) is 9°C above the b.p. 115°C of pyridine, whereas **STPY1** loses its solvent at a temperature 22°C ~~above~~ below the b.p. 128°C of α-picoline. It is also noted that stronger H:G interactions are operating in **STPY** crystals with a higher enthalpy of solvent release, $\Delta H = 41.5\ kJmol^{-1}$. On the other hand, a lower enthalpy value 26.4 $kJmol^{-1}$ for desolvation in **STPY1** is an indication of weaker H:G interactions in the latter compound. This result appears to be inconsistent with the idea of linking enthalpies with hydrogen bonding strengths only. Thus, enthalpies should be considered as a measure of the sum total of all energy changes that occur during desolvation. Typically, correlation studies of thermodynamic parameters like enthalpies of desolvation with structural data such as hydrogen bond distances (Å) are conducted in trying to understand these salient molecular details.

For compounds **STPY** and **STPY1**, typically high and overlapping Ea values (see **Table 11.4.1**) were obtained and as such they did not give an intuitive indication of whether there is any kinetic difference in the desolvation processes between the two compounds. It is thus not easy to advance a reasonable physical interpretation of what is going on at the molecular level.

(ii) **STPY2** and **STPY26** in **Figures 11.3.3 (a)-(b)**

From theoretical % losses, 26.5 for **STPY2** and 29.6 for **STPY26** single-step desolvation and 1:1 H:G compositions were indicated by the TGA results which are consistent with the microanalytical and density measurements.

The peaks A and B on the DSC thermograms are attributed to the processes of solvent-release and host fusion respectively. However, it will be noted that there exists a persistent and rather broad ~~anomalous~~ peak C in **STPY1**, **STPY2** and **STPY26** solvates.

Attempts to elucidate this event involved heating the samples for several hours at the threshold temperature of desolvation and then obtaining the reproducible DSC and XRD pattern of the resulting species. No evidence of any polymorphic phase change was recorded. Instead, the XRD patterns that were obtained upon desolvation of all three compounds matched that of form I of **ST** (*Jamshed*)[95]. It was suggested that probably a short-lived metastable form is obtained upon desolvation which quickly reverts to the more stable Form I (Jamshed *et al*)[95].

These two compounds did not produce linear plots of -logß versus 1/T and thus they were not amenable to kinetic investigation by the method of Flynn and Wall[126]. No other method of studying kinetics was attempted.

REFERENCES

141. E. Weber, K.Skobridis, A. Wierig, L.J. Barbour, M.R. Caira, L.R. Nassimbeni: *Chem.Ber.* **126,** 1141, (1993).

142. L. Lavelle: *J.Chem.Soc.Dalton Trans,* 3511, (1992).

143. L. Lavelle, L.R. Nassimbeni, M.L. Niven, M.W. Taylor: *Acta Cryst.* **C45,** 591, (1989).

144. M.H. Moore, L.R. Nassimbeni, M.L. Niven: *Inorganica Chimica Acta,* **132,** 61, (1987).

145. D.R. Bond, G.E. Jackson, L.R. Nassimbeni: *S.Afr.J.Chem.* **36(1),** 19, (1983).

CHAPTER 12

SUBCONTENTS

12. POWDER XRD CHARACTERIZATION OF ST COMPOUNDS

12.1 NOTES ON THE DSC-XRD DUAL CHARACTERIZATION OF ST

Numerous workers have attempted to isolate and characterize the polymorphs of sulfathiazole[88-94, 146-155]. Not until recently[95], has there been a definite consensus about the number of its distinct polymorphic forms. It was imperative to identify the starting material in order to assign the polymorphs resulting from desolvation and get an idea of the extent and proliferation of phase changes brought about by inclusion. It was noted that neither the DSC nor the XRD technique was adequate by itself in elucidating the complicated polymorphism of sulfathiazole, but that the two should complement each other to eliminate ambiguities. Shown side-by-side below **(Figure 12.1 (a)-(b))** are the XRD diffractogram and DSC thermogram which enabled the identification of the starting drug material as Form III (Jamshed *et al*)[95], **cf.Figure 1.30.**

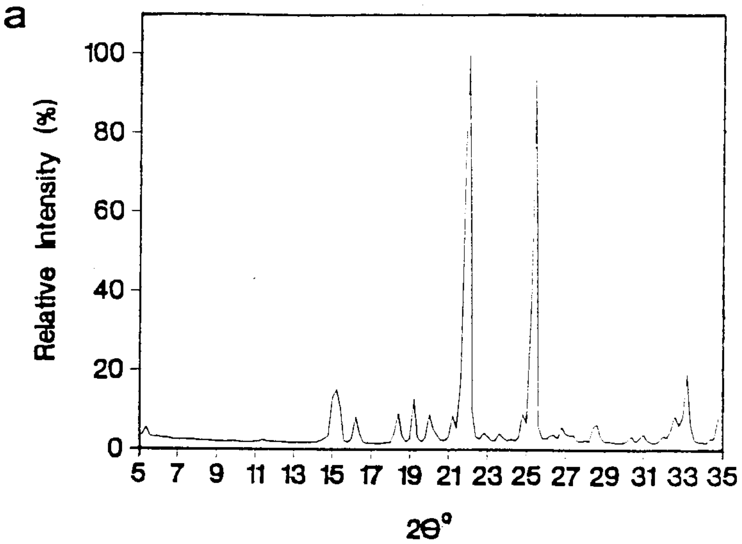

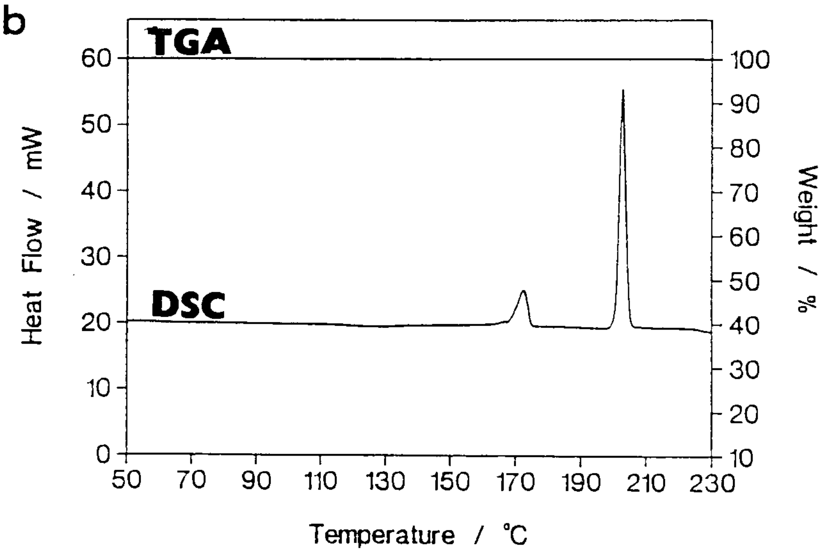

Figure 12.1 (a)-(b) X-ray powder pattern and the TG and DSC plots of the starting material - Sulfathiazole (Suppliers: Aldrich Chemical Company, *Inc*, *USA*)

This identification was rather tricky due to the close resemblance of the XRD patterns for Forms III and IV (see **Figure 1.30**) as well as the obscure melting points that were reported for these forms[136-155].

12.2 EXPERIMENTAL POWDER PATTERNS

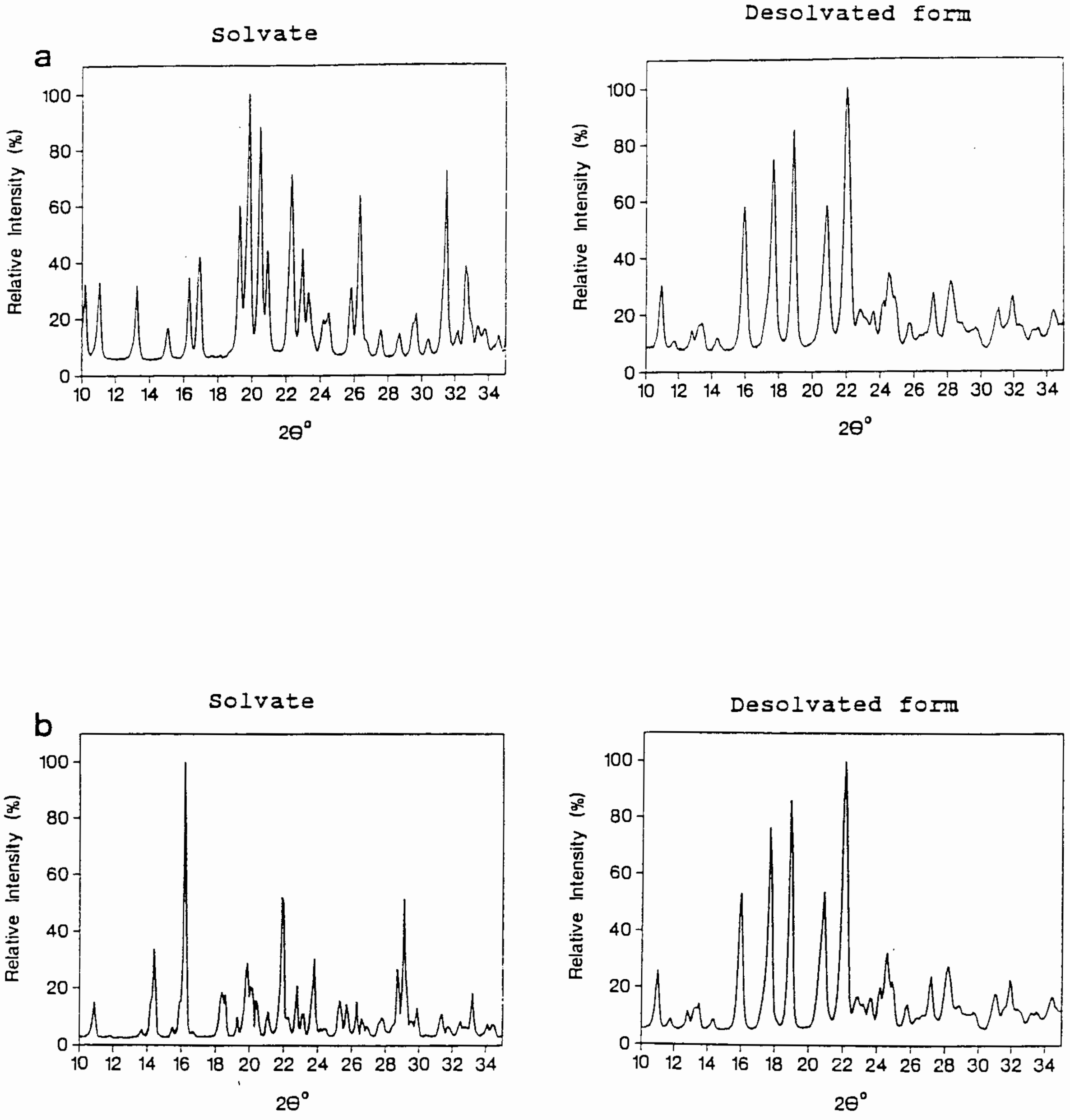

12.2.1 Experimental powder patterns of the solvates as well as the desolvated species for (a) **STPY** and (b) **STPY1**.

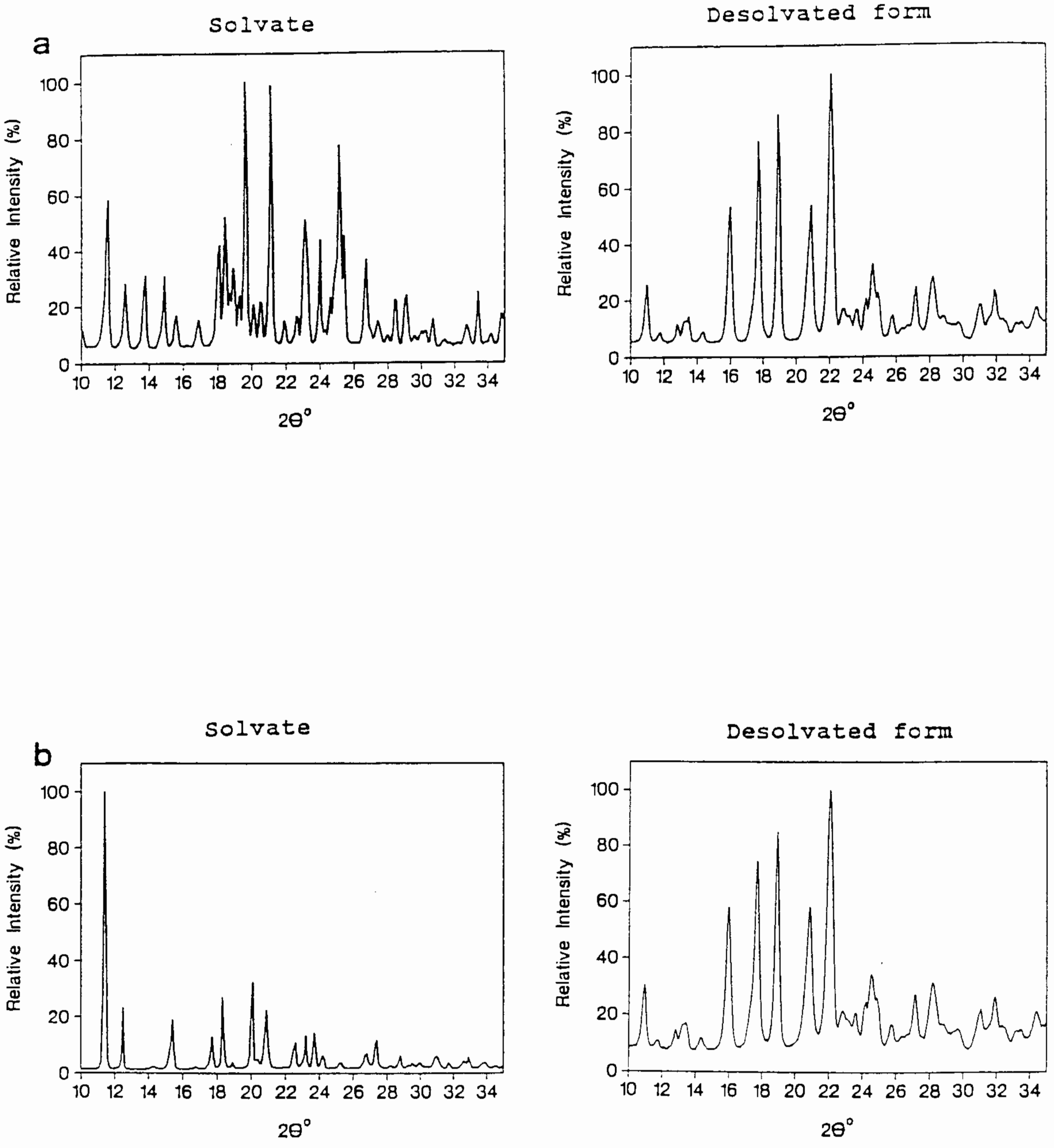

12.2.2 Experimental powder patterns of the solvates as well as the desolvated species for (a) **STPY2** and (b) **STPY26**.

12.3 DISCUSSION

A glance at the XRD patterns for the solvated species indicates that they are all evidently different. This is consistent with the single crystal X-ray analyses (discussed in **CHAPTER 13**) whereby the crystal packing modes have been found to be different in three of the solvates.

Furthermore, the good quality XRD patterns for solvates and their reproducibilities were indicative of the high degree of crystallinities and purities of these compounds. However, the XRD patterns for the desolvated species are common for all compounds: Form I (see **Figure 1.30**) is obtained upon the desolvation of all four compounds. Thus, a polymorphic interconversion scheme is established based on the experimental results as follows:-

$$\text{Form III} \xrightarrow[\text{solvents}]{\text{pyridine}} \begin{array}{c}\text{Four } \textbf{ST} \\ \text{solvates} \\ \text{of pyridines}\end{array} \xrightarrow{\text{heat}} \text{Form I}$$

Due to the subtle phase changes that occur at temperatures above 150°C i.e. after the process of solvent-release has taken place, it was further proposed that the other known polymorphic forms[95] were probably formed and could not be effectively identified using only DSC-XRD techniques and that they are metastable forms which quickly revert to the more stable Form I.

The evidence in support of this view was obtained from the desorption studies of the compound, **STPY26**. Some samples of **STPY26** showed a melting endotherm (DSC) at about 196°C which is the documented literature[150,154,156] melting point for Form II.

It was concluded from this study that the predominance of Form I as the only identifiable product of desorption is an indication of its stability compared to the other three polymorphic forms[95].

CHAPTER 13

STRUCTURE SOLUTIONS AND DESCRIPTIONS FOR ST SOLVATES

REFERENCES

146. D.C. Grove, G.L. Keenan: *J.Chem.Soc.,* **63,** 97, (1941).

147. H. Miyazaki: *Jap.J.Pharm.Chem.,* **19,** 133, (1947), *Chem.Abstr.* **45,** 3559h, (1947).

148. M. Kuhnert-Brandstätter, A. Martinek: *Mikrochim.Acta,* 909, (1965), *Chem.Abstr.,* **64,** 1403b, (1966).

149. R.J. Mesley, E.E. Houghton: *J.Pharm.Pharmacol.,* **19,** 295, (1967).

150. M.A. Moustafa, J.E. Carless: *J.Pharm.Pharmacol.,* **21,** 359, (1969).

151. E.G. Shami, P.D. Bernado, E.S. Rattie, L.J. Ravin: *J.Pharm.Sci.,* **61,** 1318, (1972).

152. M. Kanke, K. Sekiguchi: *Chem.Pharm.Bull.,* **21,** 871, (1973).

153. J.E. Carless, D. Jordan: *J.Pharm.Pharmacol.,* **26,** Suppl. 86P., (1974).

154. M. Lagas, C.F. Lerk: *Int.J.Pharm.,* **8,** 11, (1981).

155. A. Burger, R.D. Dialer: *Pharm.Acta Helv.,* **58,** 72, (1983).

156. S.S. Yang, J.K. Guillory: *J.Pharm.Sci.* **61,** 26, (1972).

CHAPTER 13

13.1 STRUCTURE SOLUTIONS AND DESCRIPTIONS FOR ST SOLVATES

13.1.1. GENERAL LAYOUT OF THIS CHAPTER

In contrast to the **SST** solvates where isormorphism and a number of other common structural features were encountered, the present series of compounds manifests an interesting structural variety which necessitates that each structure solution and description should be discussed independently of the others. The chapter is concluded with a comparison of the common, unusual and divergent structural trends that were identified among these compounds.

The presentation style is otherwise the same as that adopted in **CHAPTER SEVEN** with the tables of essential crystallographic information being appended at the end of the chapter as follows:-

TABLE 13a	Intensity Data Collection and Structure Refinements,	
TABLE 13b	Listing of Hydrogen bonds	
TABLE 13c	(i)	Fractional Atomic Coordinates,
	(ii)	Thermal Parameters,
	(iii)	Bond Lengths (Å)
	(iv)	Bond Angles (°), and
	(v)	Torsion Angles (°) for compound **STPY**.

Corresponding **TABLES 13d (i) - (v)** for compound **STPY1** and
TABLES 13e (i) - (v) for compound **STPY2**.

For convenience sake, the structure factor tables have been appended on the computer diskette as APPENDIX 2.

13.1.2 THE HOST COMPOUND - SULFATHIAZOLE

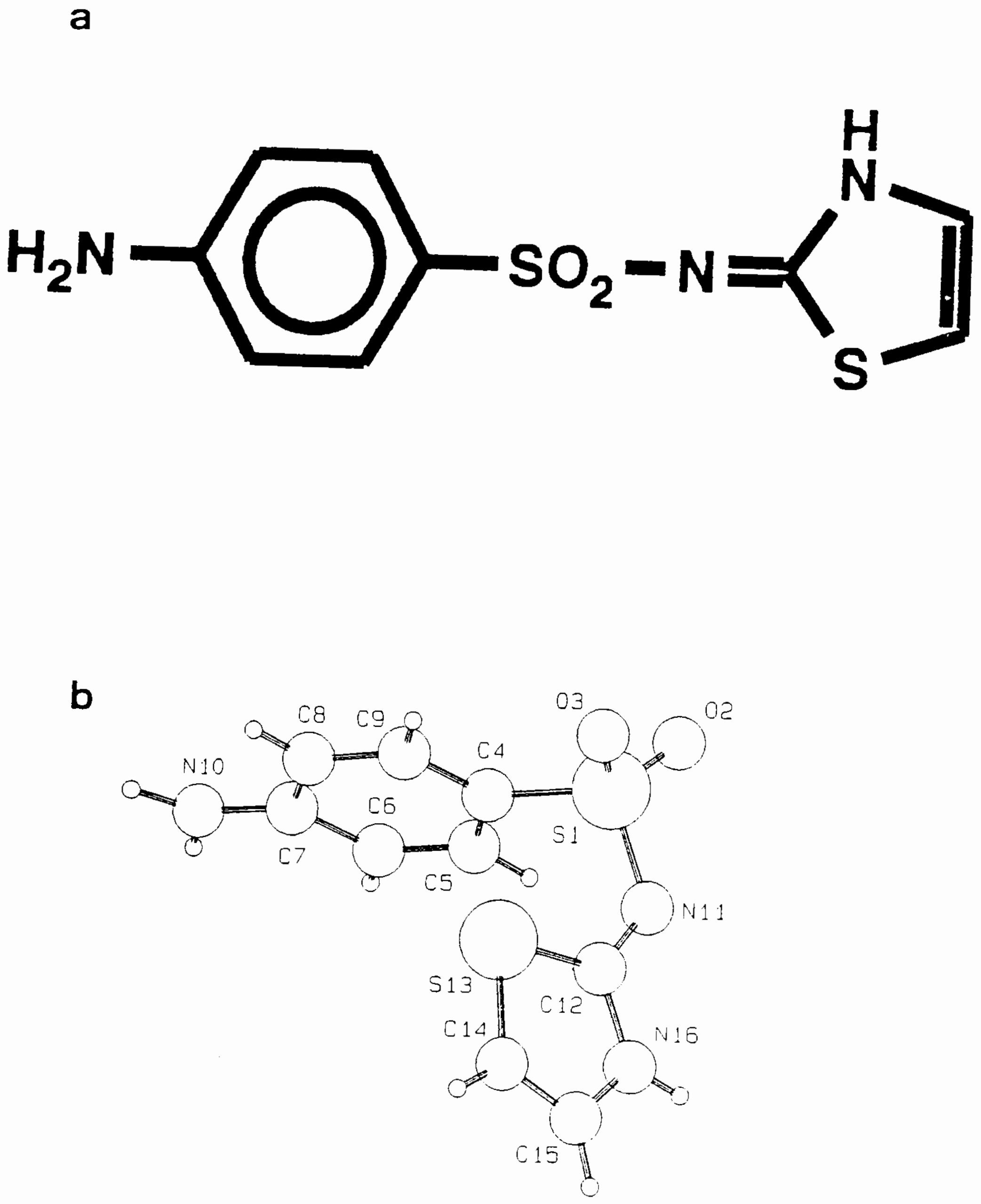

Figure 13.1.2 (a) A structural diagram of sulfathiazole and
(b) The molecular structure of **ST** obtained from the **STPY** crystal structure indicating the atomic nomenclature that was adopted in this study.

13.1.3 STRUCTURE SOLUTION AND REFINEMENT OF STPY

Large spear-shaped crystals were harvested for this compound. A suitable specimen was crushed and immersed in silicone oil so as to be examined in plane-polarized light under the microscope. The emergence of a uniaxial interference figure indicated that the crystal belongs to the tetragonal, trigonal or hexagonal system. The symmetry displayed by the oscillation and Weissenberg photographs *(4/m)* indicated a tetragonal space group. The only systematically absent reflections were 00l, l = 4n + 1, 2 or 3, thus implying two possible space groups in this system, namely $P4_1$ (no.76) or $P4_3$ (no.78)[157], which are enantiomorphously-related.

A single crystal was mounted in a 0.3mm Lindemann capillary tube containing mother liquor for intensity-data collection. Details of intensity-data collection appear in **Table 13a**. The reflections collected were h: 0 to 10, k: 0 to 10 and l: -24 to 24 in order to pursue the resolution of absolute structure.

The structure was solved by direct methods using program SHELX 86. Solution involved tangent refinement of the phases of 200 reflections with large (>1.2) E-values using 4516 unique triple phase relationships. The solution with lowest combined figure of merit, CFOM = 0.101, yielded an E-map which revealed 19 non-hydrogen atoms. These atoms were refined isotropically using the program SHELX 76.

The remaining 14 non-hydrogen atoms were located from subsequent weighted difference electron density ($\Delta\rho$) syntheses.

The hydrogen atoms which were located in $\Delta\rho$ maps were included in idealized positions in a riding model with C-H 1.00Å, except for the amino hydrogens, which were allowed to refine freely. Hydrogen atoms were treated isotropically with common variable U_{iso} thermal parameters assigned to chemically equivalent groups of atoms. Details of the final refinement appear also in **Table 13a.**

At this point an attempt to resolve the question of absolute structure was made by invoking the program SHELX 93[158]. This program treats the two sets of reflections hkl and hk$\bar{l}$ as being independent i.e. without merging symmetry-related reflections.

The refinement based on F_o^2 was carried out using the above-mentioned program. The weighted R-index obtained is wR2 = 0.238 which is notably higher than R1 = 0.0828 obtained by refining on F_0. The merits of the agreement index wR2 have been discussed by Sheldrick in the SHELX 93 manual. (See footnote for definition of wR2 below). The value S = 0.996 is the restrained goodness of fit that was obtained for all data.

Note: $wR2 = [\Sigma(w(F_o^2 - F_c^2)^2 / \Sigma(w(F_o^2)^2]^{\frac{1}{2}}$

Refinement of the structure in space group $P4_1$ yielded $x = 0.9001 \pm 0.2056$ for the Flack parameter[159], while refinement in space group $P4_3$ yielded $x = 0.0744 \pm 0.2046$. The expected value of x is zero within three esd's, for the correct absolute structure and it was therefore concluded that the crystal chosen for analysis belonged to $P4_3$. The final parameters reported in this text refer to this choice of space group.

13.1.4 DISCUSSION OF THE STPY STRUCTURE

The three main features of interest in this and related structures are:-

(i) The H:G relationships which occur commonly via the host (N-H)...N(guest) intermolecular hydrogen bond and possible correlation of the length of this bond with desolvation enthalpy values obtained from DSC measurements.

(ii) The nature of guest inclusion which involves occupation of either distinct channels or cavities within the crystal, and

(iii) Crystal and molecular packing in which the space group symmetry prescribes how the host and guest molecules should be orientated in relation to each other.

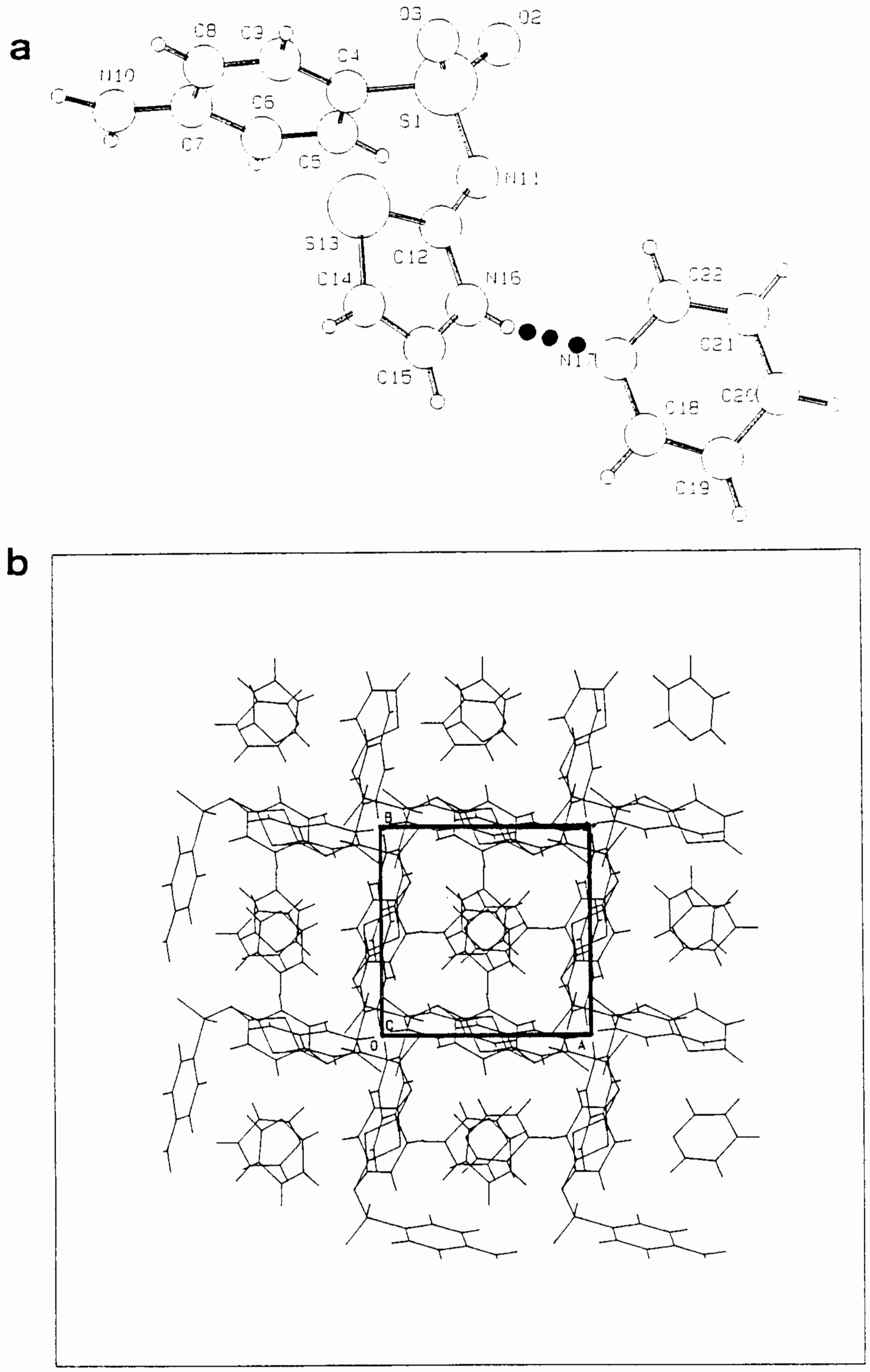

Figure 13.1.4 (a) The 1:1 H:G asymmetric unit of **STPY** with the intermolecular N-H...N hydrogen bond, 2.77(1)Å indicated by means of a dotted line.

(b) The crystal packing of **STPY** drawn in projection along [001]. The pyridine molecules are located at the centre of the unit cell.

Figure 13.1.4 (b) indicates the pyridine molecules in the centre and sulfathiazole molecules at the unit cell corners and edges. The molecules of the host compound are related to each other by a four-fold screw axis along z and the pyridines are stacked in a channel parallel to the second four-fold screw axis. The channel occupation of the pyridine molecules is more clearly revealed in **Figures 13.1.4 (c) - (e).**

In **Figure 13.1.4 (e)**, the hatching represents the area occupied by the host **ST** molecules alone at successive sections of the unit cell parallel to the ab-plane. A sense of continuity of the channel is conveyed in **Figure 13.1.4 (d).**

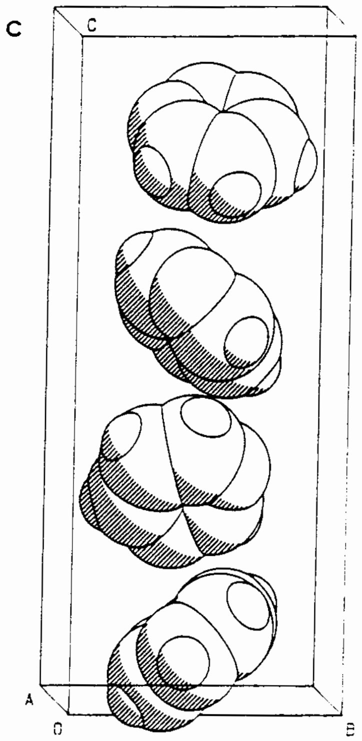

Figure 13.1.4 (c) Space-filling representation of the guest pyridine molecules in **STPY.** The molecules occupy a continuous channel defined by a four-fold screw axis parallel to c.

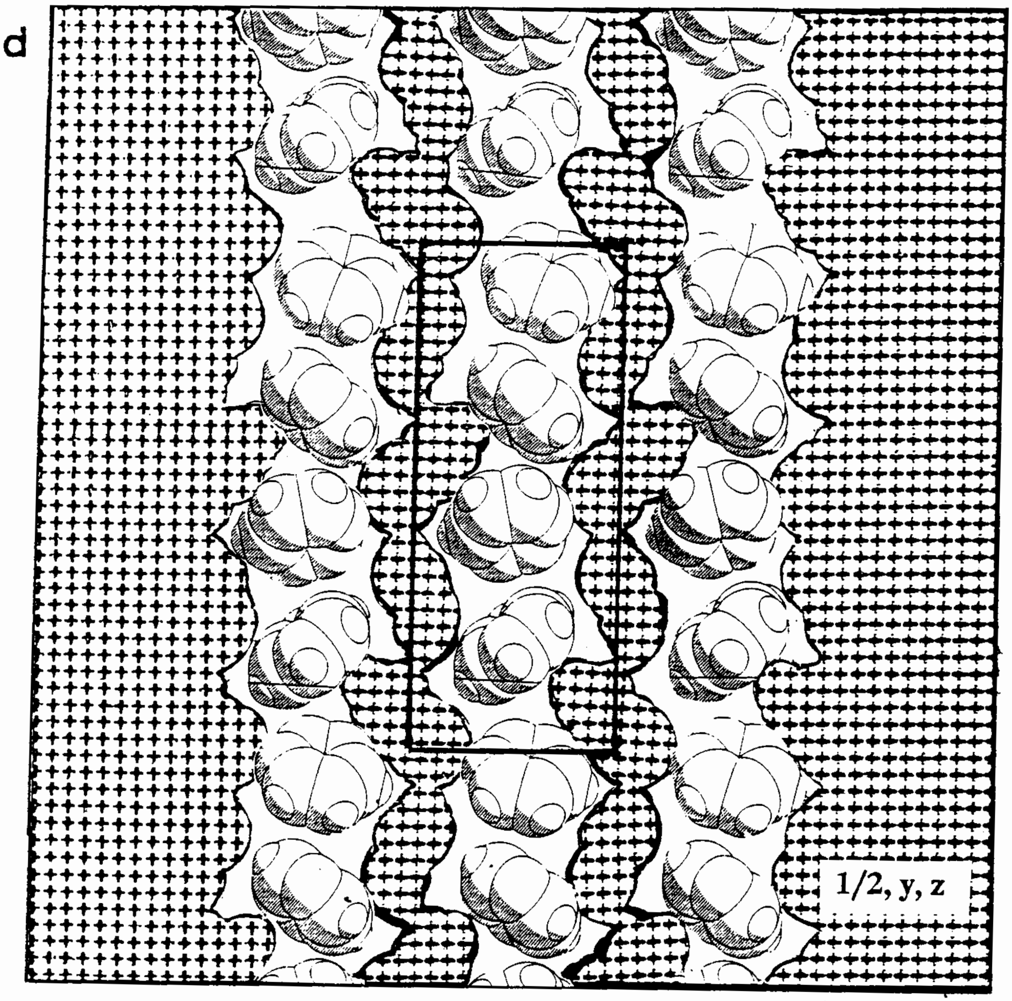

Figure 13.1.4 (d) A cross section of the cell at ½, y, z showing guest molecules drawn with van der Waals radii in a channel and the host molecules represented by the hatched area.

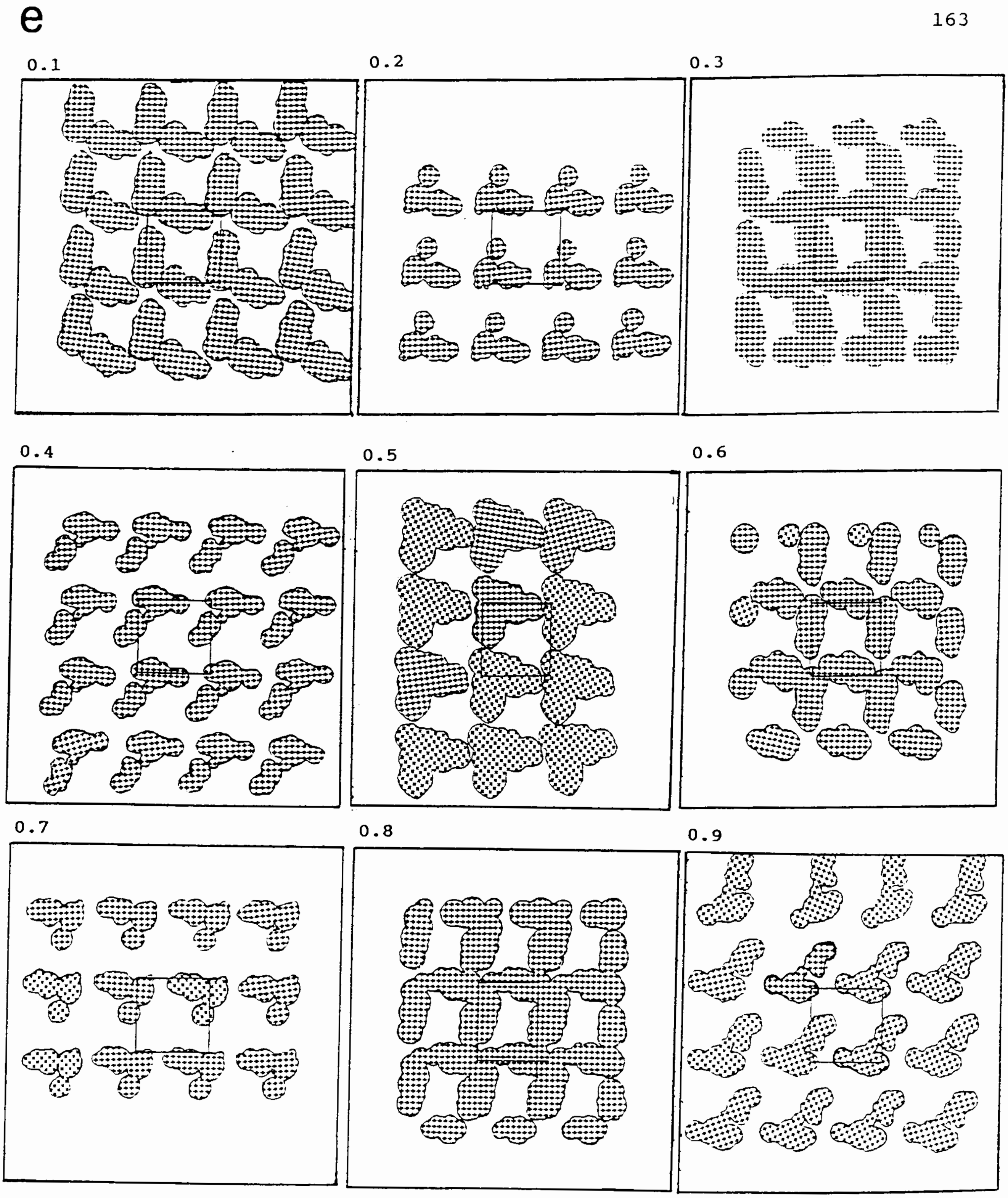

Figure 13.1.4 (e) Successive cross sections of the cell at intervals of 0.1 along c. The hatched area represents occupation by host ST molecules.

The host molecules in this structure are linked by N(10) - H(101)...O(2) hydrogen bonds while the guest molecules are hydrogen bonded to the host molecules (see **Table 13 b**). Thus, this structure may be described as a *coordinato clathrate in a coordination-assisted host lattice.*

13.1.5 STRUCTURE SOLUTION AND REFINEMENT OF STPY1

From oscillation and Weissenberg photographs, the diffraction symmetry (Laue symmetry) was determined as *2/m,* indicating the monoclinic crystal system. A primitive lattice was indicated by superposition of levels h 1 l and h 2 l, whose reflections overlapped. The h o l level showed no systematic absences. Inspection of the o k o reflections showed that they were systematically absent for k odd. Since these were the only systematically absent reflections, the space group was identified as $P2_1$ (No.4) or $P2_1/m$ (No.11).

A single cystal was mounted in mother liquor for intensity data collection, details of which appear in **Table 13 a**. It was found that the reference reflection intensities chosen to monitor the progress of data collection increased significantly with time. This was interpreted as growth of the crystal while immersed in mother liquor. For this reason, it was decided to collect only the reflections h: -12 to +12, k: 0 to 15, l: 0 to 15 i.e. this set includes reflections with k ≥ 0 only.

The structure was solved by direct methods using program SHELX 86. The mean $|E^2-1|$ value for general reflections was 0.754, indicating the acentric space group $P2_1$ (theoretical values: 0.968 centric crystal, 0.736 acentric crystal). Solution involved tangent refinement of the phases of 361 reflections with large (>1.2) E-values using 6662 unique triple phase relationships.

The solution with the lowest combined figure of merit (CFOM = 0.022) yielded an E-map which revealed 35 non-hydrogen atoms. Since the unit cell content is four 1:1 host:guest complexes, space group $P2_1$ requires the asymmetric unit to consist of two independent host:guest units. The E-map thus yielded 76% of the total number of 46 non-hydrogen atoms. These atoms were refined isotropically using the program SHELX 76.

From a subsequent weighted difference electron density ($\Delta\rho$) synthesis, the remaining 11 non-hydrogen atoms were located.

While most of the hydrogen atoms were located in $\Delta\rho$ syntheses, all of them were included in a riding model with C-H 1.00Å, except for the amino hydrogen atoms which were allowed to refine freely.

Hydrogen atoms were treated isotropically with common variable U_{iso} thermal parameters assigned to chemically-equivalent groups. Details of the final refinement are listed in **TABLE 13 a**.

The question of the absolute structure of the crystal specimen chosen for analysis was considered. Since the non-centrosymmetric space group $P2_1$ belongs to monoclinic class 2, neglect of anomalous dispersion corrections can lead to errors in the refined y-coordinates[160-161].

Final refinement of the structure was carried out with anomalous dispersion corrections applied to the S atom scattering factors and the procedure adopted to determine the absolute structure was to perform separate refinements of both polarities with the available 'half data-set' (with non-negative k only). As expected under these circumstances, these refinements yielded the same R_G factor[109,161] ($R_G = 0.0704$) but very slightly different y-coordinates. The resulting bond lengths and bond angles for the refined structure and its inverse were carefully compared. It was found, however, that there were no significant differences between these parameters for the two alternatives, thus indicating that the available data could not distinguish the absolute structure. The atomic coordinates listed in **Table 13 d (i)** are those of the original model (i.e. those obtained from the refinement preceding inversion of the structure).

In retrospect, the determination of the absolute structure for this compound by collection of a full data-set would not have yielded reliable results because of systematic errors in the data due to crystal growth during data-collection[162]. The latter was evident from an overall increase of 7% in the reference reflection intensities for the half data-set and since this variation was anisotropic (i.e. different for the three reference reflections) correction for this effect was not feasible. Failure to determine the absolute strcture in this case was not considered a major setback since the main aim of the analysis, namely the determination of the mode of inclusion of the guest by the host, was nevertheless achieved.

13.1.6 DISCUSSION OF THE STPY1 STRUCTURE

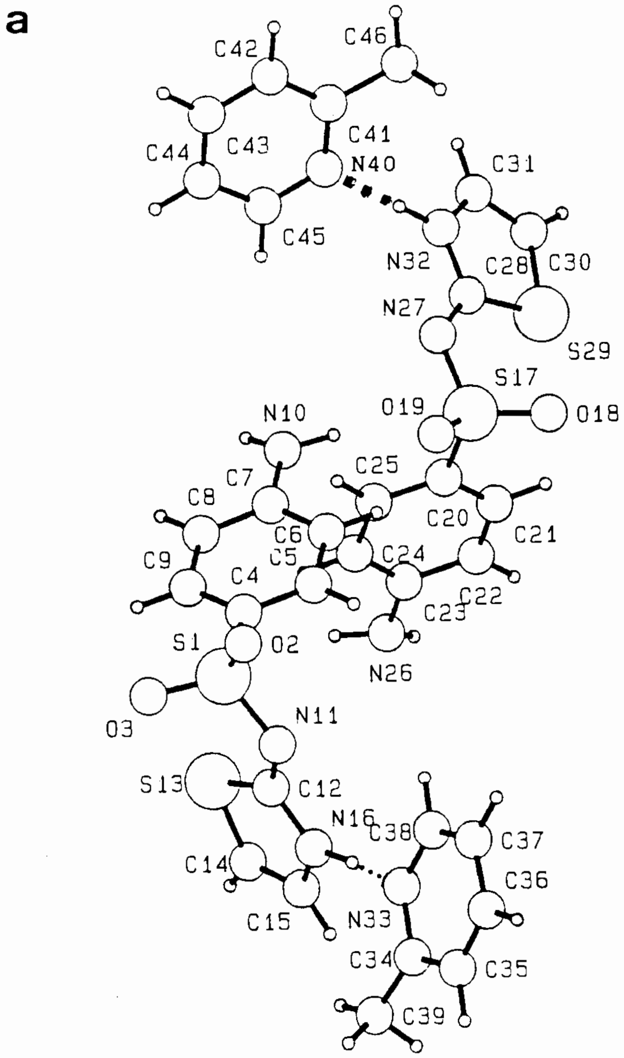

Figure 13.1.6 (a) The asymmetric unit of **STPY1** consisting of two independent 1:1 H:G components. Atomic nomenclature and host-guest intermolecular N-H...N hydrogen bonds (dotted lines) are indicated.

The diagram in **Figure 13.1.6 (a)** illustrates the two crystallographically-independent 1:1 H:G units in the crystal of **STPY1**. Each of these units is associated by host (N-H)...N(guest) hydrogen bonding. In one unit the hydrogen bond N(16)-H(16)...N(33) has an N...N distance of 2.768(9)Å, while in the other, the hydrogen bond N(32)-H(32)...N(40) has an N...N distance of 2.78(1)Å. The two distances are not statistically different, therefore an average of 2.77(1)Å will be quoted henceforth.

Statistical calculations involving comparable molecular parameters for each of the independent host-guest units in the asymmetric unit reveal that no significant differences exist between these parameters.

As observed in the other two structures, namely **STPY** and **STPY2**, the amino hydrogens and sulfonamide oxygens are responsible for host:host binding; thus the structure contains an interwoven network of host:guest and host:host hydrogen bonds which are ultimately responsible for the stability of the crystal. This structure, like **STPY**, can thus be described as a *coordinato clathrate in a coordination-assisted host lattice*.

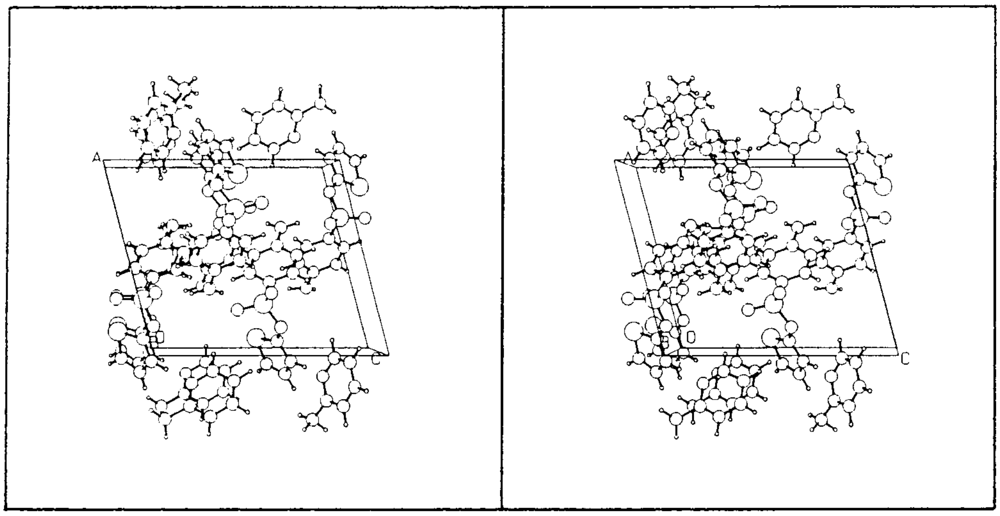

Figure 13.1.6 (b) Stereoview of the crystal packing within the structure of **STPY1**.

The stereo diagram in **Figure13.1.6 (b)** shows asymmetric units that are related to each other by means of two-fold screw axes.

Diagrams in **Figure 13.1.6 (c)** and **(d)** reveal that there exist continuous channels parallel to c in which the guest molecules are trapped and engage in hydrogen bonding with the host.

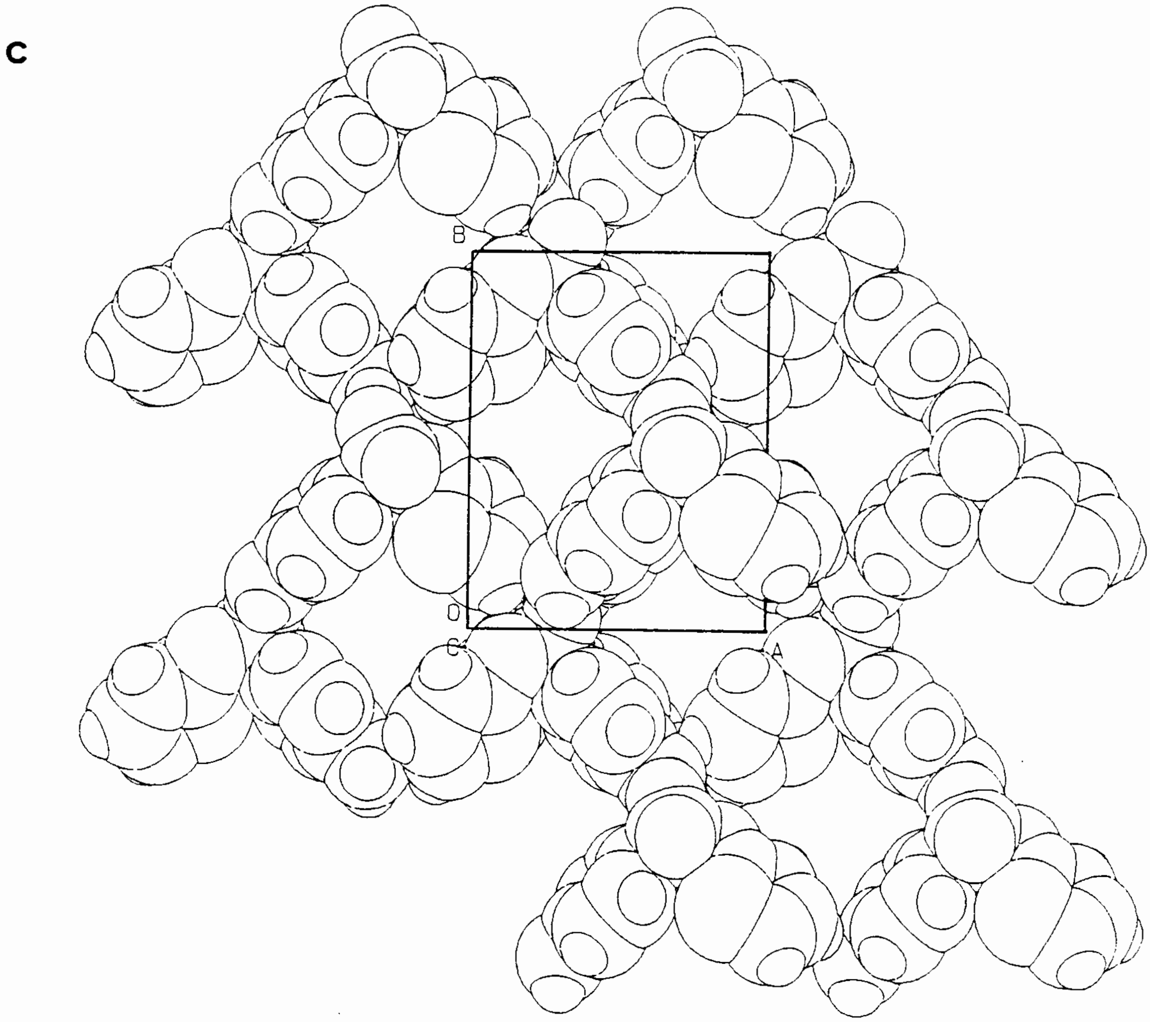

Figure 13.1.6 (c) A view of channels parallel to c as they are created by the host structure is represented by host molecules only. Atoms are drawn with van der Waals radii.

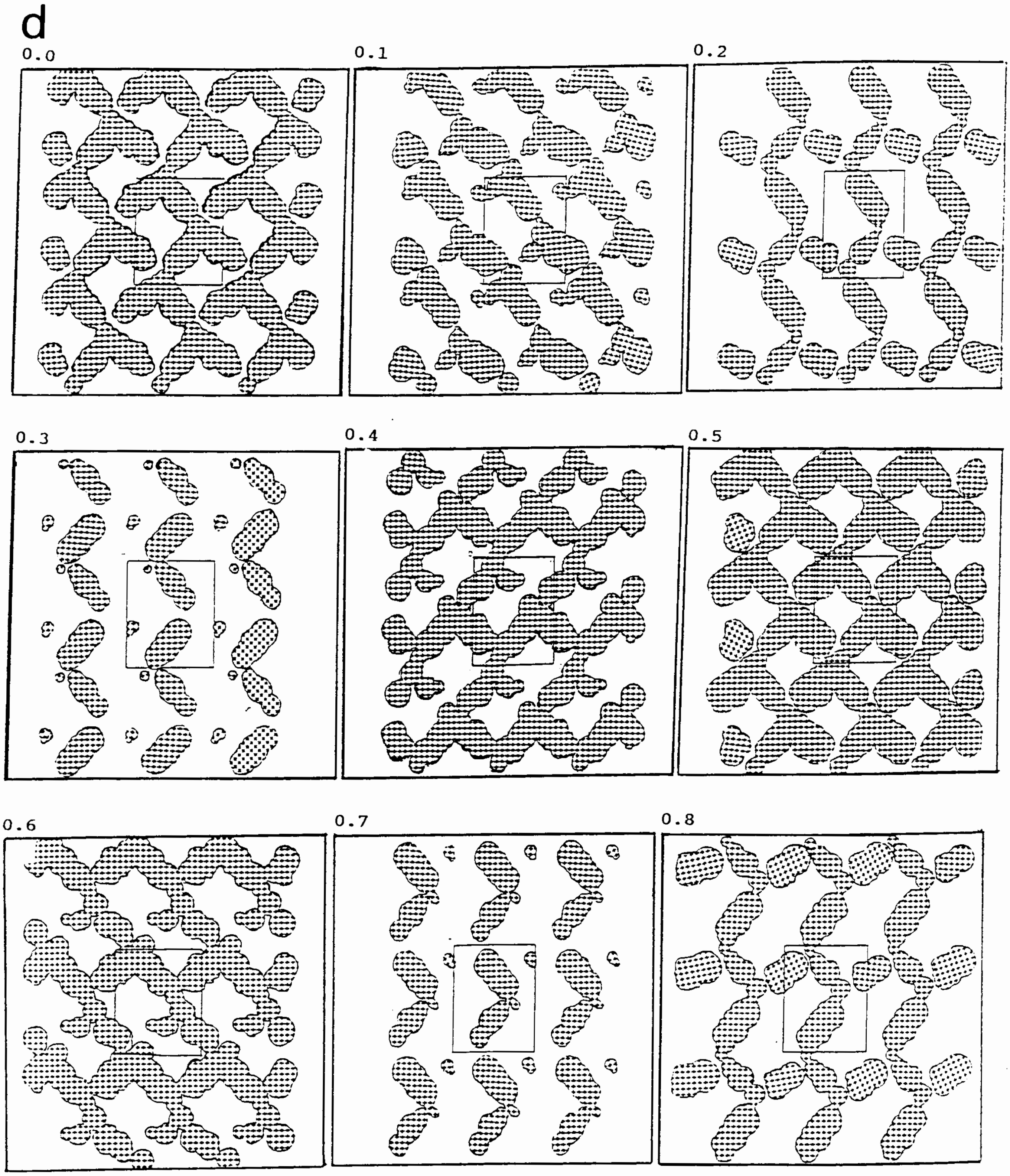

Figure 13.1.6 (d) A diagram of cross-sections of the unit cell along c indicating the presence of continuous channels in this direction. The hatched regions are occupied by host **ST** molecules.

This structure is accordingly described as a *coordinato clathrate in a coordination-assisted host lattice.*

13.1.7 STRUCTURE SOLUTION AND REFINEMENT OF STPY2

A single crystal which extinguished uniformly under plane-polarized light was mounted in mother liquor in a sealed Lindemann tube for preliminary X-ray photography. From oscillation and Weissenberg photographs, the Laue symmetry *2/m* was evident, confirming that this species is monoclinic. A survey of zero-and upper-level photographs yielded the conditions for non-extinction of reflections as hkl: none, hol: l=2n, oko: k=2n, indicating space group $P2_1/c$ (no.14). An alternative unit cell with $\beta = 98^{\circ}$ consistent with the condition hol: h+l=2n, was chosen. The final setting of the crystal is thus $P2_1/n$.

For intensity data-collection, a~~n~~ ~~equant~~ crystal fragment was cut from a larger crystal and mounted as described above. Crystal data and data-collection parameters are listed in **Table 13 a.**

One of the S atoms of the ST molecule was located by examining the Harker peaks in a three-dimensional sharpened Patterson synthesis. After refinement of the S atom position, a weighted difference electron-density ($\Delta\rho$) synthesis revealed the second S atom as well as several light atoms. Successive refinements and $\Delta\rho$ syntheses revealed the remaining non-hydrogen atoms. Isotropic refinement yielded R = 0.108. After several cycles of anisotropic refinement, all of the hydrogen atoms were located in $\Delta\rho$ syntheses. These were included in idealized positions in a riding model with C-H 1.00Å, except for the amino hydrogen atoms which were allowed to refine freely. Hydrogen atoms were treated isotropically with common variable U_{iso} thermal parameters assigned to chemically-equivalent groups. Details of the final refinement are also listed in **Table 13 a**.

13.1.8 DISCUSSION OF THE STPY2 STRUCTURE

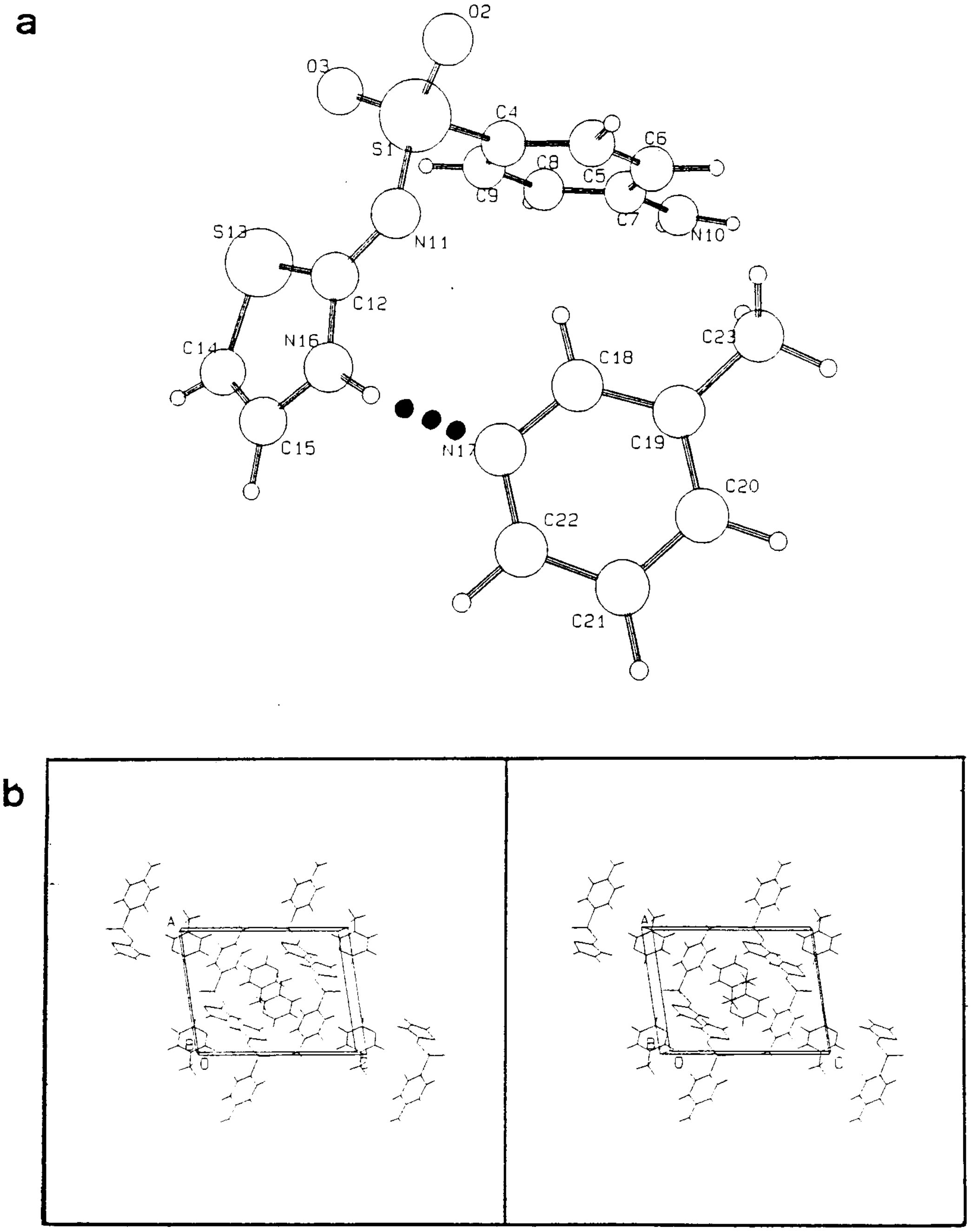

Figure 13.1.8 (a) A diagram of the asymmetric unit of **STPY2** with atom nomenclature and hydrogen bonding indicated by a dotted line.

(b) Stereoview of crystal packing in **STPY2** viewed along (010).

The hydrogen bonding scheme that is shown in **Figure 13.1.8 (a)** above is the same as that of **STPY** and **STPY1**. The host molecules are associated by means of a hydrogen bond N(10)-H(102)...O(2), 3.064(4)Å, while the hydrogen bond N(16)-H(16)...N(17), 2.833(4)Å is responsible for host:guest association. No unusual features are evident with regard to either the conformation of the host molecules or the nature of H:G molecular association. The molecular parameters **Tables 13 e (i)-(v)** are well within acceptable limits.

However, the space group for this compound *($P2_1/n$)* contains a greater number of symmetry elements than those of **STPY** *($P4_3$)* and **STPY1** *($P2_1$)* resulting in a distinctly different type of crystal packing shown in **Figure 13.1.8 (b)**.

The solvent molecules exist as centrosymmetric pairs related to each other by means of the two-fold screw axis and n-glide plane. **Figure 13.1.8 (c)** is a stereo diagram showing the guest molecules alone in space-filling representation with the arrangement just described being illustrated. The guest molecules are trapped in cavities within the crystal. Sections along all three directions using the program MOLMAP did not indicate the existence of channels.

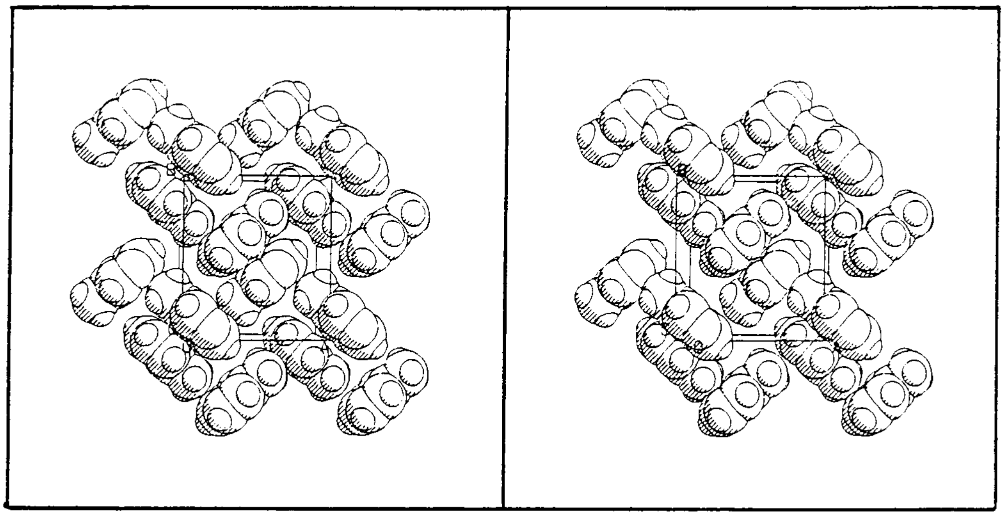

Figure 13.1.8 A stereo diagram of guest molecules only in **STPY2** in space-filling representation indicating cavity occupation by the solvent molecules. For clarity, only one centrosymetrically-related pair of guest molecules is drawn (related by $\bar{1}$ at $\frac{1}{2},\frac{1}{2},\frac{1}{2}$ at the unit cell centre). Analogous pairs exist at other centres of symmetry.

The structure of **STPY2** may also be described as *a coordinato clathrate in a coordination-assisted* host lattice; but in contrast to **STPY** and **STPY1**, guest molecules occupy cavities rather than channels.

13.1.9 DISCUSSION OF ST CRYSTAL STRUCTURES AND CONCLUSION

The choice of pyridine solvents resulted in a common mode of H:G association, namely host (N-H)...N(guest) hydrogen bond among the three compounds, thus making the inclusion trend systematic in this way.

The strength of this H:G interaction is influenced by a combination of factors. Common among these is the effect of the methyl substituent at different positions in the pyridine ring. Its steric effect influences the packing arrangements in the three crystal structures while its position influences the basicity of the N hetero-atom. It is evident however, from the pK_a values listed in section 2.1 that the methyl substituent at different positions of the pyridine ring does not influence the basicity so significantly.

In an attempt to correlate structural results with thermodynamic results, the values of DSC enthalpies of desolvation were compared with N...N hydrogen bond distances among the compounds.

The enthalpy of guest release in **STPY** is 41.5kJmol^{-1} and the corresponding hydrogen bond length, N(16)-H(16)...N(17) is 2.77(1)Å. When these data are compared with the corresponding data for **STPY2** (26.7 kJmol^{-1} and 2.833(4)Å for the enthalpy of desolvation and hydrogen bond distance respectively) it appears that the shorter the N...N distance, the higher the ΔH for desolvation.

However, we note that for **STPY1**, which has an average N...N distance of 2.77(1)Å, i.e. the same as that observed in **STPY**, the enthalpy change is only 24.6 kJmol^{-1}. This indicates that an attempt to correlate N...N distance with enthalpy for desolvation is not justified in this series of compounds, although such a correlation has been reported for other inclusion compounds of pyridine[127]. It was emphasized earlier (see section **11.5 (i)**) that the measured enthalpy for desolvation will generally be affected not only by the host-guest hydrogen bonded distances, but also by the nature of structural rearrangement occurring on desolvation.

On the subject of conformation and chemical behaviour of the host molecules in the solvates, it was noted that the imido tautomeric form of sulfathiazole is invariant in all three structures where N(16) instead of N(11) is protonated (See **Figure 13.1.2 (a)**). This is consistent with the results of structure solutions of sulfathiazole polymorphs by Kruger *et al*[93-94]. The same result was obtained in the study of the **SST** series of solvates in the present work.

With regard to the conformations of **ST** molecules in the three compounds, an inspection of torsion angles (**Tables 13 c(v), d(v) and e(v)**), especially those that define the conformation of the **ST** molecules uniquely, shows that there are no major conformational differences in moving from one structure to the next, except possibly in the structure of compound **STPY2**. For instance τ C(12)-N(11)-S(1)-C(4) is equal to -66.7(6)° in **STPY**, -61.2(5)° in **STPY1** approximating to a gauche conformation while it is -92.6(2)° in **STPY2** which is slightly different from the other two. It is not surprising that sulfathiazole should adopt a similar conformation throughout these compounds since their structures are characterized by a common H:H bond, N-H...O as well as a common H:G interaction, N-H...N.

In general, satisfactory characterization studies of the **ST** solvates have been carried out resulting in the determination of 1:1 stoichiometries by microanalysis, density measurements, TGA and ultimately confirmed by structure solutions.

The challenge of solving difficult structures, particularly those in the two polar space groups $P2_1$ and $P4_3$ for **STPY** and **STPY1** respectively was tackled successfully. This task was made even more difficult by the relative instability of these compounds resulting in crystal decompositions during handling with the result that several unsuccessful data collections were attempted.

A studious collection and analysis of thermal and XRD data ensured that the subject of sulfathiazole pseudopolymorphism is adequately addressed namely that sulfathiazole forms stoichiometric solvates with pyridines and its methyl substituted derivatives. The solvates were described as *coordinato clathrates in a coordination-assisted host lattice*.

TABLE 13 a Details of Intensity Data Collections and Structure Refinements

COMPOUND	STPY	STPY1	STPY2
Molecular formula	$C_9H_9N_3O_2S_2.C_5H_5N$	$C_9H_9N_3O_2S_2.C_6H_7N$	$C_9H_9N_3O_2S_2.C_6H_7N$
Guest	Pyridine	2-Methylpyridine	3-Methylpyridine
H:G Ratio	1:1	1:1	1:1
Crystal system	tetragonal	monoclinic	monoclinic
Space group	$P4_3$	$P2_1$	$P2_1/n$
a/Å	8.646(3)	10.744(2)	10.620(4)
b/Å	8.646(3)	12.915(2)	11.452(2)
c/Å	20.88(1)	12.687(2)	14.249(2)
α/°	90	90	90
β/°	90	104.93(2)	98.40(2)
γ/°	90	90	90
V/Å^3	1560(1)	1701.0(5)	1714(5)
Z	4	4	4
D_m/gcm^{-3}	1.419	1.358	1.350
D_c/gcm^{-3}	1.423	1.361	1.347
F(000)	696	728	728
μ(MoKα)/cm^{-1}	3.38	3.13	3.10
Crystal size/mm	0.50x0.65x0.40	0.35x0.50x0.65	0.20x0.65x0.50
Range scanned,θ/°	1-25	1-25	1-25
Index range	10,10,± 24	± 12,15,15	12,-13,± 16
Scan width,ω/°	0.80+0.35tanθ	0.85+0.35tanθ	0.85+0.35tanθ
Aperture width/mm	1.12+1.05tanθ	1.12+0.35tanθ	1.12+1.05tanθ
No.of reflections collected	3148	3283	3366
No. of unique reflections	2738	2869	2698
No.of reflections observed ($I_o>2\sigma(I_o)$)	2413	2538	2402
No.of parameters refined	208	431	220
R	0.083	0.053	0.040
Rw	*S	0.057	0.049

Table 13 a (continued)	Intensity Data Collection and Structure Refinements		
	STPY	STPY1	STPY2
Max shift/esd	0.02	0.787	1.37
Absorption correction factor range	0.8650-0.9967	0.8415-0.0089	0.9696-1.0000
Crystal stability (%)	-2.2	+7.0	+1.7
$\Delta\rho$:max,min/eÅ^{-3}	+0.55,-0.72	+0.16,-0.24	+0.26,-0.24

Note: (*) denotes refinement on F^2 with SHELX 93 which yielded wR2 = 0.238 and S (goodness of fit) = 0.997

TABLE 13 a Details of Intensity Data Collections and Structure Refinements

COMPOUND	STPY	STPY1	STPY2
Molecular formula	$C_9H_9N_3O_2S_2.C_5H_5N$	$C_9H_9N_3O_2S_2.C_6H_7N$	$C_9H_9N_3O_2S_2.C_6H_7N$
Guest	Pyridine	2-Methylpyridine	3-Methylpyridine
H:G Ratio	1:1	1:1	1:1
Crystal system	tetragonal	monoclinic	monoclinic
Space group	$P4_3$	$P2_1$	$P2_1/n$
a/Å	8.646(3)	10.744(2)	10.620(4)
b/Å	8.646(3)	12.915(2)	11.452(2)
c/Å	20.88(1)	12.687(2)	14.249(2)
α/°	90	90	90
β/°	90	104.93(2)	98.40(2)
γ/°	90	90	90
V/Å^3	1560(1)	1701.0(5)	1714(5)
Z	4	4	4
D_m/gcm^{-3}	1.419(2)	1.358(1)	1.350(2)
D_c/gcm^{-3}	1.423	1.361	1.347
F(000)	696	728	728
μ(MoKα)/cm^{-1}	3.38	3.13	3.10
Crystal size/mm	0.50x0.65x0.40	0.35x0.50x0.65	0.20x0.65x0.50
Range scanned,θ/°	1-25	1-25	1-25
Index range	10,10,± 24	± 12,15,15	12,-13,± 16
Scan width,ω/°	$0.80+0.35\tan\theta$	$0.85+0.35\tan\theta$	$0.85+0.35\tan\theta$
Aperture width/mm	$1.12+1.05\tan\theta$	$1.12+0.35\tan\theta$	$1.12+1.05\tan\theta$
No.of reflections collected	3148	3283	3366
No. of unique reflections	2738	2869	2698
No.of reflections observed $(I_o>2\sigma(I_o))$	2413	2538	2402
No.of parameters refined	208	431	220
R	0.083	0.053	0.040
Rw	*S	0.057	0.049

Table 13 b Distances (Å) and angles (°) for Hydrogen bonds

Donor-H		Donor-Acceptor		H...Acceptor		Donor-H...Acceptor	
STPY							
N(16)-H(16)	0.86(1)	N(16)...N(17)	2.77(1)	H(16)...N(17)	1.93(1)	N(16)-H(16)...N(17)	164.1(8)
N(10)-H(101)	1.04(9)	N(10)...O(2)^a	2.98(1)	H(101)...O(2)^a	1.95(4)	N(10)-H(101)...O(2)^a	171(8)
	(a) x, -1 + y, z						
STPY1							
N(10)-H(102)	1.00(2)	N(10)...O(19)	2.947(8)	H(102)...O(19)	1.98(3)	N(10)-H(102)...O(19)	163(3)
N(16)-H(16)	1.00(9)	N(16)...N(33)	2.768(9)	H(16)...N(33)	1.784(9)	N(16)-H(16)...N(33)	166.8(7)
N(32)-H(32)	1.00(1)	N(32)...N(40)	2.78(1)	H(32)...N(40)	1.79(1)	N(32)-H(32)...N(40)	178.2(7)
N(10)-H(101)	1.00(5)	N(10)...O(3)^a	3.158(9)	H(101)...O(3)^a	2.20(6)	N(10)-H(101)...O(3)^a	160(2)
N(26)-H(262)	1.00(5)	N(26)...O(2)^b	3.02(1)	H(262)...O(2)^b	2.05(5)	N(26)-H(262)...O(2)^b	163(4)
	(a) 1-x, $-\frac{1}{2}$+y, 1-z			(b) -1+y, z			
STPY2							
N(16)-H(16)	1.00(4)	N(16)...N(17)	2.833(4)	H(16)...N(17)	1.919(4)	N(16)-H(16)...N(17)	150.6(3)
N(10)-H(102)	0.73(3)	N(10)...O(2)^a	3.064(4)	H(102)...O(2)^a	2.47(3)	N(10)-H(102)...O(2)^a	140(3)
	(a) $1\frac{1}{2}$-x, $-\frac{1}{2}$+y, $\frac{1}{2}$-z						

ABLE 13 c (i) Fractional atomic coordinates (x 10^4)
and Thermal Parameters ($Å^2$ x 10^3)
with e.s.d. s in parentheses for Compound **STPY**

Atom	x/a	y/b	z/c	Uiso/Uequiv(*)
S(1)	1367(1)	789(1)	9947(0)	41(1) *
O(2)	87(5)	1793(5)	9880(3)	57(2) *
O(3)	1977(6)	641(6)	10585(2)	53(2) *
C(4)	845(6)	-1068(7)	9694(3)	37(2) *
C(5)	236(7)	-1248(7)	9075(3)	39(2) *
C(6)	-184(9)	-2683(8)	8871(3)	49(2) *
C(7)	-9(8)	-3996(7)	9253(3)	45(2) *
C(8)	634(8)	-3772(7)	9868(3)	49(2) *
C(9)	1039(7)	-2343(8)	10078(3)	43(2) *
N(10)	-443(11)	-5429(8)	9064(4)	72(3) *
N(11)	2657(6)	1388(6)	9458(2)	44(2) *
C(12)	4023(8)	701(7)	9442(3)	45(2) *
S(13)	4706(2)	-846(2)	9891(1)	63(1) *
C(14)	6484(10)	-746(13)	9521(5)	78(4) *
C(15)	6505(9)	394(12)	9099(4)	69(3) *
N(16)	5155(7)	1190(8)	9052(3)	55(2) *
N(17)	4888(8)	3987(8)	8418(3)	67(3) *
C(18)	5876(16)	4536(14)	8001(7)	105(5) *
C(19)	6005(21)	6004(15)	7810(7)	120(7) *
C(20)	4906(18)	7020(15)	8067(8)	112(6) *
C(21)	3855(15)	6461(17)	8492(8)	109(5) *
C(22)	3880(10)	4975(14)	8639(5)	81(4) *

$$U_{eq} = (1/3) \sum_i \sum_j U_{ij} a_i^* a_j^* a_i \cdot a_j$$

Hydrogen atomic coordinates (Å x 10^4) for **STPY**.

Parent atom	H	x/a	y/b	z/c
C(5)	H(5)	122	-396	8807
C(6)	H(6)	-602	-2792	8463
C(8)	H(8)	782	-4621	10135
C(9)	H(9)	1452	-2225	10487
N(10)	H(101)	-244(93)	-6462(54)	9307(43)
N(10)	H(102)	-524(89)	-5409(62)	8706(52)
C(14)	H(14)	7312	-1402	9606
C(15)	H(15)	7372	632	8855
N(16)	H(16)	5035	1951	8792
C(18)	H(18)	6559	3830	7819
C(19)	H(19)	6769	6328	7526
C(20)	H(20)	4896	8057	7949
C(21)	H(21)	3128	7115	8677
C(22)	H(22)	3129	4609	8920

TABLE 13 c (ii) Anisotropic atoms for **STPY** have thermal parameters ($Å^2$ x 10^3) of the form :

$$\exp[-2\pi^2(U_{11}h^2a^{*2} + U_{22}k^2b^{*2} + U_{33}l^2c^{*2} + 2U_{23}klb^*c^* + 2U_{13}hla^*c^* + 2U_{12}hka^*b^*)]$$

Atom	U11	U22	U33	U23	U13	U12
S(1)	39(1)	41(1)	42(1)	0(1)	5(1)	0(1)
O(2)	45(3)	56(3)	70(4)	-4(3)	12(3)	4(2)
O(3)	56(3)	61(3)	41(3)	3(2)	3(2)	8(2)
C(4)	29(3)	42(3)	39(3)	2(3)	6(2)	5(2)
C(5)	37(3)	43(3)	38(3)	5(3)	0(3)	6(3)
C(6)	57(4)	53(4)	38(3)	6(3)	2(3)	2(3)
C(7)	50(4)	42(3)	43(3)	3(3)	12(3)	1(3)
C(8)	54(4)	43(3)	49(4)	11(3)	2(3)	2(3)
C(9)	37(3)	56(4)	38(3)	8(3)	4(3)	1(3)
N(10)	115(7)	47(4)	56(4)	6(4)	3(4)	8(4)
N(11)	41(3)	42(3)	48(3)	7(2)	3(2)	3(2)
C(12)	53(4)	47(4)	34(3)	0(3)	3(3)	18(3)
S(13)	43(1)	84(1)	60(1)	22(1)	10(1)	12(1)
C(14)	47(5)	116(8)	71(6)	18(6)	16(4)	17(5)
C(15)	52(4)	92(6)	64(6)	6(5)	21(4)	5(4)
N(16)	49(3)	72(4)	45(3)	3(3)	10(3)	3(3)
N(17)	57(4)	70(5)	73(5)	12(4)	20(4)	2(3)
C(18)	117(9)	76(7)	123(11)	14(6)	76(8)	19(6)
C(19)	166(14)	83(8)	110(11)	28(7)	64(10)	1(8)
C(20)	132(12)	72(8)	133(13)	24(7)	13(10)	10(7)
C(21)	85(8)	100(10)	142(12)	28(9)	8(8)	36(7)
C(22)	54(5)	102(8)	85(7)	10(6)	20(5)	9(5)

TABLE 13 c (iii) Bond lengths (Angstrom) with e.s.d. s in parentheses for Compound **STPY**

S(1)	- O(2)	1.414(5)
S(1)	- O(3)	1.437(5)
S(1)	- C(4)	1.751(6)
S(1)	- N(11)	1.599(6)
C(4)	- C(5)	1.404(9)
C(4)	- C(9)	1.374(9)
C(5)	- C(6)	1.36 (1)
C(6)	- C(7)	1.40 (1)
C(7)	- C(8)	1.41 (1)
C(7)	- N(10)	1.35 (1)
C(8)	- C(9)	1.36 (1)
N(11)	- C(12)	1.32 (9)
C(12)	- S(13)	1.736(7)
C(12)	- N(16)	1.341(9)
S(13)	- C(14)	1.72 (1)
C(14)	- C(15)	1.32 (2)
C(15)	- N(16)	1.36 (1)
N(17)	- C(18)	1.31 (2)
N(17)	- C(22)	1.30 (1)
C(18)	- C(19)	1.34 (2)
C(19)	- C(20)	1.40 (2)
C(20)	- C(21)	1.36 (2)
C(21)	- C(22)	1.32 (2)

TABLE 13 c (iv) Bond angles (degrees) with e.s.d. s in parentheses for Compound **STPY**

C(4)	- S(1)	- N(11)	106.5(3)
O(3)	- S(1)	- N(11)	111.4(3)
O(3)	- S(1)	- C(4)	107.0(3)
O(2)	- S(1)	- N(11)	106.5(3)
O(2)	- S(1)	- C(4)	109.3(3)
O(2)	- S(1)	- O(3)	115.8(3)
S(1)	- C(4)	- C(9)	121.9(5)
S(1)	- C(4)	- C(5)	118.5(4)
C(5)	- C(4)	- C(9)	119.6(6)
C(4)	- C(5)	- C(6)	119.3(6)
C(5)	- C(6)	- C(7)	122.3(7)
C(6)	- C(7)	- N(10)	123.3(7)
C(6)	- C(7)	- C(8)	116.8(6)
C(8)	- C(7)	- N(10)	119.9(7)
C(7)	- C(8)	- C(9)	121.4(7)
C(4)	- C(9)	- C(8)	120.7(6)
S(1)	- N(11)	- C(12)	119.6(5)
N(11)	- C(12)	- N(16)	121.7(6)
N(11)	- C(12)	- S(13)	129.5(5)
S(13)	- C(12)	- N(16)	108.8(5)
C(12)	- S(13)	- C(14)	91.3(4)
S(13)	- C(14)	- C(15)	110.4(7)
C(14)	- C(15)	- N(16)	114.5(8)
C(12)	- N(16)	- C(15)	115.4(7)
C(18)	- N(17)	- C(22)	115.7(1)
N(17)	- C(18)	- C(19)	126.7(1)
C(18)	- C(19)	- C(20)	115.1(1)
C(19)	- C(20)	- C(21)	118.7(1)
C(20)	- C(21)	- C(22)	119.1(1)
N(17)	- C(22)	- C(21)	124.4(1)

TABLE 13 c (v) Torsion angles (degrees) with e.s.d. s in parentheses for Compound **STPY**

(RIGHT-HAND RULE,KLYNE & PRELOG.(1960).EXPERIENTIA,16,521)
(E.S.D.'S, FOLLOWING STANFORD & WASER,ACTA CRYST.(1972).A28,213)

C(4)	- S(1)	- N(11)	- C(12)	-66.7(6)
O(3)	- S(1)	- N(11)	- C(12)	49.6(6)
O(2)	- S(1)	- N(11)	- C(12)	176.7(5)
O(3)	- S(1)	- C(4)	- C(5)	-179.0(5)
O(2)	- S(1)	- C(4)	- C(5)	55.0(6)
O(3)	- S(1)	- C(4)	- C(9)	0.1(6)
O(2)	- S(1)	- C(4)	- C(9)	-126.0(6)
N(11)	- S(1)	- C(4)	- C(9)	119.3(6)
N(11)	- S(1)	- C(4)	- C(5)	-59.6(6)
S(1)	- C(4)	- C(9)	- C(8)	-179.6(5)
S(1)	- C(4)	- C(5)	- C(6)	-179.6(5)
C(5)	- C(4)	- C(9)	- C(8)	-1(1)
C(9)	- C(4)	- C(5)	- C(6)	1(1)
C(4)	- C(5)	- C(6)	- C(7)	-1(1)
C(5)	- C(6)	- C(7)	- C(8)	0(1)
C(5)	- C(6)	- C(7)	- N(10)	178.8(7)
C(6)	- C(7)	- C(8)	- C(9)	1(1)
N(10)	- C(7)	- C(8)	- C(9)	-178.1(7)
C(7)	- C(8)	- C(9)	- C(4)	-1(1)
S(1)	- N(11)	- C(12)	- S(13)	0(1)
S(1)	- N(11)	- C(12)	- N(16)	-178.1(5)
N(11)	- C(12)	- N(16)	- C(15)	178.5(7)
N(11)	- C(12)	- S(13)	- C(14)	-178.6(7)
S(13)	- C(12)	- N(16)	- C(15)	0.0(8)
N(16)	- C(12)	- S(13)	- C(14)	-0.3(6)
C(12)	- S(13)	- C(14)	- C(15)	0.5(8)
S(13)	- C(14)	- C(15)	- N(16)	-1(1)
C(14)	- C(15)	- N(16)	- C(12)	1(1)
C(18)	- N(17)	- C(22)	- C(21)	-3(1)
C(22)	- N(17)	- C(18)	- C(19)	4(1)
N(17)	- C(18)	- C(19)	- C(20)	-3(1)
C(18)	- C(19)	- C(20)	- C(21)	2(1)
C(19)	- C(20)	- C(21)	- C(22)	-1(1)
C(20)	- C(21)	- C(22)	- N(17)	2(1)

TABLE 13 d (i)

Fractional atomic coordinates (${}_{3}$x 10^4)
and Thermal Parameters (Å^2 x 10^3)
with e.s.d. s in parentheses for Compound **STPY1**

Atom	x/a	y/b	z/c	Uiso/Uequiv(*)
S(1)	2634(1)	9335(0)	5201(1)	42(1) *
O(2)	3194(4)	10308(4)	5617(5)	60(2) *
O(3)	2314(4)	9234(4)	4041(4)	60(2) *
C(4)	3735(5)	8344(5)	5748(5)	39(2) *
C(5)	4200(6)	8207(5)	6868(5)	47(2) *
C(6)	5113(7)	7481(6)	7269(6)	52(2) *
C(7)	5614(6)	6854(5)	6572(5)	43(2) *
C(8)	5127(7)	6988(5)	5452(6)	52(2) *
C(9)	4196(6)	7731(6)	5040(5)	49(2) *
N(10)	6564(7)	6141(5)	6973(5)	64(3) *
N(11)	1420(4)	9188(4)	5695(4)	43(2) *
C(12)	677(5)	8375(5)	5423(5)	42(2) *
S(13)	815(2)	7314(2)	4612(2)	67(1) *
C(14)	-589(8)	6783(7)	4789(8)	76(3) *
C(15)	-1069(7)	7359(6)	5453(7)	65(3) *
N(16)	-381(5)	8265(5)	5794(5)	52(2) *
S(17)	7134(1)	4591(2)	9843(1)	46(1) *
O(18)	7102(4)	4593(4)	10970(4)	57(2) *
O(19)	6779(4)	5554(4)	9258(4)	56(2) *
C(20)	6016(6)	3644(5)	9191(5)	44(2) *
C(21)	5542(6)	2954(6)	9822(6)	56(2) *
C(22)	4642(7)	2227(7)	9340(6)	60(3) *
C(23)	4214(6)	2147(6)	8186(6)	53(2) *
C(24)	4730(7)	2879(6)	7587(6)	58(3) *
C(25)	5618(6)	3590(6)	8072(5)	54(2) *
N(26)	3321(8)	1449(6)	7720(6)	79(3) *
N(27)	8509(5)	4290(5)	9686(4)	51(2) *
C(28)	9194(6)	3565(6)	10276(5)	53(2) *
S(29)	8835(2)	2762(2)	11271(2)	82(1) *
C(30)	10266(11)	2111(9)	11431(10)	102(5) *
C(31)	10962(9)	2498(8)	10782(9)	89(4) *
N(32)	10366(5)	3301(6)	10165(6)	70(3) *
N(33)	-1073(6)	9924(5)	6903(5)	62(2) *
C(34)	-2289(7)	10244(7)	6778(8)	73(3) *
C(35)	-2505(12)	11131(9)	7383(10)	101(5) *
C(36)	-1500(15)	11612(13)	8042(9)	125(7) *
C(37)	-297(14)	11276(12)	8132(10)	128(6) *
C(38)	-111(9)	10425(7)	7572(7)	79(4) *
C(39)	-3300(8)	9677(10)	5972(13)	133(7) *
N(40)	11461(6)	4364(7)	8718(6)	77(3) *
C(41)	12587(7)	4857(7)	9053(7)	67(3) *
C(42)	13087(9)	5396(8)	8311(8)	84(4) *
C(43)	12442(12)	5435(10)	7241(9)	104(5) *
C(44)	11303(12)	4921(11)	6905(9)	113(5) *
C(45)	10829(10)	4416(10)	7684(9)	103(4) *
C(46)	13247(9)	4809(10)	10240(8)	93(3)

$$U_{eq} = (1/3) \sum_i \sum_j U_{ij} a_i^* a_j^* a_i \cdot a_j$$

Hydrogen atom coordinates (Å x 10^4) for **STPY1**

Parent atom	H	x/a	y/b	z/c
C(5)	H(5)	3860	8646	7380
C(6)	H(6)	5437	7392	8077
C(8)	H(8)	5457	6546	4936
C(9)	H(9)	3858	7823	4234
N(10)	H(101)	6752(68)	5579(38)	6495(14)
N(10)	H(102)	6818(64)	5980(47)	7771(12)
C(14)	H(14)	-985	6126	4440
C(15)	H(15)	-1859	7163	5684
N(16)	H(16)	-650	8787	6275
C(21)	H(21)	5854	2986	10635
C(22)	H(22)	4283	1747	9807
C(24)	H(24)	4428	2873	6772
C(25)	H(25)	5983	4079	7619
N(26)	H(261)	3268(76)	776(25)	8099(22)
N(26)	H(262)	3310(78)	1211(45)	6969(32)
C(30)	H(30)	10544	1513	11938
C(31)	H(31)	11826	2226	10757
N(32)	H(32)	10777	3678	9654
C(35)	H(35)	-3400	11390	7314
C(36)	H(36)	-1649	12230	8469
C(37)	H(37)	454	11648	8612
C(38)	H(38)	785	10164	7665
C(39)	H(391)	-4136	10034	5931
C(39)	H(392)	-3296	8987	6332
C(39)	H(393)	-3192	9577	5219
C(42)	H(42)	13933	5761	8565
C(43)	H(43)	12795	5833	6707
C(44)	H(44)	10821	4908	6118
C(45)	H(45)	9969	4072	7449
C(46)	H(461)	14135	5102	10368
C(46)	H(462)	13303	4053	10414
C(46)	H(463)	12780	5171	10721

TABLE 13 d (ii) Anisotropic atoms for **STPY1** have thermal parameters ($\text{Å}^2 \times 10^3$) of the form :

$$\exp[-2\pi^2(U_{11}h^2a^{*2} + U_{22}k^2b^{*2} + U_{33}l^2c^{*2} + 2U_{23}klb^*c^* + 2U_{13}hla^*c^* + 2U_{12}hka^*b^*)]$$

Atom	U11	U22	U33	U23	U13	U12
S(1)	42(1)	32(1)	56(1)	3(1)	19(1)	0(1)
O(2)	52(3)	36(2)	96(4)	-1(2)	26(3)	-6(2)
O(3)	66(3)	60(3)	58(3)	16(2)	24(2)	12(3)
C(4)	36(3)	36(3)	47(3)	0(3)	16(2)	0(2)
C(5)	55(3)	42(3)	49(3)	0(3)	24(3)	6(3)
C(6)	62(4)	49(4)	47(3)	2(3)	18(3)	8(3)
C(7)	42(3)	33(3)	56(4)	1(3)	17(3)	1(2)
C(8)	63(4)	41(4)	58(4)	-11(3)	26(3)	6(3)
C(9)	50(4)	48(4)	46(3)	-2(3)	7(3)	6(3)
N(10)	71(4)	52(4)	69(4)	0(3)	20(3)	18(3)
N(11)	37(2)	35(3)	58(3)	-4(2)	15(2)	-2(2)
C(12)	40(3)	29(3)	55(3)	3(3)	8(2)	0(2)
S(13)	68(1)	43(1)	94(2)	-22(1)	31(1)	-14(1)
C(14)	74(5)	47(4)	105(6)	-12(4)	18(5)	-26(4)
C(15)	47(4)	57(4)	91(5)	-4(4)	16(4)	-20(3)
N(16)	42(3)	46(3)	74(4)	0(3)	25(2)	-5(2)
S(17)	49(1)	39(1)	51(1)	-4(1)	12(1)	-1(1)
O(18)	62(3)	56(3)	56(2)	-8(2)	19(2)	-4(2)
O(19)	61(3)	42(3)	63(3)	2(2)	9(2)	3(2)
C(20)	46(3)	41(3)	45(3)	-2(3)	14(3)	-7(3)
C(21)	53(4)	62(5)	52(4)	4(3)	15(3)	-3(3)
C(22)	64(4)	60(5)	57(4)	1(3)	16(3)	-17(4)
C(23)	51(4)	52(4)	57(4)	-3(3)	15(3)	-7(3)
C(24)	65(4)	59(4)	50(4)	0(3)	13(3)	-9(3)
C(25)	61(4)	56(4)	47(3)	1(3)	16(3)	-13(3)
N(26)	93(5)	71(5)	67(4)	-10(4)	10(4)	-41(4)
N(27)	47(3)	43(3)	62(3)	-4(3)	13(2)	-5(3)
C(28)	49(3)	49(4)	58(4)	-2(3)	5(3)	-2(3)
S(29)	81(1)	71(1)	91(2)	27(1)	18(1)	9(1)
C(30)	86(7)	80(7)	124(9)	34(6)	-1(6)	23(6)
C(31)	66(5)	82(7)	106(7)	2(6)	-2(5)	31(5)
N(32)	50(3)	71(4)	86(4)	-7(4)	12(3)	0(3)
N(33)	62(4)	42(3)	87(4)	7(3)	30(3)	10(3)
C(34)	58(4)	53(4)	115(7)	26(4)	36(4)	6(4)
C(35)	118(8)	92(8)	118(8)	45(7)	79(7)	56(7)
C(36)	164(13)	127(12)	84(7)	-25(7)	30(8)	35(11)
C(37)	140(11)	123(11)	94(7)	-36(7)	-17(7)	45(9)
C(38)	87(6)	64(5)	75(5)	-8(4)	0(4)	5(4)
C(39)	46(5)	82(7)	263(17)	3(10)	27(7)	-3(5)
N(40)	55(3)	77(5)	95(5)	-5(4)	14(3)	1(4)
C(41)	50(4)	66(5)	83(5)	-16(4)	14(4)	9(4)
C(42)	74(6)	81(7)	102(7)	-22(5)	31(5)	-18(5)
C(43)	117(8)	102(9)	93(7)	-14(6)	27(6)	-34(7)
C(44)	137(10)	107(9)	80(6)	-8(6)	4(6)	-21(8)
C(45)	87(6)	91(7)	111(7)	4(7)	-8(6)	-25(6)

TABLE 13 d (iii) Bond lengths (Angstrom) with e.s.d. s in parentheses for Compound **STPY1**

S(1)	- O(2)	1.434(5)
S(1)	- O(3)	1.428(5)
S(1)	- C(4)	1.760(6)
S(1)	- N(11)	1.597(5)
C(4)	- C(5)	1.391(9)
C(4)	- C(9)	1.38(1)
C(5)	- C(6)	1.36(1)
C(6)	- C(7)	1.40(1)
C(7)	- C(8)	1.393(9)
C(7)	- N(10)	1.372(9)
C(8)	- C(9)	1.39(1)
N(11)	- C(12)	1.310(8)
C(12)	- S(13)	1.743(7)
C(12)	- N(16)	1.346(9)
S(13)	- C(14)	1.72(1)
C(14)	- C(15)	1.32(1)
C(15)	- N(16)	1.39(1)
S(17)	- O(18)	1.439(5)
S(17)	- O(19)	1.449(6)
S(17)	- C(20)	1.764(6)
S(17)	- N(27)	1.589(6)
C(20)	- C(21)	1.38(1)
C(20)	- C(25)	1.374(9)
C(21)	- C(22)	1.37(1)
C(22)	- C(23)	1.42(1)
C(23)	- C(24)	1.41(1)
C(23)	- N(26)	1.34(1)
C(24)	- C(25)	1.35(1)
N(27)	- C(28)	1.302(9)
C(28)	- S(29)	1.752(8)
C(28)	- N(32)	1.347(9)
S(29)	- C(30)	1.72(1)
C(30)	- C(31)	1.34(1)
C(31)	- N(32)	1.36(1)
N(33)	- C(34)	1.34(1)
N(33)	- C(38)	1.32(1)
C(34)	- C(35)	1.43(1)
C(34)	- C(39)	1.48(1)
C(35)	- C(36)	1.34(1)
C(36)	- C(37)	1.34(2)
C(37)	- C(38)	1.35(1)
N(40)	- C(41)	1.34(1)
N(40)	- C(45)	1.31(1)
C(41)	- C(42)	1.39(1)
C(41)	- C(46)	1.49(1)
C(42)	- C(43)	1.36(1)
C(43)	- C(44)	1.36(1)
C(44)	- C(45)	1.39(1)

TABLE 13 d (iv) Bond angles (degrees) with e.s.d. s in parentheses for Compound **STPY1**

C(4)	- S(1)	- N(11)	107.0(2)
O(3)	- S(1)	- N(11)	112.9(2)
O(3)	- S(1)	- C(4)	107.4(2)
O(2)	- S(1)	- N(11)	105.5(2)
O(2)	- S(1)	- C(4)	108.5(2)
O(2)	- S(1)	- O(3)	115.2(3)
S(1)	- C(4)	- C(9)	118.5(4)
S(1)	- C(4)	- C(5)	121.6(4)
C(5)	- C(4)	- C(9)	119.8(5)
C(4)	- C(5)	- C(6)	120.4(6)
C(5)	- C(6)	- C(7)	121.3(6)
C(6)	- C(7)	- N(10)	121.5(6)
C(6)	- C(7)	- C(8)	117.8(6)
C(8)	- C(7)	- N(10)	120.7(6)
C(7)	- C(8)	- C(9)	121.0(5)
C(4)	- C(9)	- C(8)	119.7(6)
S(1)	- N(11)	- C(12)	119.7(4)
N(11)	- C(12)	- N(16)	120.3(5)
N(11)	- C(12)	- S(13)	130.3(4)
S(13)	- C(12)	- N(16)	109.4(4)
C(12)	- S(13)	- C(14)	91.5(3)
S(13)	- C(14)	- C(15)	110.9(6)
C(14)	- C(15)	- N(16)	114.1(7)
C(12)	- N(16)	- C(15)	114.1(5)
C(20)	- S(17)	- N(27)	108.3(3)
O(19)	- S(17)	- N(27)	106.0(2)
O(19)	- S(17)	- C(20)	107.4(3)
O(18)	- S(17)	- N(27)	112.7(2)
O(18)	- S(17)	- C(20)	106.2(3)
O(18)	- S(17)	- O(19)	115.9(3)
S(17)	- C(20)	- C(25)	120.8(5)
S(17)	- C(20)	- C(21)	119.0(5)
C(21)	- C(20)	- C(25)	120.2(6)
C(20)	- C(21)	- C(22)	120.4(6)
C(21)	- C(22)	- C(23)	120.8(7)
C(22)	- C(23)	- N(26)	120.6(7)
C(22)	- C(23)	- C(24)	115.9(6)
C(24)	- C(23)	- N(26)	123.4(7)
C(23)	- C(24)	- C(25)	122.5(6)
C(20)	- C(25)	- C(24)	120.0(6)
S(17)	- N(27)	- C(28)	120.6(4)
N(27)	- C(28)	- N(32)	121.8(6)
N(27)	- C(28)	- S(29)	130.1(5)
S(29)	- C(28)	- N(32)	108.1(5)
C(28)	- S(29)	- C(30)	91.0(4)
S(29)	- C(30)	- C(31)	111.6(8)
C(30)	- C(31)	- N(32)	112.5(9)
C(28)	- N(32)	- C(31)	116.6(6)
C(34)	- N(33)	- C(38)	120.0(7)
N(33)	- C(34)	- C(39)	116.7(8)
N(33)	- C(34)	- C(35)	118.1(8)

TABLE 13 d (v) Torsion angles (degrees) with e.s.d. s in parentheses for Compound **STPY1**

(RIGHT-HAND RULE,KLYNE & PRELOG.(1960).EXPERIENTIA,16,521)
(E.S.D.'S, FOLLOWING STANFORD & WASER,ACTA CRYST.(1972).A28,213)

C(4)	- S(1)	- N(11)	- C(12)	-67.2(5)
O(3)	- S(1)	- N(11)	- C(12)	50.8(5)
O(2)	- S(1)	- N(11)	- C(12)	177.4(4)
O(3)	- S(1)	- C(4)	- C(5)	-177.6(5)
O(2)	- S(1)	- C(4)	- C(5)	57.3(6)
O(3)	- S(1)	- C(4)	- C(9)	6.2(6)
O(2)	- S(1)	- C(4)	- C(9)	-118.9(5)
N(11)	- S(1)	- C(4)	- C(9)	127.7(5)
N(11)	- S(1)	- C(4)	- C(5)	-56.1(9)
S(1)	- C(4)	- C(9)	- C(8)	175.9(5)
S(1)	- C(4)	- C(5)	- C(6)	-175.6(5)
C(5)	- C(4)	- C(9)	- C(8)	-0.4(9)
C(9)	- C(4)	- C(5)	- C(6)	0.6(9)
C(4)	- C(5)	- C(6)	- C(7)	0.2(3)
C(5)	- C(6)	- C(7)	- C(8)	-1.1(6)
C(5)	- C(6)	- C(7)	- N(10)	178.0(6)
C(6)	- C(7)	- C(8)	- C(9)	1.3(3)
N(10)	- C(7)	- C(8)	- C(9)	-177.8(6)
C(7)	- C(8)	- C(9)	- C(4)	-0.6(5)
S(1)	- N(11)	- C(12)	- S(13)	3.6(8)
S(1)	- N(11)	- C(12)	- N(16)	-177.0(4)
N(11)	- C(12)	- N(16)	- C(15)	-179.1(6)
N(11)	- C(12)	- S(13)	- C(14)	-179.3(6)
S(13)	- C(12)	- N(16)	- C(15)	0.4(7)
N(16)	- C(12)	- S(13)	- C(14)	1.2(6)
C(12)	- S(13)	- C(14)	- C(15)	-2.6(7)
S(13)	- C(14)	- C(15)	- N(16)	3.3(9)
C(14)	- C(15)	- N(16)	- C(12)	-2.4(8)
C(20)	- S(17)	- N(27)	- C(28)	-77.8(6)
O(19)	- S(17)	- N(27)	- C(28)	167.2(5)
O(18)	- S(17)	- N(27)	- C(28)	39.4(6)
O(19)	- S(17)	- C(20)	- C(21)	-137.9(6)
O(18)	- S(17)	- C(20)	- C(21)	-13.3(6)
O(19)	- S(17)	- C(20)	- C(25)	42.0(6)
O(18)	- S(17)	- C(20)	- C(25)	166.6(5)
N(27)	- S(17)	- C(20)	- C(25)	-72.1(6)
N(27)	- S(17)	- C(20)	- C(21)	108.0(8)
S(17)	- C(20)	- C(25)	- C(24)	-177.9(5)
S(17)	- C(20)	- C(21)	- C(22)	178.1(5)
C(21)	- C(20)	- C(25)	- C(24)	2.0(4)
C(25)	- C(20)	- C(21)	- C(22)	-1.9(7)
C(20)	- C(21)	- C(22)	- C(23)	2.1(7)
C(21)	- C(22)	- C(23)	- C(24)	-2.4(2)
C(21)	- C(22)	- C(23)	- N(26)	-178.9(7)
C(22)	- C(23)	- C(24)	- C(25)	2.7(8)
N(26)	- C(23)	- C(24)	- C(25)	179.0(7)

TABLE 13 d (iv) (continued)

C(35)	- C(34)	- C(39)	125.1(8)
C(34)	- C(35)	- C(36)	119.4(6)
C(35)	- C(36)	- C(37)	120.5(4)
C(36)	- C(37)	- C(38)	119.2(7)
N(33)	- C(38)	- C(37)	122.6(5)
C(41)	- N(40)	- C(45)	119.1(8)
N(40)	- C(41)	- C(46)	117.2(7)
N(40)	- C(41)	- C(42)	120.1(8)
C(42)	- C(41)	- C(46)	122.7(8)
C(41)	- C(42)	- C(43)	120.7(9)
C(42)	- C(43)	- C(44)	118.8(8)
C(43)	- C(44)	- C(45)	118.1(4)
N(40)	- C(45)	- C(44)	123.1(9)

TABLE 13 d (v) (continued)

C(23)	- C(24)	- C(25)	- C(20)	-2.5(1)
S(17)	- N(27)	- C(28)	- S(29)	2.4(9)
S(17)	- N(27)	- C(28)	- N(32)	-179.5(5)
N(27)	- C(28)	- N(32)	- C(31)	-176.5(7)
N(27)	- C(28)	- S(29)	- C(30)	176.7(7)
S(29)	- C(28)	- N(32)	- C(31)	1.9(9)
N(32)	- C(28)	- S(29)	- C(30)	-1.6(6)
C(28)	- S(29)	- C(30)	- C(31)	0.9(9)
S(29)	- C(30)	- C(31)	- N(32)	0.0(5)
C(30)	- C(31)	- N(32)	- C(28)	-1.3(3)
C(34)	- N(33)	- C(38)	- C(37)	-1.4(6)
C(38)	- N(33)	- C(34)	- C(39)	176.8(8)
C(38)	- N(33)	- C(34)	- C(35)	0.1(7)
N(33)	- C(34)	- C(35)	- C(36)	0.3(4)
C(39)	- C(34)	- C(35)	- C(36)	-176.4(8)
C(34)	- C(35)	- C(36)	- C(37)	0.6(3)
C(35)	- C(36)	- C(37)	- C(38)	-1.9(5)
C(36)	- C(37)	- C(38)	- N(33)	2.4(3)
C(41)	- N(40)	- C(45)	- C(44)	3.2(2)
C(45)	- N(40)	- C(41)	- C(46)	177.8(9)
C(45)	- N(40)	- C(41)	- C(42)	-1.3(7)
N(40)	- C(41)	- C(42)	- C(43)	0.2(6)
C(46)	- C(41)	- C(42)	- C(43)	-178.8(8)
C(41)	- C(42)	- C(43)	- C(44)	-0.9(7)
C(42)	- C(43)	- C(44)	- C(45)	2.6(5)
C(43)	- C(44)	- C(45)	- N(40)	-3.8(3)

TABLE 13 e (i) Fractional atomic coordinates ($\times 10^4$) and Thermal Parameters ($Å^2 \times 10^3$) with e.s.d. s in parentheses for Compound **STPY2**

Atom	x/a	y/b	z/c	Uiso/Uequiv(*)
S(1)	5019(1)	7558(1)	1523(1)	48(0) *
O(2)	4750(2)	8772(2)	1644(1)	70(1) *
O(3)	5017(2)	7144(2)	566(1)	62(1) *
C(4)	6524(2)	7256(2)	2152(2)	43(1) *
C(5)	6937(2)	7841(2)	2989(2)	49(1) *
C(6)	8079(3)	7555(2)	3522(2)	52(1) *
C(7)	8831(2)	6677(2)	3229(2)	51(1) *
C(8)	8422(3)	6114(2)	2373(2)	54(1) *
C(9)	7280(3)	6391(2)	1841(2)	49(1) *
N(10)	9954(3)	6375(3)	3772(2)	77(1) *
N(11)	4038(2)	6866(2)	2071(1)	48(1) *
C(12)	3664(2)	5800(2)	1817(2)	45(1) *
S(13)	3856(1)	5003(1)	809(1)	75(0) *
C(14)	3041(4)	3847(3)	1188(3)	92(2) *
C(15)	2651(3)	4070(3)	2020(3)	76(1) *
N(16)	3007(2)	5159(2)	2369(2)	55(1) *
N(17)	3265(2)	5782(2)	4312(2)	63(1) *
C(18)	4212(3)	6542(3)	4534(2)	65(1) *
C(19)	4723(3)	6840(3)	5447(2)	64(1) *
C(20)	4194(3)	6294(3)	6166(2)	72(1) *
C(21)	3222(4)	5513(3)	5950(2)	76(1) *
C(22)	2781(3)	5280(3)	5022(2)	68(1) *
C(23)	5792(4)	7697(4)	5635(3)	109(2) *

$$U_{eq} = (1/3) \sum_i \sum_j U_{ij} a_i^* a_j^* a_i \cdot a_j$$

Hydrogen atom coordinates (Å) for **STPY2.**

Parent atom	H	x/a	y/b	z/c
C(5)	H(5)	6391	8467	3208
C(6)	H(6)	8384	7986	4122
C(8)	H(8)	8979	5507	2141
C(9)	H(9)	6983	5973	1233
N(10)	H(101)	10184(28)	6697(25)	4385(22)
N(10)	H(102)	10330(30)	5909(29)	3605(22)
C(14)	H(14)	2860	3102	828
C(15)	H(15)	2166	3504	2365
N(16)	H(16)	2795	5463	2985
C(18)	H(18)	4570	6924	4000
C(20)	H(20)	4529	6476	6843
C(21)	H(21)	2849	5111	6468
C(22)	H(22)	2059	4719	4864
C(23)	H(231)	6055	7792	6334
C(23)	H(232)	5475	8461	5353
C(23)	H(233)	6539	7434	5335

TABLE 13 e (ii) Anisotropic atoms for **STPY2** have thermal parameters ($Å^2 \times 10^3$) of the form :

$$\exp[-2\pi^2(U_{11}h^2a^{*2} + U_{22}k^2b^{*2} + U_{33}l^2c^{*2} + 2U_{23}klb^*c^* + 2U_{13}hla^*c^* + 2U_{12}hka^*b^*)]$$

Atom	U11	U22	U33	U23	U13	U12
S(1)	52(0)	46(0)	42(0)	10(0)	-4(0)	-6(0)
O(2)	68(1)	44(1)	89(1)	18(1)	-13(1)	-1(1)
O(3)	66(1)	80(1)	37(1)	11(1)	-3(1)	-18(1)
C(4)	46(1)	41(1)	39(1)	4(1)	0(1)	-5(1)
C(5)	57(2)	42(1)	45(1)	-4(1)	2(1)	4(1)
C(6)	62(2)	47(1)	44(1)	-8(1)	-6(1)	3(1)
C(7)	54(2)	42(1)	53(1)	-1(1)	-3(1)	-1(1)
C(8)	58(2)	47(1)	55(2)	-7(1)	8(1)	3(1)
C(9)	62(2)	47(1)	38(1)	-3(1)	2(1)	-5(1)
N(10)	67(2)	70(2)	85(2)	-24(2)	-23(2)	23(1)
N(11)	52(1)	45(1)	46(1)	0(1)	4(1)	-4(1)
C(12)	43(1)	46(1)	45(1)	4(1)	3(1)	0(1)
S(13)	95(1)	66(1)	71(1)	-21(0)	33(0)	-25(0)
C(14)	118(3)	59(2)	106(3)	-20(2)	38(2)	-31(2)
C(15)	79(2)	59(2)	91(2)	9(2)	12(2)	-25(2)
N(16)	56(1)	56(1)	55(1)	6(1)	10(1)	-10(1)
N(17)	61(2)	74(2)	55(1)	8(1)	7(1)	5(1)
C(18)	64(2)	75(2)	56(2)	9(1)	14(1)	4(2)
C(19)	61(2)	68(2)	63(2)	-1(1)	10(1)	5(1)
C(20)	91(2)	74(2)	51(2)	-1(2)	15(2)	16(2)
C(21)	97(3)	74(2)	63(2)	7(2)	30(2)	-2(2)
C(22)	70(2)	66(2)	72(2)	5(2)	18(2)	5(2)
C(23)	114(3)	119(3)	95(3)	-16(3)	16(3)	-35(3)

TABLE 13 e (iii) Bond lengths (Angstrom) with e.s.d. s in parentheses for Compound **STPY2**

S(1)	-	O(2)	1.435(3)
S(1)	-	O(3)	1.443(2)
S(1)	-	C(4)	1.749(3)
S(1)	-	N(11)	1.601(3)
C(4)	-	C(5)	1.382(4)
C(4)	-	C(9)	1.387(4)
C(5)	-	C(6)	1.373(4)
C(6)	-	C(7)	1.386(4)
C(7)	-	C(8)	1.392(4)
C(7)	-	N(10)	1.368(4)
C(8)	-	C(9)	1.370(4)
N(11)	-	C(12)	1.318(3)
C(12)	-	S(13)	1.740(3)
C(12)	-	N(16)	1.342(4)
S(13)	-	C(14)	1.711(4)
C(14)	-	C(15)	1.336(6)
C(15)	-	N(16)	1.376(4)
N(17)	-	C(18)	1.332(4)
N(17)	-	C(22)	1.331(4)
C(18)	-	C(19)	1.378(4)
C(19)	-	C(20)	1.388(5)
C(19)	-	C(23)	1.494(5)
C(20)	-	C(21)	1.366(5)
C(21)	-	C(22)	1.363(4)

TABLE 13 e (iv) Bond angles (degrees) with e.s.d. s in parentheses for Compound **STPY2**

C(4)	- S(1)	- N(11)	105.3(1)
O(3)	- S(1)	- N(11)	112.7(1)
O(3)	- S(1)	- C(4)	107.1(1)
O(2)	- S(1)	- N(11)	105.4(1)
O(2)	- S(1)	- C(4)	108.3(1)
O(2)	- S(1)	- O(3)	117.3(1)
S(1)	- C(4)	- C(9)	120.3(2)
S(1)	- C(4)	- C(5)	119.8(1)
C(5)	- C(4)	- C(9)	119.8(2)
C(4)	- C(5)	- C(6)	120.3(2)
C(5)	- C(6)	- C(7)	120.5(2)
C(6)	- C(7)	- N(10)	120.4(2)
C(6)	- C(7)	- C(8)	118.7(2)
C(8)	- C(7)	- N(10)	120.9(6)
C(7)	- C(8)	- C(9)	121.0(2)
C(4)	- C(9)	- C(8)	119.7(2)
S(1)	- N(11)	- C(12)	121.1(1)
N(11)	- C(12)	- N(16)	120.5(2)
N(11)	- C(12)	- S(13)	130.1(1)
S(13)	- C(12)	- N(16)	109.3(1)
C(12)	- S(13)	- C(14)	91.1(1)
S(13)	- C(14)	- C(15)	111.7(2)
C(14)	- C(15)	- N(16)	112.9(3)
C(12)	- N(16)	- C(15)	115.0(2)
C(18)	- N(17)	- C(22)	117.6(2)
N(17)	- C(18)	- C(19)	124.5(3)
C(18)	- C(19)	- C(23)	121.1(2)
C(18)	- C(19)	- C(20)	116.0(2)
C(20)	- C(19)	- C(23)	122.9(2)
C(19)	- C(20)	- C(21)	120.2(2)
C(20)	- C(21)	- C(22)	119.2(3)
N(17)	- C(22)	- C(21)	122.4(3)

TABLE 13 e (v) Torsion angles (degrees) with e.s.d. s in parentheses for Compound **STPY2**

(RIGHT-HAND RULE,KLYNE & PRELOG.(1960).EXPERIENTIA,16,521)
(E.S.D.'S, FOLLOWING STANFORD & WASER,ACTA CRYST.(1972).A28,213)

C(4)	- S(1)	- N(11)	- C(12)	-92.6(2)
O(3)	- S(1)	- N(11)	- C(12)	23.9(2)
O(2)	- S(1)	- N(11)	- C(12)	153.1(2)
O(3)	- S(1)	- C(4)	- C(5)	161.1(2)
O(2)	- S(1)	- C(4)	- C(5)	33.7(2)
O(3)	- S(1)	- C(4)	- C(9)	-22.2(2)
O(2)	- S(1)	- C(4)	- C(9)	-149.6(2)
N(11)	- S(1)	- C(4)	- C(9)	98.1(2)
N(11)	- S(1)	- C(4)	- C(5)	-78.6(2)
S(1)	- C(4)	- C(9)	- C(8)	-175.9(2)
S(1)	- C(4)	- C(5)	- C(6)	175.5(2)
C(5)	- C(4)	- C(9)	- C(8)	0.8(4)
C(9)	- C(4)	- C(5)	- C(6)	-1.2(4)
C(4)	- C(5)	- C(6)	- C(7)	-0.0(4)
C(5)	- C(6)	- C(7)	- C(8)	1.7(4)
C(5)	- C(6)	- C(7)	- N(10)	-178.5(2)
C(6)	- C(7)	- C(8)	- C(9)	-2.1(4)
N(10)	- C(7)	- C(8)	- C(9)	178.1(2)
C(7)	- C(8)	- C(9)	- C(4)	0.9(4)
S(1)	- N(11)	- C(12)	- S(13)	-11.8(3)
S(1)	- N(11)	- C(12)	- N(16)	169.3(2)
N(11)	- C(12)	- N(16)	- C(15)	178.9(2)
N(11)	- C(12)	- S(13)	- C(14)	-179.0(2)
S(13)	- C(12)	- N(16)	- C(15)	-0.2(3)
N(16)	- C(12)	- S(13)	- C(14)	-0.1(2)
C(12)	- S(13)	- C(14)	- C(15)	0.3(3)
S(13)	- C(14)	- C(15)	- N(16)	-0.5(4)
C(14)	- C(15)	- N(16)	- C(12)	0.4(4)
C(18)	- N(17)	- C(22)	- C(21)	-0.4(4)
C(22)	- N(17)	- C(18)	- C(19)	0.1(4)
N(17)	- C(18)	- C(19)	- C(20)	0.1(4)
N(17)	- C(18)	- C(19)	- C(23)	179.6(3)
C(18)	- C(19)	- C(20)	- C(21)	-0.2(4)
C(23)	- C(19)	- C(20)	- C(21)	-179.6(3)
C(19)	- C(20)	- C(21)	- C(22)	-0.1(5)
C(20)	- C(21)	- C(22)	- N(17)	0.4(5)

REFERENCES

157. T. Hahn, A. Vos: International Tables for X-Ray Crystallography, **vol.A,** Space Group Symmetry, Kluwer Academic Publishers, (1992).

158. G.M. Sheldrick: *J.Appl.Cryst.* (in preparation), (1993).

159. G. Bernadelli, H.D. Flack: *Acta Cryst.,* **A40,** 500, (1985).

160. D.W.J. Cruickshank, W.S. McDonald: *Acta Cryst.,* **23,** 9, (1967).

161. D.H. Templeton: *Z. Kristallogr.,* **113,** 234, (1960).

162. P.G. Jones: *Acta Cryst.,* **A40,** 660, (1984).

CHAPTER 14

CONCLUSION

CHAPTER 14

14.1 CONCLUSION

The main objective of the research that was conducted was achieved, namely to gain an insight into the pseudopolymorphism of the antimicrobial drugs sulfathiazole and succinylsulfathiazole.

The following summary of structures is tabulated below in support of this claim:

Table 14.1.1 Summary of the Structures that were solved.

COMPOUND	GUEST	H:G	SPACE GR	GUEST TOPOLOGY
SSTDI	1,4-dioxane	1:1	$P\bar{1}$	channel
SSTBU	1-butanol	1:1	$P\bar{1}$	cavity
SSTPE	1-pentanol	1:1	$P\bar{1}$	cavity
STPY	pyridine	1:1	$P4_3$	channel
STPY1	2-methylpyridine	1:1	$P2_1$	channel
STPY2	3-methylpyridine	1:1	$P2_1/n$	cavity

Four of the above six compounds, namely **SSTDI**, **STPY**, **STPY1** and **STPY2** are hitherto unknown compounds that have not been reported in the literature despite the effort that had been previously devoted to investigating the polymorphic and pseudopolymorphic behaviour of these two drug substances. This observation led us to propose that any future work of this kind should begin with a fuller and more comprehensive battery of recrystallizations from a wide range of solvents.

The use of highly sensitive and discriminating experimental techniques such as TGA, DSC and XRD yielded accurate stoichiometries of these compounds together with full details of their crystal structures.

A high level of consistency between structure and thermodynamics was evident in cases such as that of compound **SSTDI**, where the observed two-step loss of solvent from TGA-DSC thermograms (**see Figure 5.3 (c)**) was confirmed by the three-dimensional structural results showing two crystallographically-distinct sites occupied by the dioxane molecules, namely that one guest molecule is not bonded to the host while the other one is tightly bound by means of hydrogen bonds. This is definitely consistent with the appearance of two TGA-DSC peaks for solvent release shown in **Figure 5.3 (c)**.

Of interest in this project was the identification and correct assignment of the pure polymorphs of the drugs resulting from desolvation processes. In some cases this was not an easy task, for example, the identification of polymorphic forms III and IV of sulfathiazole (Jamshed *et al*)[95]. However, the complementary use of DSC and XRD powder methods ensured unambiguous characterization of the compounds.

APPENDICES 1 AND 2

Tables of structure factors are contained in a computer diskette as follows:

APPENDIX 1

DISFT.DOC	for SSTDI
BUSFT.DOC	for SSTBU
PESFT.DOC	for SSTPE

APPENDIX 2

PYSFT.DOC	for STPY1
Y1SFT.DOC	for STPYI
Y2SFT.DOC	for STPY2

The files have been stored as simple text files which have been formatted using the software program MS WORD 5.0.